

# COMPUTATION OF GRAVITY CURRENTS IN ESTUARIES

PROEFSCHRIFT

TER VERKRIJGING VAN DE GRAAD VAN DOCTOR IN DE  
TECHNISCHE WETENSCHAPPEN AAN DE TECHNISCHE  
HOGESCHOOL DELFT, OP GEZAG VAN DE RECTOR  
MAGNIFICUS PROF. IR. H. R. VAN NAUTA LEMKE, HOOG-  
LERAAR IN DE AFDELING DER ELEKTROTECHNIEK,  
VOOR EEN COMMISSIE UIT DE SENAAT TE VERDEDIGEN  
OP WOENSDAG 2 DECEMBER 1970 TE 14 UUR

DOOR

CORNELIS BOUDEWIJN VREUGDENHIL

wiskundig ingenieur

geboren te Delft

UITGEVERIJ WALTMAN - DELFT

This thesis is also published as publication no. 86 of the Delft Hydraulics Laboratory.

## STELLINGEN

1.

Van een wiskundig model voor gelaagde stroming in een getij-rivier, dat werkt met meer dan twee lagen, moet geen belangrijk beter resultaat verwacht worden dan van een twee-lagen-model.

2.

De wijze waarop Boulot en Daubert bij hun berekening van een zouttong het uiteinde van die tong behandelen is niet juist.

F. Boulot & A. Daubert, *Modèle mathématique de la remontée de la salinité sous une forme stratifiée en régime non-permanent*, XIIIth Congress IAHR, Kyoto 1969, C 38.

3.

Bij de berekening van waterslag-verschijnselen kan de methode van de starre waterkolom worden toegepast wanneer een maatgevend tijds-interval voor de verschijnselen groter is dan ongeveer twintig maal de looptijd (heen en terug) van een drukgolf in de leiding.

4.

De afleiding van de vergelijkingen voor de voortplanting van lange golven in ondiep water door middel van integratie in verticale richting over de waterdiepte verdient de voorkeur boven een afleiding door een reeks-ontwikkeling naar een kleine parameter.

5.

De door Di Toro voorgestelde formulering voor de menging in een getijrivier verschilt niet essentieel van het door hem betwijfelde dispersie-model.

D. M. di Toro, *Maximum entropy mixing in estuaries*, J. ASCE, **95**, HY (1969) 1247-1271.

6.

Een differentie-methode ter oplossing van hyperbolische differentiaalvergelijkingen voor de voortplanting van lange golven dient stabiel te zijn op lange termijn bij een constante tijdstap.

7.

Het door Sharp gesignaleerde verschijnsel van cavitatiebellen op regelmatige afstanden in een buisleiding waarin een onderdruk golf optreedt, wordt door hem onjuist geïnterpreteerd. Het verschijnsel is voor buisleidingen van praktische afmetingen niet van belang.

B. B. Sharp, Rupture of the water-column, Proc. 2nd Australasian Conf. Hydr. Fluid Mech. (1965) A 169-177.

B. B. Sharp, The growth and collapse of cavities produced by a rarefaction wave with special reference to rupture of the water-column. Ph. D. Thesis, Melbourne 1965.

8.

Teneinde het verschil tussen de naar Euler en Lagrange genoemde beschouwingswijzen voor de afleiding van de bewegingsvergelijkingen van een vloeistof tot zijn recht te laten komen, verdient het de voorkeur, bij de eerstgenoemde methode van een vast volume-element uit te gaan.

9.

De door Streeter en Wylie beschreven „method of specified time-intervals” voor waterslag-berekeningen mag niet gelijkwaardig worden geacht met de karakteristieken-methode.

V. L. Streeter & E. B. Wylie, Hydraulic transients, Mc Grawhill Book Cy., New York 1967.

10.

Bij het onderzoek van wind-effecten op ondiep water dient de invloed van de wind op de bodem-schuifspanning in aanmerking te worden genomen.

## CONTENTS

CHAPTER 1	INTRODUCTION	
1.1	Gravity currents and mathematical models . . . . .	9
1.2	Literature . . . . .	10
1.3	Outline . . . . .	11
CHAPTER 2	MATHEMATICAL DESCRIPTION	
2.1	Basic equations . . . . .	13
2.2	Effects of turbulence . . . . .	15
2.3	Approximations . . . . .	15
CHAPTER 3	TWO-LAYER MODEL	
3.1	General . . . . .	18
3.2	Integration . . . . .	19
3.3	Rectangular channel . . . . .	24
3.4	Definition of the interface . . . . .	27
CHAPTER 4	FLOW STRUCTURE	
4.1	Introduction . . . . .	30
4.2	Mixing-length hypothesis . . . . .	30
4.3	Velocity and density profiles . . . . .	32
4.4	Frictional and mixing coefficients . . . . .	36
4.5	Convection through the interface . . . . .	37
CHAPTER 5	BOUNDARY CONDITIONS	
5.1	Initial conditions . . . . .	38
5.2	Number and character of boundary conditions . . . . .	40
5.3	Critical flow . . . . .	42
5.4	Schematized sea . . . . .	43
5.5	Supercritical flow . . . . .	44
CHAPTER 6	BAROTROPIC AND BAROCLINIC APPROXIMATIONS	
6.1	Singular perturbation problem . . . . .	46
6.2	Barotropic approximation . . . . .	46
6.3	Baroclinic approximation . . . . .	48
6.4	Matching and uniform approximation . . . . .	51

CHAPTER 7	APPLICATIONS OF THE MODEL WITHOUT MIXING	
7.1	Rotterdam Waterway . . . . .	54
7.2	Velocity profiles . . . . .	62
7.3	Interfacial friction . . . . .	64
CHAPTER 8	APPLICATION OF THE MODEL WITH MIXING . . .	67
	CONCLUSIONS . . . . .	71
	REFERENCES . . . . .	75
	NOTATION . . . . .	79
	SUMMARY . . . . .	83
	SAMENVATTING . . . . .	85
	APPENDIX	
1	Numerical method . . . . .	87
2	Energy equations . . . . .	95
3	Characteristics . . . . .	100
4	Estimates of approximations . . . . .	104

## INTRODUCTION

**1.1 Gravity currents and mathematical models**

In several fields phenomena occur which can be characterized as gravity currents, i.e., currents caused by differences in the specific weight of a fluid. Examples are to be found in oceanography, meteorology, civil engineering. In many cases an important engineering interest is present. This may concern questions of water management (salt intrusion in estuaries or in ground-water, dispersion of cooling water or pollutants), shipping (navigational consequences of currents, maintenance of channels: silt and sand transport), constructions (effects on bridge piers, tunnels, pipe-lines).

To analyse and predict gravity currents, one can take recourse to hydraulic and mathematical models, both of which need support from field data. Each kind of model has its own possibilities and peculiarities. As far as mathematical models are concerned, the major question is, whether a satisfactory mathematical description can be given for the relevant physical processes. In most of the cases mentioned above, turbulence plays an important part. In many of them also tidal effects are present. A practical limitation of mathematical models is usually formed by the computational effort required to obtain a sufficient degree of detail, either necessary to adequately represent the problem or desired for the engineering evaluation. Generally, e.g., it is impossible yet to include vertical variations systematically, as the mathematical formulation is not sufficiently known and the computational effort may be very great. The approach in the set-up of a mathematical model, therefore, is determined both by the requirements from the point of view of the applications and by the possibilities in the mathematical description of the physical processes.

In the present study, attention is limited to gravity currents in estuaries. For most of the estuarial problems mentioned above, some knowledge of the distribution of velocities and densities is required. The degree of detail varies. In studies of salt-penetration, e.g., the mean currents generally will be sufficient information. In the design of a cooling-water outfall, however, both the velocity and density profiles are rather important.

An indication of the possibilities in mathematical models for estuarine gravity currents can be derived from a consideration of literature on the subject. This is done in the following section. It turns out that some experience has been obtained only with models in one spatial dimension, as far as time-dependent cases are concerned. Extension to two horizontal dimensions is mainly a computational question. The limited physical knowledge concerning turbulent flow in a stratified fluid is the main drawback to an extension with the vertical dimension.

In the present study one of the one-dimensional approaches, viz. the two-layer

model, is worked out. A similar method is applicable to different situations, e.g., flow of heated water in a lake. For the case of estuaries, the model is extended with a rough estimate of the velocity- and density-profiles, with the layer mean values as parameters.

## 1.2 Literature

In the abundant literature on gravity currents relatively few references are available dealing with more or less detailed mathematical models, suitable for prediction purposes. A first distinction can be made with respect to the type of estuary considered. The classification usually made consists of three types: the fully stratified or salt-wedge type, the partly mixed type and the vertically homogeneous or well-mixed type. About the only paper giving motivated quantitative limits for these types is that by Hansen and Rattray (1966). They find that the classification depends not only on the ratio between the tidal and river flows, mentioned by most authors, but also on a stability parameter (internal Froude number). A second distinction in the mathematical models is made by considering whether or not tidal variations are taken into account.

Models which do not represent tidal variations can give only limited information with regard to the applications mentioned in the preceding section. Mainly for the well-mixed case, Van der Burgh (1968) and Ippen and Harleman (1961) treat the one-dimensional case. The latter paper refers to conditions at low-water slack rather than to tidal mean conditions. See also Harleman and Abraham (1966). Hansen and Rattray (1966) and Hansen (1967) take the vertical variations of velocity and salinity into account. In an analysis of flume measurements, Harleman and Ippen (1967) conclude that Hansen and Rattray's model applies to the central part of the intrusion area only.

Models considering tidal variations use either depth mean quantities with a diffusion-like term to describe the longitudinal dispersion of salt, or a two-layer scheme similar to the one in the present study. The former possibility naturally will apply best to well-mixed conditions. However, Stigter and Siemons (1967) also found very good correspondence to measurements in the Rotterdam Waterway which is of the partly mixed type. The relation between the coefficient of dispersion and the determining conditions still seems to be an unsolved question.

The two-layer model has been described by Schijf and Schönfeld (1953). The model, of course, applies best to salt-wedge type estuaries. Again, however, it may be applicable in less extreme conditions too. Voogt (1966) attempted a numerical solution of the equations, but did not arrive at useful results for an estuary, because of computational difficulties. The method in some respects resembles that developed in the present study. Boulot and Daubert (1969), using a different numerical method, applied the model to the Rhône River, which, because of the small tidal range in the Mediterranean, actually approaches the salt-wedge type (see also Boulot, Braconnot and Mar-

vaud (1967)). They tried to determine the main empirical parameter, the interfacial frictional coefficient, by comparison of numerical results to prototype-data. They state that this is a difficult task, as the salt-wedge is probably never in dynamical equilibrium, due to the daily variations in the river discharge and the tidal range. Application of the two-layer model to the partly mixed Rotterdam Waterway has been described by Vreugdenhil (1970).

For completeness some applications can be mentioned for two-dimensional areas, which do not concern estuaries. Schmitz (1964, 1967) computed the response of a layered sea to a wind-field. With modified assumptions for the shear stresses at the interface and the bottom, the method would be an equivalent of the two-layer model without mixing in the present study. It could be applied to wide estuaries. A similar method for the flow of warm over cold water is described by Wada (1969). The two-layer model has been applied in meteorology to simulate the behaviour of a cold front (Kasahara, Isaacson and Stoker (1965)). In this case no frictional terms were included.

It may be concluded, firstly, that only one-dimensional models have been checked reasonably against prototype-data. However, the verifications have not been very complete. Therefore, as a second conclusion, the value of these mathematical models is still limited. Much more should be known about the empirical parameters in each model. On the other hand, it should be made clear in which situations each model is applicable. As a third conclusion, models taking vertical variations into account have hardly come into the picture yet, due to the difficulties in reasonably formulating the behaviour of the flow.

### 1.3 Outline

From the preceding sections it has become clear that, on the one hand, the mathematical model should not be too complicated, and that on the other hand, it should give sufficient information to be applicable to the engineering problems. In the present study it is shown that a two-layer model meets these requirements. The following chapters describe the derivation and application of such a model.

It is important to know the possibilities and limitations of a mathematical model. Therefore Chapters 2 and 3 deal with the basic equations and the schematization into a two-layer system. The treatment essentially takes turbulence effects into account. Equations for the two-layer schematization are derived both for the general case and for the case in which the exchange between the layers is left out of consideration.

Chapter 4 treats the effects of turbulence in some more detail, using a mixing-length hypothesis. In this way it turns out to be possible to derive velocity and density profiles, given the mean values in each layer and some geometrical parameters. These profiles agree with data from nature to a limited accuracy. This opens the possibility to derive some information on the velocity and density profiles from a two-layer model. Also some remarks are made on the frictional and mixing coefficients at the inter-

face and their relation to the local conditions. This relation is not useful as it contains unknown empirical parameters.

The mathematical model is completed by a set of boundary and initial conditions, discussed in Chapter 5. The boundary condition at the rivermouth presents some difficulties, as several kinds of supercritical flow can occur. A method is proposed which includes a part of the sea, such that the river-mouth adjusts itself to the various conditions. The sea is treated schematically as a one-dimensional channel. In the case without mixing, an alternative method can be used, based on critical flow at the river-mouth. Still the complications of supercritical flow must be taken into account.

The mathematical properties of the equations are discussed in Chapter 6. Two types of waves are identified, viz., fast surface waves and slow internal waves. This has consequences for a numerical solution of the equations. An approximation is constructed which describes the internal waves only. This approximation can be derived by considering the singular perturbation problem, describing the influence of the small relative density difference  $\varepsilon$ .

In Chapters 7 and 8 applications are made to the Rotterdam Waterway, for which extensive measurements are available. A quite reasonable reproduction is obtained, to some extent also for the velocity and density profiles. By hindcasting a number of flume tests some information is gathered concerning the interfacial frictional coefficient, as depending on the overall conditions.

There follows a discussion of the results and a conclusion on the applicability of the model.

## MATHEMATICAL DESCRIPTION

### 2.1 Basic equations

The basic equations for sea-water are discussed rather completely by Eckart (1962). In the following only a schematic derivation is given.

The equation of mass-conservation for a non-homogeneous fluid reads

$$\frac{\partial \varrho}{\partial t} + \frac{\partial}{\partial x_j}(\varrho v_j) - \theta \frac{\partial^2 \varrho}{\partial x_j \partial x_j} = 0 \quad (2.1.1)$$

where  $\varrho$  = density  
 $t$  = time  
 $x_j$  = coordinate (cf. fig. 1)  
 $v_j$  = velocity-component in  $x_j$ -direction  
 $\theta$  = coefficient of molecular diffusion

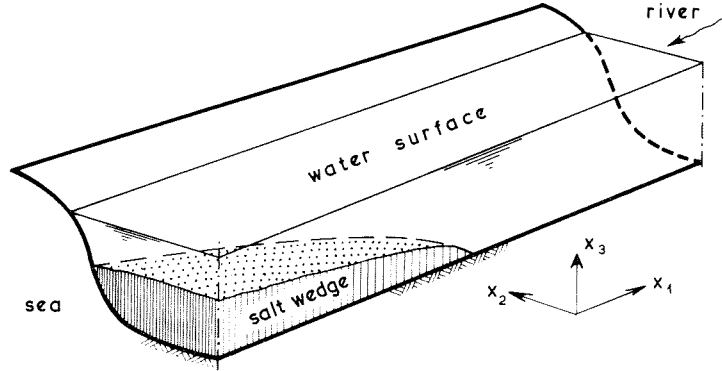


Fig. 1. Coordinates.

The summation-convention is used, i.e. if in one term a letter subscript is repeated, this term should be summed over all possible values of the subscript.

Salinity is defined as the mass of dissolved salt per unit-mass of sea-water (a more precise definition is given by Wooster c.s. 1969). The mass of salt per unit volume can be expressed by  $\varrho S$ . The equation of continuity for dissolved salt now reads

$$\frac{\partial}{\partial t}(\varrho S) + \frac{\partial}{\partial x_j}(\varrho S v_j) - D_s = 0 \quad (2.1.2)$$

where  $D_s$  denotes the molecular diffusion term. Combining eqs. (2.1.1) and (2.1.2) one finds

$$\frac{\partial S}{\partial t} + v_j \frac{\partial S}{\partial x_j} + \theta \frac{S}{\varrho} \frac{\partial^2 \varrho}{\partial x_j \partial x_j} - \frac{1}{\varrho} D_s = 0 \quad (2.1.3)$$

which means that the salinity of a fluid element remains constant except for diffusive effects. Now for simplicity temperature is assumed to be constant. This is not essential, as the influence of temperature can be treated in the same way as that of salinity. With the assumption, density is a function of salinity and pressure only, so

$$\frac{\partial \varrho}{\partial t} + v_j \frac{\partial \varrho}{\partial x_j} = \frac{\partial \varrho}{\partial S} \left( \frac{\partial S}{\partial t} + v_j \frac{\partial S}{\partial x_j} \right) + \frac{\partial \varrho}{\partial p} \left( \frac{\partial p}{\partial t} + v_j \frac{\partial p}{\partial x_j} \right)$$

Introducing this into (2.1.1) together with (2.1.3) one derives

$$\frac{\partial v_j}{\partial x_j} = -\frac{1}{\varrho} \frac{\partial \varrho}{\partial p} \left( \frac{\partial p}{\partial t} + v_j \frac{\partial p}{\partial x_j} \right) - \varrho^{-2} D_s \frac{\partial \varrho}{\partial S} + \theta \varrho^{-1} \left( 1 + \frac{S}{\varrho} \frac{\partial \varrho}{\partial S} \right) \frac{\partial^2 \varrho}{\partial x_j \partial x_j} \quad (2.1.4)$$

The first term on the right-hand side represents the effect of compressibility. With respect to the tidal phenomena to be considered, compressible or acoustic effects are not important, as they take place on a very much smaller time-scale. The other terms denote effects of molecular diffusion. For the turbulent flow considered, the molecular diffusion in this respect is unimportant. This means that both members of eq. (2.1.4) vanish:

$$\frac{\partial v_j}{\partial x_j} = 0 \quad (2.1.5)$$

This equation is to be used in connection with eq. (2.1.1) as an independent equation. From the two equations it is derived that

$$\frac{\partial \varrho}{\partial t} + v_j \frac{\partial \varrho}{\partial x_j} = 0$$

i.e. the density of a fluid element is conserved. The preceding argument shows that this property is a consequence of the conservation of dissolved salt and the neglect of compressibility and diffusion.

The equations of motion for a non-homogeneous fluid read (e.g. Oswatitsch 1959):

$$\frac{\partial}{\partial t}(\varrho v_k) + \frac{\partial}{\partial x_j}(\varrho v_k v_j) + \frac{\partial p}{\partial x_k} + \varrho g \delta_{k3} - \varrho \nu \frac{\partial^2 v_k}{\partial x_j \partial x_j} = 0 \quad k = 1, 2, 3 \quad (2.1.6)$$

where  $g$  = acceleration of gravity  
 $\nu$  = kinematic viscosity coefficient  
 $\delta_{kj}$  = Kronecker-delta (= 1 if  $k = j$ , else 0)

In this equation the geostrophic acceleration is left out, which implies that the investigation is limited to relatively narrow estuaries, where no lateral circulation exists.

## 2.2 Effects of turbulence

To separate the turbulent fluctuations from the tidal ones, a moving time-average is applied, denoted by a bar over a symbol:

$$v_j = \bar{v}_j + v'_j$$

Here the prime denotes the deviation from the average. For details of the process cf. e.g. Hinze (1959). The averaging interval should be so large that turbulent fluctuations vanish. On the other hand it should be so small that tidal variations are retained. This procedure is not free from theoretical difficulties (Lumley and Panofsky 1964, Okubo 1964). It supposes that the spectrum of the quantity under consideration shows a gap between the tidal and turbulent frequencies. This may be doubtful, due among other factors to the occurrence of internal waves. However, when dealing with measurements, there does not seem to be an alternative to the time-averaging process.

Applying this procedure to eqs. (2.1.1), (2.1.5) and (2.1.6) one obtains

$$\frac{\partial \bar{q}}{\partial t} + \frac{\partial}{\partial x_j} (\bar{q} \bar{v}_j + \overline{q' v'_j}) - \theta \frac{\partial^2 \bar{q}}{\partial x_j \partial x_j} = 0 \quad (2.2.1)$$

$$\frac{\partial \bar{v}_j}{\partial x_j} = 0 \quad (2.2.2)$$

$$\frac{\partial}{\partial t} (\bar{q} \bar{v}_k) + \frac{\partial}{\partial x_j} (\bar{q} \bar{v}_k \bar{v}_j + \overline{q' v'_k v'_j}) + \frac{\partial \bar{p}}{\partial x_k} + \bar{q} g \delta_{k3} - \bar{q} \nu \frac{\partial^2 \bar{v}_k}{\partial x_j \partial x_j} = 0 \quad (k = 1, 2, 3) \quad (2.2.3)$$

In the latter equation the Boussinesq-approximation (Boussinesq 1903) has been applied, which states that in the equation of motion variations of the density may be neglected except in the gravity-term (this exception is of importance in the derivation of the energy-equations (Appendix 2)). In this way a number of additional terms are suppressed, describing correlations between density and velocity fluctuations. The approximation is not necessary at this stage, but it considerably simplifies the equations.

## 2.3 Approximations

Some of the terms in eqs. (2.2.1) to (2.2.3) may be neglected. In this section their order of magnitude is estimated. Some of the neglects are applied only after the integration-process which is described in the following Chapter. The estimates are based on the fact that the equations are to be applied to a shallow and relatively narrow estuary. This means that the longitudinal length scale  $L$  is much larger than the vertical and lateral ones  $h$  and  $b$ . If a characteristic longitudinal velocity is called  $U$ , the vertical and lateral velocities will be of the order  $hU/L$  and  $bU/L$  from considerations of

continuity (eq. (2.2.2)). The relative intensity of turbulence is called  $r$ , defined by

$$\overline{v_j'^2} \sim r^2 U^2$$

It is assumed to have the same order of magnitude in all directions. Disregarding a coefficient of correlation, which is smaller than unity, it follows that also terms like  $\overline{v_k' v_j'}$  are of the order  $r^2 U^2$ . The time-scale which is related to the tidal period, is called  $T$ . It is not independent of the preceding scales and it will be of the order  $L/U$ .

First the equation of vertical motion is investigated. In the turbulent and viscous stress terms (third and last in eq. (2.2.3)) the vertical derivatives will dominate the others, as the stresses are comparable but the length scales rather different. The convective acceleration terms (second in the equation) are all of the same order of magnitude, as the different length scales are compensated by the magnitude of the velocities. The relative order of magnitude of the six terms in eq. (2.2.3) ( $k = 3$ ) now becomes

$$\left(\frac{h}{L}\right)^2 \frac{U^2}{gh}, \left(\frac{h}{L}\right)^2 \frac{U^2}{gh}, r^2 \frac{U^2}{gh}, (1), 1, \frac{h}{L} \frac{U^2}{gh} \frac{v}{Uh}$$

The order of magnitude of the pressure-term is between parentheses because it is derived below. The parameter  $h/L$  and the Froude number  $U(gh)^{-\frac{1}{2}}$  are small and the Reynolds number  $Re = Uh/\nu$  is large ( $\sim 10^6$ ), so all terms are negligible as compared to the gravity-term  $\bar{\rho}g$ . Only the pressure-term remains to balance the gravity-term. It follows that the pressure distribution is quasi-hydrostatic:

$$\frac{\partial \bar{p}}{\partial x_3} = -\bar{\rho}g \quad (2.3.1)$$

As the pressure vanishes at the free surface  $x_3 = h_s$ , the pressure can be written as

$$\bar{p} = g \int_{x_3}^{h_s} \bar{\rho} dx_3 \quad (2.3.2)$$

In the equation of longitudinal motion ( $k = 1$ ) the pressure-gradient  $\partial \bar{p} / \partial x_1$  plays a part. From (2.3.2) it is found to consist of two terms:

$$\frac{\partial \bar{p}}{\partial x_1} = g \int_{x_3}^{h_s} \frac{\partial \bar{\rho}}{\partial x_1} dx_3 + g \bar{\rho}_s \frac{\partial h_s}{\partial x_1}$$

where  $\bar{\rho}_s$  is the density at the surface. The first term in the right-hand member is of the order  $gh\Delta\rho/L$ , where  $\Delta\rho$  is a characteristic density difference (e.g. between pure sea and fresh water). To this term the normal turbulent stress-gradient  $\partial/\partial x_1(\bar{\rho} \overline{v_1'^2})$  is compared. The ratio is of the order

$$r^2 U^2 \left( gh \frac{\Delta\rho}{\bar{\rho}} \right)^{-1} = r^2 F_i^2$$

Here the internal Froude number  $F_i$  will not be very much larger than unity; moreover,  $r \sim 0.1$ , so the turbulent term may be neglected as a first approximation. This is much less convincing than in the case of homogeneous flow. The ratio between the main components of the viscous and turbulent stress terms is

$$\bar{q}v \frac{\partial^2 \bar{v}_1}{\partial x_3^2} \bigg/ \frac{\partial}{\partial x_3} (\bar{q} \overline{v'_1 v'_3}) \sim r^{-2} Re^{-1}$$

As the Reynolds-number is much larger than  $r^{-2}$ , the viscous terms may be neglected.

Finally, in the equation of continuity (2.2.1) the ratio of the three turbulent terms is determined mainly by the length scales, so that at least the longitudinal one  $\partial/\partial x_1 (\overline{\varrho' v'_1})$  may be neglected. The ratio of the main molecular and turbulent terms is (again disregarding a coefficient of correlation)

$$\theta \frac{\partial^2 \bar{q}}{\partial x_3^2} \bigg/ \frac{\partial}{\partial x_3} (\overline{\varrho' v'_3}) \sim (\gamma r Re)^{-1} \theta/\nu$$

where  $\gamma^2 \Delta \varrho^2 = \overline{\varrho'^2}$ . As  $\nu/\theta \gg 1$  for water, and  $Re$  is large, the molecular terms again turn out to be negligible.

## TWO-LAYER MODEL

## 3.1 General

The system of differential equations, derived in Chapter 2 is incomplete, as a specification of the turbulent terms is still missing. However, before going more deeply into this question, it is noted that the equations are too complicated to warrant a direct solution. Some schematization is necessary and permitted from the point of view of the applications. In this section a choice is made for the simplest schematization, still showing the main features of interest (cf. Chapter 1). For many purposes the tidal fluctuations are essential, so a further time-averaging process is not allowable. The remaining possibility is some schematization of the profiles in a cross-section of the estuary.

Any schematization of this kind can be characterized by the number of parameters involved (fig. 2). The first method is to characterize the situation at a cross-section by three quantities: the water level  $h_s$ , the mean velocity  $\langle \bar{u} \rangle$  and the mean density  $\langle \bar{\rho} \rangle$ . The symbol  $\langle \rangle$  is used to denote a cross-sectional mean value. This "one-dimensional model" has been applied by Stigter and Siemons (1967). It gives quite useful results as far as the longitudinal salt-distribution is concerned. However it does not give any information about the distribution of the velocity and salinity in a cross-section.

A schematization using four parameters can be constructed in several ways. One is the two-layer model without exchange between the layers. The densities (salinities) of the layers being fixed to those of pure sea and river water, the four parameters are the water level  $h_s$ , the level of the interface  $h_i$ , and the mean velocities  $u_1$  and  $u_2$  in each layer. This model has been proposed by Schijf and Schönfeld (1953). Applications have been described by Boulot, Braconnot and Marvaud (1967), Boulot and Daubert (1969) and the present author (1970).

A model with six parameters is obtained if the exchange of water and salt through the interface is included in the two-layer model. The additional parameters are the mean densities  $\rho_1$  and  $\rho_2$  in each layer.

Similar models can be constructed, using ever more parameters to describe each cross-section. Although this permits more detail, it should be stressed that the more detailed models also meet more difficulties in formulating boundary conditions and specifying empirical parameters. This is demonstrated in the present study for the two-layer models with and without interfacial mixing. Therefore for the time being no more detailed schematizations are discussed.

A general method to derive equations for a schematized situation is the method of integral relations (e.g. Dorodnitsyn 1964). The differential equations are multiplied by a weight function and integrated over the cross-section. This is repeated with a

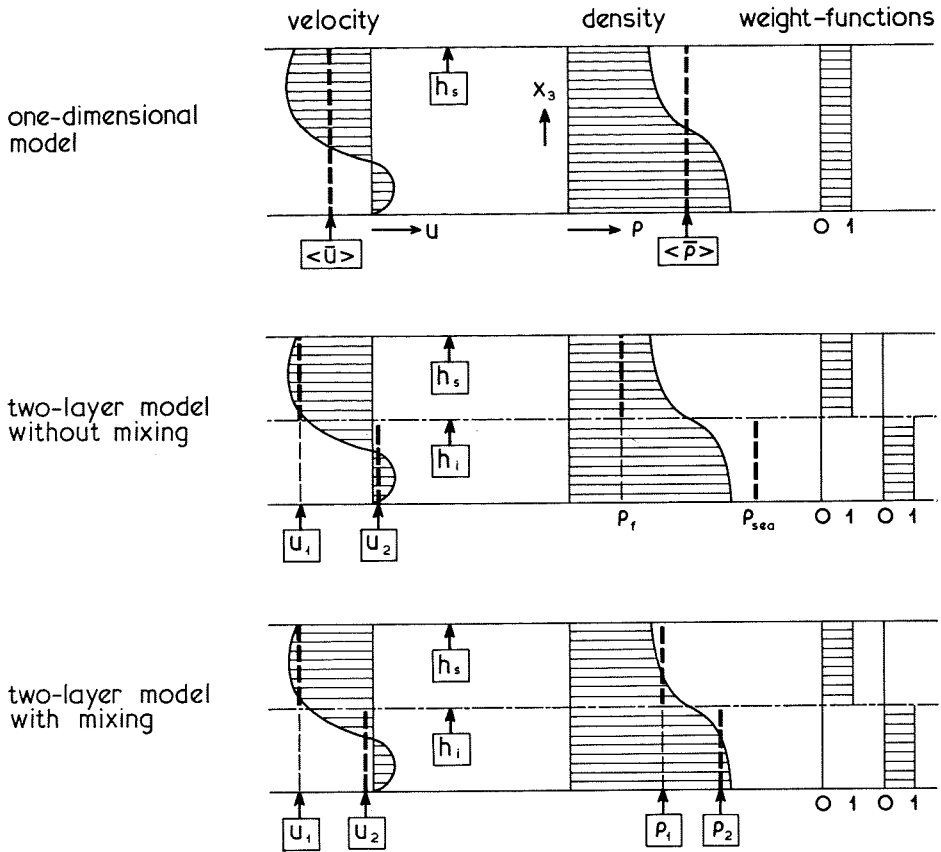


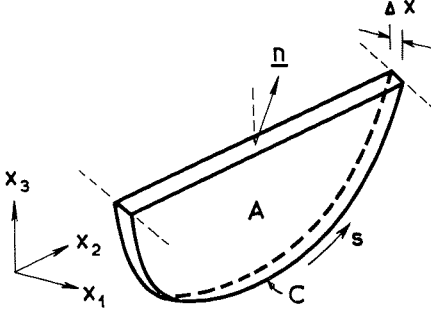
Fig. 2. Schematizations (parameters in boxes).

number of independent weight functions such that a sufficient number of equations is obtained to determine the parameters characterizing the profiles. The weight functions are indicated in fig. 2. For the two-layer model they are block functions, equalling unity in one layer and vanishing in the other. This is shown in detail in the following section. From this description it is seen that such a schematization can be applied to any case, not only when the physical situation clearly shows a two-layer structure (salt-wedge type). Of course not all situations are represented equally well by a two-layer model. However, in this study the two-layer model is found to be very well applicable to a partly mixed estuary.

### 3.2 Integration

To obtain the two-layer model, eqs. (2.2.1), (2.2.2) and (2.2.3) for  $k = 1$  are multiplied by a weight function and integrated over the cross-sectional area. The weight-functions are such that the integration is limited to either the upper or the lower layer.

Fig. 3. Integration over a cross-section.



The level of the interface  $h_i$  is discussed in section 3.4. For the time being it is only assumed not to be inclined laterally. The same assumption is made for the water-level  $h_s$ .

By considering a cross-sectional slice of infinitesimal thickness (fig. 3), one derives the following relations by means of the Gauss-theorem:

$$\iint_A \frac{\partial f_j}{\partial x_j} dA = \frac{\partial}{\partial x_1} \iint_A f_1 dA + \int_C f_j \frac{n_j}{\sqrt{1-n_1^2}} ds \quad (3.2.1)$$

$$\iint_A \frac{\partial f}{\partial x_1} dA = \frac{\partial}{\partial x_1} \iint_A f dA + \int_C f \frac{n_1}{\sqrt{1-n_1^2}} ds \quad (3.2.2)$$

Also

$$\iint_A \frac{\partial f}{\partial t} dA = \frac{\partial}{\partial t} \iint_A f dA - \int_C f \left( n_2 \frac{dX_2}{dt} + n_3 \frac{dX_3}{dt} \right) / \sqrt{1-n_1^2} ds \quad (3.2.3)$$

where  $C$  is the contour of the slice,  $X_j(t)$  are its coordinates as a function of time and  $n_j$  is the outward unit normal vector on the circumferential boundary of the slice. The sense of the contour integration is clockwise with respect to the  $x_1$ -axis. In all these formulae, the reduced normal vector  $n_j^* = n_j / \sqrt{1-n_1^2}$  plays a part. For the interface (i) and the surface (s) these read:

$$n_{ij}^* = \left( -\frac{\partial h_i}{\partial x_1}, 0, 1 \right)$$

$$n_{sj}^* = \left( -\frac{\partial h_s}{\partial x_1}, 0, 1 \right)$$

Integrating eq. (2.2.2) over the lower layer and applying (3.2.1) one finds

$$\int_i \bar{v}_j n_{ij}^* ds + \int_b \bar{v}_j n_{bj}^* ds + \frac{\partial}{\partial x_1} \iint_{A_2} \bar{v}_1 dA = 0$$

where  $A_2$  denotes the cross-sectional area below the interface (fig. 4). Now the bottom is assumed to be impermeable, so

$$\bar{v}_j n_{bj}^* = 0 \quad \text{at the bottom} \quad (3.2.4)$$

At the interface, the vertical velocity  $W_i$  relative to it is defined by

$$\frac{\partial h_i}{\partial t} - \bar{v}_j n_{ij}^* = -W_i \quad (3.2.5)$$

With these conditions, the integrated equation becomes

$$b_i \frac{\partial h_i}{\partial t} + \frac{\partial}{\partial x_1} (A_2 u_2) + b_i w_i = 0 \quad (3.2.6)$$

Here  $b_i$  is the width of the interface; further by definition

$$u_2 = A_2^{-1} \iint_{A_2} \bar{v}_1 dA \quad \text{mean velocity in the lower layer}$$

$$w_i = b_i^{-1} \int_i W_i ds$$

The same procedure is applied to the equation of mass-continuity (2.2.1). This gives

$$\begin{aligned} & \frac{\partial}{\partial t} \iint_{A_2} \bar{\rho} dA - \frac{\partial h_i}{\partial t} \int_i \bar{\rho} ds + \frac{\partial}{\partial x_1} \iint_{A_2} (\bar{\rho} \bar{v}_1 + \overline{\rho' v'_1}) dA + \\ & + \int_i \bar{\rho} \bar{v}_j n_{ij}^* ds + \int_i \overline{\rho' v'_j} n_{ij}^* ds + \int_b \bar{\rho} \bar{v}_j n_{bj}^* ds + \int_b \overline{\rho' v'_j} n_{bj}^* ds = 0 \end{aligned}$$

The latter two terms, representing the net water-flux and the turbulent mass-flux normal to the bottom, vanish because of the impermeability. Applying eq. (3.2.5) one finds

$$\frac{\partial}{\partial t} (\rho_2 A_2) + \frac{\partial}{\partial x_1} (\rho_2 A_2 u_2 + F_2) + b_i f_i + w_i \rho_i b_i = 0 \quad (3.2.7)$$

where

$$\rho_2 = A_2^{-1} \iint_{A_2} \bar{\rho} dA \quad \text{mean density in the lower layer}$$

$$F_2 = \iint_{A_2} (\bar{\rho} \bar{v}_1 - \rho_2 u_2 + \overline{\rho' v'_1}) dA$$

$$f_i = b_i^{-1} \int_i \overline{\rho' v'_j} n_{ij}^* ds$$

$$\rho_i = w_i^{-1} b_i^{-1} \int_i \bar{\rho} W_i ds$$

(the subscript  $i$  is not subject to the summation-convention).

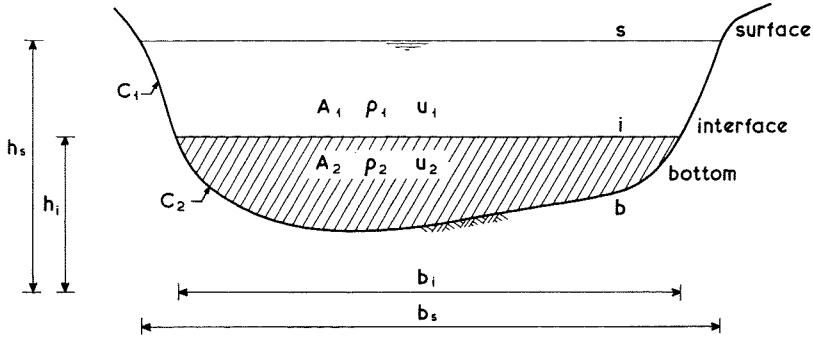


Fig. 4. Cross-section in a two-layer system.

The quantity  $F_2$  is the mass-flux through the area  $A_2$  per unit time, apart from convection by the mean flow. In section 2.3 it has been shown that the term  $\overline{\varrho'v_1'}$  is not important. The remaining part is the mass-flux by dispersion, due to the non-uniform distributions of the density  $\bar{\varrho}$  and the velocity  $\bar{v}_1$ .

The quantity  $f_i$  is the turbulent mass flux through the interface per unit area. Its main part is  $\overline{\varrho'v_3'}$ . In case of a stable stratification upward velocities generally will be accompanied by positive density differences, so  $f_i$  will be positive. The term  $w_i \varrho_i b_i$  represents the convective flux through the interface.

Finally, the integration process is applied to the equation of motion in longitudinal direction (2.2.3 with  $k = 1$ ). This results in

$$\begin{aligned} & \frac{\partial}{\partial t} \iint_{A_2} \bar{\varrho} \bar{v}_1 dA - \frac{\partial h_i}{\partial t} \int_i \bar{\varrho} \bar{v}_1 ds + \frac{\partial}{\partial x_1} \iint_{A_2} (\bar{\varrho} \bar{v}_1^2 + \bar{\varrho} \overline{v_1'^2}) dA + \\ & + \int_i \bar{\varrho} \bar{v}_1 \bar{v}_j n_{ij}^* ds + \int_i \bar{\varrho} \overline{v_1' v_j'} n_{ij}^* ds + \int_b \bar{\varrho} \overline{v_1' v_j'} n_{bj}^* ds + \\ & + \int_b \bar{\varrho} \bar{v}_1 \bar{v}_j n_{bj}^* ds + \frac{\partial}{\partial x_1} \iint_{A_2} \bar{p} dA + \int_i \bar{p} n_{i1}^* ds + \int_b \bar{p} n_{b1}^* ds = 0 \end{aligned}$$

This can be written as

$$\begin{aligned} & \frac{\partial}{\partial t} (\varrho_2 A_2 u_2) + \frac{\partial}{\partial x_1} (\varrho_2 A_2 u_2^2) - \tau_i b_i + \tau_b C_2 + w_i \varrho_i u_i b_i + \\ & + \frac{\partial}{\partial x_1} \iint_{A_2} \bar{p} dA + \int_i \bar{p} n_{i1}^* ds + \int_b \bar{p} n_{b1}^* ds = 0 \end{aligned} \quad (3.2.8)$$

with the definitions

$$\tau_i = -b_i^{-1} \int_i \bar{\varrho} \overline{v_1' v_j'} n_{ij}^* ds \quad \text{interfacial shear stress}$$

$$\tau_b = +C_2^{-1} \int_b \bar{\varrho} \bar{v}_1' v_j' n_{bj}^* ds \quad \text{bottom shear stress}$$

$C_2 =$  wetted perimeter of lower layer (interface excluded)

$$u_i = (w_i \varrho_i b_i)^{-1} \int_i \bar{\varrho} \bar{v}_1 W_i ds$$

The different signs in the definitions of the shear stresses are caused by the different positive directions illustrated in fig. 5.

In eq. (3.2.8) the term with  $\bar{\varrho} \bar{v}_1'^2$  has been neglected in accordance with section 2.3. In addition, some approximation has been introduced in the acceleration terms, viz.

$$\iint_{A_2} \bar{\varrho} \bar{v}_1 dA \simeq \varrho_2 A_2 u_2, \quad \iint_{A_2} \bar{\varrho} \bar{v}_1^2 dA \simeq \varrho_2 A_2 u_2^2$$

The former is again the Boussinesq-approximation.

In the same way equations for the upper layer can be derived. Assuming the pressure and the turbulent stresses to vanish at the surface, one obtains:

$$b_s \frac{\partial h_s}{\partial t} - b_i \frac{\partial h_i}{\partial t} + \frac{\partial}{\partial x_1} (A_1 u_1) - b_i w_i = 0 \quad (3.2.9)$$

$$\frac{\partial}{\partial t} (\varrho_1 A_1) + \frac{\partial}{\partial x_1} (\varrho_1 A_1 u_1 + F_1) - b_i f_i - w_i \varrho_i b_i = 0 \quad (3.2.10)$$

$$\begin{aligned} & \frac{\partial}{\partial t} (\varrho_1 A_1 u_1) + \frac{\partial}{\partial x_1} (\varrho_1 A_1 u_1^2) + \tau_i b_i + \tau_w C_1 - w_i \varrho_i u_i b_i + \\ & + \frac{\partial}{\partial x_1} \iint_{A_1} \bar{p} dA - \int_i \bar{p} n_{i1}^* ds = 0 \end{aligned} \quad (3.2.11)$$

where  $\tau_w$  is the shear stress at the solid boundary and  $C_1$  the corresponding wetted perimeter. The last term of eq. (3.2.11) bears a negative sign, because the same (upward) normal vector as before has been applied.

For any distribution of the density, the pressure-terms in eqs. (3.2.8) and (3.2.11) can be evaluated, using the hydrostatic pressure-distribution (2.3.1).

The dispersive terms  $F_1$  and  $F_2$  in eqs. (3.2.10) and (3.2.7) are to be compared to the terms representing the convective salt flux,  $\varrho_1 A_1 u_1$  and  $\varrho_2 A_2 u_2$  respectively. The density-difference  $\varrho_{1,2} - \varrho_f$  has been denoted by  $\Delta \varrho_{1,2}$ ,  $\varrho_f$  being the density of fresh water. It is difficult to make this comparison for a general case. In Appendix 4 the dispersive terms for a specific case are found to be unimportant. In the present study they are neglected. If for other estuaries these terms are important, empirical expressions have to be introduced.

### 3.3 Rectangular channel

The equations (3.2.6) to (3.2.11) within the assumptions are still general with respect to the shape of the cross-section, provided it is not so wide as to show a significant lateral circulation. For a given shape, approximations may be made to relate the pressure-terms to the layer thickness and the mean densities. The simplest assumption is lateral uniformity of the density-distribution. In the present study, the additional, not necessary, assumption is made that the cross-section is rectangular.

With these assumptions, the pressure-terms in the equation of motion for the upper layer (3.2.11), after division by the (constant) width  $b$ , become

$$\begin{aligned}
 & \frac{\partial}{\partial x_1} \int_{h_i}^{h_s} \bar{p} dx_3 + \bar{p}_i \frac{\partial h_i}{\partial x_1} = \\
 & = \frac{\partial}{\partial x_1} \int_{h_i}^{h_s} g \bar{q}(x_3 - h_i) dx_3 + g \frac{\partial h_i}{\partial x_1} \int_{h_i}^{h_s} \bar{q} dx_3 = \\
 & = \frac{\partial}{\partial x_1} \left\{ \frac{1}{2} g \varrho_1 a_1^2 + g \int_{h_i}^{h_s} (x_3 - h_i) (\bar{q} - \varrho_1) dx_3 \right\} + g \varrho_1 a_1 \frac{\partial h_i}{\partial x_1} \quad (3.3.1)
 \end{aligned}$$

where  $a_1$  is the thickness of the upper layer.

Similarly for the lower layer (eq. (3.2.8)):

$$\begin{aligned}
 & \frac{\partial}{\partial x_1} \int_{h_b}^{h_i} \bar{p} dx_3 - \bar{p}_i \frac{\partial h_i}{\partial x_1} + \bar{p}_b \frac{\partial h_b}{\partial x_1} = \\
 & = \frac{\partial}{\partial x_1} \left\{ a_2 \bar{p}_i + g \int_{h_b}^{h_i} (x_3 - h_b) \bar{q} dx_3 \right\} - g \varrho_1 a_1 \frac{\partial h_i}{\partial x_1} + g (\varrho_1 a_1 + \varrho_2 a_2) \frac{\partial h_b}{\partial x_1} = \\
 & = \frac{\partial}{\partial x_1} \left\{ g \varrho_1 a_1 a_2 + \frac{1}{2} g \varrho_2 a_2^2 + g \int_{h_b}^{h_i} (x_3 - h_b) (\bar{q} - \varrho_2) dx_3 \right\} + \\
 & - g \varrho_1 a_1 \frac{\partial h_i}{\partial x_1} - g (\varrho_1 a_1 + \varrho_2 a_2) I \quad (3.3.2)
 \end{aligned}$$

where  $h_b$  is the bottom-level,  $a_2$  is the thickness of the lower layer and  $I$  is the bottom slope (positive if the bottom slopes downward in  $x_1$ -direction). Usually, the integrals in the right-hand members of (3.3.1) and (3.3.2) are neglected. In the method of integral relations, however, one would introduce an expression for the density profiles in terms of the characteristic parameters, after which the integration could be carried out. This method works well if a reasonable density profile can be specified, which is possible if a large number of layers is used. In the present case, only two layers are discerned. If the mixing between the layers is not taken into account, the densities  $\varrho_1$  and  $\varrho_2$  are fixed (see the next section) and only the levels of the surface and the interface are left to describe the profile. This is hardly possible as the latter

only can serve to define a mean density over the water depth, but not the shape of the profile. So the integral cannot be approximated. If, on the other hand, the mixing is included, a useful though complicated expression for the profile can be derived (section 4.3). However, in this case both integrals are rather unimportant with respect to the other terms in (3.3.1) and (3.3.2), as shown in Appendix 4.

In that section, the integral terms are compared to other important terms in eqs. (3.3.1) and (3.3.2). For the upper layer (eq. (3.3.1)) the main term is  $\varrho_1 g \partial h / \partial x$ , as follows from the behaviour of the mathematical model, especially from the characteristic velocities. Due to the relatively small density differences involved in the integral, it is quite small compared to this dominating term. For the lower layer, however, the term

$$\frac{\partial}{\partial x_1} \{ \frac{1}{2} g (\varrho_2 - \varrho_1) a_2^2 \}$$

is important. The integral in eq. (3.3.2) may amount to 20% of the value of the dominating term if the model without mixing is considered. For the case with mixing, the ratio is less than 5%.

It must be concluded that for the model with mixing a proper estimate of the integral can be made, but is not necessary. For the model without mixing it would be desired, but it is not possible. Yet in the latter case the integral is not of decisive importance. Therefore in both cases it is neglected.

The equations (3.2.6) ... (3.2.11) can now be specialized to the case of a rectangular cross-section.

$$\frac{\partial}{\partial t} (\varrho_1 a_1) + \frac{\partial}{\partial x} (\varrho_1 a_1 u_1) - f_i - \varrho_i w_i = 0 \quad (3.3.3)$$

$$\frac{\partial}{\partial t} (\varrho_2 a_2) + \frac{\partial}{\partial x} (\varrho_2 a_2 u_2) + f_i + \varrho_i w_i = 0 \quad (3.3.4)$$

$$\frac{\partial a_1}{\partial t} + \frac{\partial}{\partial x} (a_1 u_1) - w_i = 0 \quad (3.3.5)$$

$$\frac{\partial a_2}{\partial t} + \frac{\partial}{\partial x} (a_2 u_2) + w_i = 0 \quad (3.3.6)$$

$$\frac{\partial}{\partial t} (\varrho_1 a_1 u_1) + \frac{\partial}{\partial x} (\varrho_1 a_1 u_1^2 + \frac{1}{2} g \varrho_1 a_1^2) + g \varrho_1 a_1 \frac{\partial a_2}{\partial x} - g \varrho_1 a_1 I + \tau_i - w_i \varrho_i u_i = 0 \quad (3.3.7)$$

$$\begin{aligned} \frac{\partial}{\partial t} (\varrho_2 a_2 u_2) + \frac{\partial}{\partial x} (\varrho_2 a_2 u_2^2 + \frac{1}{2} g \varrho_2 a_2^2 + g \varrho_1 a_1 a_2) - g \varrho_1 a_1 \frac{\partial a_2}{\partial x} + \\ - g \varrho_2 a_2 I + \tau_b - \tau_i + w_i \varrho_i u_i = 0 \end{aligned} \quad (3.3.8)$$

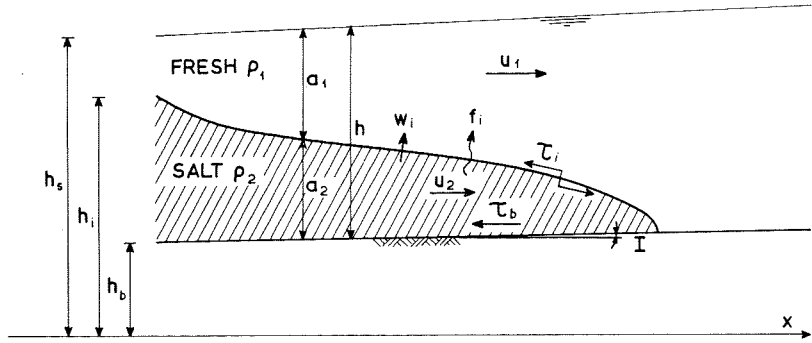


Fig. 5. Two-layer system in rectangular channel.

Here the subscript on  $x_1$  has been dropped. For convenience the notation is summarized in fig. 5. The friction at the vertical boundaries has been neglected with respect to the bottom and interfacial friction.

As a further simplification, it might be assumed that the exchange of salt and water between the layers is not important. This amounts to  $f_i = 0$  and  $w_i = 0$ . From eqs. (3.3.3) to (3.3.6) it then follows that  $\rho_1$  and  $\rho_2$  must be constants, equal to the densities of fresh water and sea water respectively. In this case the remaining four equations read

$$\frac{\partial a_1}{\partial t} + \frac{\partial}{\partial x}(a_1 u_1) = 0 \quad (3.3.9)$$

$$\frac{\partial a_2}{\partial t} + \frac{\partial}{\partial x}(a_2 u_2) = 0 \quad (3.3.10)$$

$$\frac{\partial}{\partial t}(a_1 u_1) + \frac{\partial}{\partial x}(a_1 u_1^2) + g a_1 \frac{\partial h}{\partial x} - g a_1 I + \tau_i / \rho_1 = 0 \quad (3.3.11)$$

$$\frac{\partial}{\partial t}(a_2 u_2) + \frac{\partial}{\partial x}(a_2 u_2^2) + (1 - \varepsilon) g a_2 \frac{\partial h}{\partial x} + \varepsilon g a_2 \frac{\partial a_2}{\partial x} - g a_2 I + (\tau_b - \tau_i) / \rho_2 = 0 \quad (3.3.12)$$

where  $h = a_1 + a_2$  is the total depth and the relative density difference  $(\rho_2 - \rho_1) / \rho_2$  has been denoted by  $\varepsilon$ . This system of equations is identical with that given by Schijf and Schönfeld (1953). In the terminology of section 3.1, it is a four-parameter model (parameters  $h$ ,  $a_2$ ,  $u_1$  and  $u_2$ ). The more general system (3.3.3) to (3.3.8) is a six-parameter model (additional parameters  $\rho_1$  and  $\rho_2$ ).

Upstream of the salt wedge, only one layer is present. Both systems of equations degenerate to the corresponding system if

$$a_2 = 0, \quad u_2 = u_1, \quad f_i = 0, \quad w_i = 0, \quad \tau_b = \tau_i \quad (3.3.13)$$

Then eqs. (3.3.4), (3.3.6), (3.3.8), (3.3.10) and (3.3.12) are satisfied identically. Further  $\rho_1$  must be a constant. The remaining equations are those for a single layer of homogeneous water. The latter relation of (3.3.13) physically means that the bottom friction is transferred to the interface through the vanishing lower layer. The relation  $u_2 = u_1$  is derived from the approximate dynamical equation (6.3.20), valid for the internal waves.

Similarly, the situation may occur that the upper layer vanishes. This case is treated by

$$a_1 = 0, \quad u_1 = u_2, \quad f_i = 0, \quad w_i = 0, \quad \tau_i = 0 \quad (3.3.14)$$

Then eqs. (3.3.3), (3.3.5), (3.3.7), (3.3.9) and (3.3.11) are satisfied. The remaining equations are those for a single layer of water. The zero shear stress at the surface is maintained in the vanishing surface layer.

### 3.4 Definition of the interface

So far, the derivation has been independent of the definition of the interface, except for the assumption that it is not inclined laterally. In literature no definition is found for the case of a partly mixed estuary as considered here. Generally, a definition of the interface is subject to the following requirements:

- It should be consistent with whatever physical separation there might be between the layers.
- It should be applicable to measurements, done on a routine basis.
- It should result in a useful mathematical model, with respect to the approximations involved.

In a highly stratified case there is not much of a problem, as all imaginable definitions will give approximately the same result. It should be noticed that the interface generally will move relative to the water particles. If the interface were impermeable (i.e.  $w_i = 0$  in eq. (3.3.6)), part of the salt wedge would consist of a constant quantity of water, travelling to and fro with the tide. However, from eq. (3.3.4) it can be concluded that the salinity would be decreasing, the turbulent flux  $f_i$  always being directed upwards. So the salinity distribution would not be in equilibrium.

A definition could be based on various physical criteria, such as the maximum density gradient, maximum velocity gradient, maximum shear stress, smallest degree of turbulence. However, there is no reason why these criteria would give the same result. Moreover, the knowledge of the turbulent flow-structure in density-stratified conditions is very limited, so it is not possible to select the most relevant one from the above criteria. Therefore a definition according to some physical criterion does not offer great advantages.

Concerning the approximations in the theoretical model, it has been mentioned that the neglect of the pressure-deviations in eq. (3.3.2) may be important (Appen-

dix 4). These deviations being determined by the density profile, the interface can be chosen so as to minimize the difference between the actual and the schematized density profiles. If this is done in least-squares sense:

$$\int_{h_b}^{h_i} (\bar{\varrho} - \varrho_2)^2 dx_3 + \int_{h_i}^{h_s} (\bar{\varrho} - \varrho_1)^2 dx_3 \quad \text{minimal}$$

one finds

$$2\varrho_i = \varrho_1 + \varrho_2 \quad (3.4.1)$$

where for simplicity the variations in lateral direction have been neglected. As  $\varrho_1$  and  $\varrho_2$  must be mean densities, only one degree of freedom is left and eq. (3.4.1) is an implicit equation for the level of the interface  $h_i$ . This definition is well applicable to experimental data, as only the density profile is required.

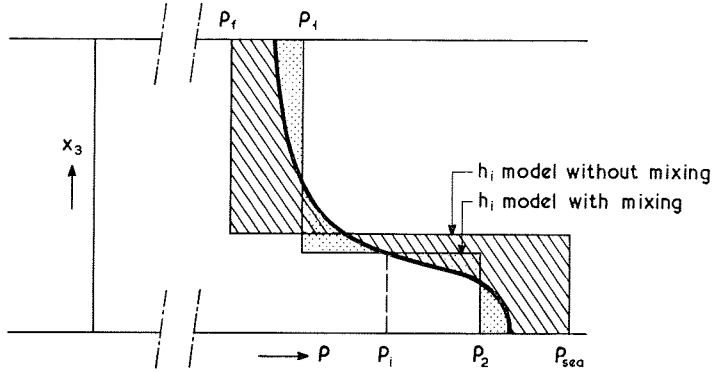


Fig. 6. Definition of the interface.

If the exchange between the layers is neglected (eqs. (3.3.9) to (3.3.12)) the values of  $\varrho_1$  and  $\varrho_2$  are fixed and for the remaining parameter  $h_i$  the definition (3.4.1) cannot be used, as it does not give a useful mass-balance. Adding eqs. (3.3.3) and (3.3.4) one finds the overall mass-balance equation:

$$\frac{\partial}{\partial t} (\langle \bar{\varrho} \rangle h) + \frac{\partial}{\partial x} (\varrho_1 a_1 u_1 + \varrho_2 a_2 u_2) = 0 \quad (3.4.2)$$

where  $\langle \bar{\varrho} \rangle = (\varrho_1 a_1 + \varrho_2 a_2)/h$  is the cross-sectional mean density, assuming that  $\varrho_1$  and  $\varrho_2$  are the mean densities in each layer. This is the case for the model with mixing. In the model without mixing, the values of  $\varrho_1$  and  $\varrho_2$  are replaced by the fresh-water density  $\varrho_f$  and the sea-water density  $\varrho_{sea}$ . The first term of eq. (3.4.2) then does not represent the rate of change of the mass per unit length, unless

$$\varrho_f a_1 + \varrho_{\text{sea}} a_2 = \langle \bar{\varrho} \rangle h$$

or

$$a_2 = h \frac{\langle \bar{\varrho} \rangle - \varrho_f}{\varrho_{\text{sea}} - \varrho_f} \quad (3.4.3)$$

As shown in Appendix 4 this causes the pressure-terms to be considerably less accurate than when (3.4.1) is used. This is one of the main drawbacks of the model without exchange.

The definitions (3.4.1) and (3.4.3) are illustrated in fig. 6.

## FLOW STRUCTURE

**4.1 Introduction**

The mathematical models, derived in section 3.3, are to be completed by expressions which relate the turbulent quantities  $\tau_i$ ,  $\tau_b$  and  $f_i$  and the convective velocity through the interface  $w_i$  to the local conditions. Not only this is necessary to obtain a closed system of differential equations, but some of these quantities (especially the bottom shear-stress  $\tau_b$ ) may be important in their own right.

On the other hand, it is desirable, though not necessary for the model, to have an expression for the profiles of velocity and density as a function of depth. This question is related to the concept of integral relations (section 3.1). The profiles have been characterized by a number of parameters, viz. the mean velocities  $u_1$ ,  $u_2$ , the mean densities  $\varrho_1$ ,  $\varrho_2$ , the levels of the interface and the surface  $h_i$  and  $h_s$ . Conversely, it must be possible to derive profiles from these parameters. This could be done e.g. by assuming polynomials, but in view of the small number of layers this will not be very successful. It is better to take the physical mechanism into account as far as possible.

The two problems just mentioned are treated in the following way. Given the parameters  $u_1$ ,  $u_2$ ,  $\varrho_1$ ,  $\varrho_2$ ,  $h_i$  and  $h_s$ , the vertical profiles of velocity and density are derived. From these profiles, conclusions are drawn concerning the shear-stresses  $\tau_i$  and  $\tau_b$  and the turbulent mass-flux  $f_i$ . The convective velocity  $w_i$  falls outside this scope and is treated separately in section 4.5.

The method of investigating these relations is the postulation of a mechanism of turbulent flow in the form of a mixing-length hypothesis. This can be based on the equation of turbulence energy, as discussed by several authors (Prandtl 1929, Ellison 1957, Townsend 1958, Stewart 1959).

**4.2 Mixing-length hypothesis**

Under certain restrictions the mixing-length hypothesis can be justified from the equation of turbulence energy. This is discussed more completely in Appendix 2. In the case of non-homogeneous flow a similar relation between the turbulent mass-flux and the density gradient can be derived by using the equation for the turbulent density fluctuations. The main assumption is a local equilibrium between production and dissipation of turbulence energy. The convection of energy by mean and turbulent velocities, and the time-rate of change of the kinetic energy per unit volume are neglected. This situation has been shown to exist for the region close to the wall in a boundary layer (e.g., Townsend 1956). For tidal flow in an estuary the assumption probably is not very well satisfied which indicates its value. Still, the resulting pro-

files may be of some use, as the production and dissipation terms apply to the instantaneous conditions (and not to steady flow).

The mixing-length hypothesis now can be formulated as follows:

$$\tau = \bar{\rho} l_\tau^2 \frac{\partial \bar{u}}{\partial z} \left| \frac{\partial \bar{u}}{\partial z} \right| \quad (4.2.1)$$

$$f = -l_f^2 \frac{\partial \bar{\rho}}{\partial z} \left| \frac{\partial \bar{u}}{\partial z} \right|$$

where  $\tau = -\bar{\rho} \overline{v_1' v_3'}$  turbulent shear-stress  
 $f = \overline{\rho' v_3'}$  turbulent mass-flux  
 $\bar{u} = \bar{v}_1$  mean longitudinal velocity  
 $z = x_3$  vertical coordinate  
 $l_\tau, l_f$  mixing lengths

In Appendix 2 it is shown that the mixing-lengths depend on the local Richardson number  $Ri$ . As insufficient knowledge is available on this relation, as well as on the vertical variation of the mixing length, an assumption has to be made. In steady, uniform, homogeneous flow a logarithmic velocity-profile is obtained if one assumes

$$l_\tau = \kappa z (1 - z/h)^{\frac{1}{2}} \quad (4.2.2)$$

where  $\kappa$  is Von Kármán's constant and  $h$  is the water-depth (the origin of  $z$  is taken at the bottom). In a two-layer system the main influence of the Richardson number is expected to occur near the interface. Therefore the following modification of (4.2.2) is proposed tentatively (Fig. 7).

$$l_\tau = \begin{cases} \kappa z (1 - z/h)^{\frac{1}{2}} \{1 - (1 - ah/a_2)z/a_2\} & 0 < z < a_2 \\ \kappa h (1 - z/h)^{\frac{1}{2}} \{\alpha + z/h - a_2/h\} & a_2 < z < h \end{cases} \quad (4.2.3)$$

*linear profile in the interface*

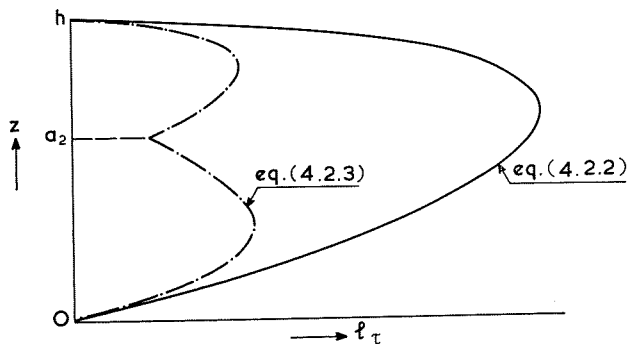


Fig. 7. Mixing length.

The parameter  $\alpha$  is to be determined empirically. For  $\alpha = a_2/h$  eq. (4.2.2) is found again.

To find a velocity profile, the variation of the shear-stress  $\tau$  still should be specified. For the case of steady, uniform flow the equation of motion (2.2.3) for  $k = 1$  reads

$$\frac{\partial \bar{p}}{\partial x_1} - \frac{\partial \tau}{\partial x_3} = 0$$

This results in a linear shear-stress profile if the densities are constant. Assuming this to approximate more general conditions too, one obtains

$$\tau = \begin{cases} \tau_b \{1 - (1 - \tau_i/\tau_b)z/a_2\} & 0 < z < a_2 \\ \tau_i(1 - z/h)(1 - a_2/h)^{-1} & a_2 < z < h \end{cases} \quad (4.2.4)$$

the values  $\tau_b$  and  $\tau_i$  at the bottom and the interface being related to the mean velocities through eqs. (3.3.7) and (3.3.8). These assumptions resemble those by Bonnefille and Goddet (1959), who found some experimental evidence.

In the equation for the turbulent mass-flux similar assumptions are made:

$$l_f = Sc^{-\frac{1}{2}} l_\tau \quad (4.2.5)$$

$$f = \begin{cases} f_i(z/a_2) & 0 < z < a_2 \\ f_i(1 - z/h)(1 - a_2/h)^{-1} & a_2 < z < h \end{cases} \quad (4.2.6)$$

where  $f_i$  is the turbulent mass-flux through the interface and  $Sc$  is the turbulent Schmidt number, defined by eq. (4.2.5) and assumed to be a constant.

Boundary conditions for the velocity and density profiles are

$$\bar{\varrho} = \varrho_b \quad \text{at} \quad z = 0$$

$$\bar{u} = 0 \quad \text{at} \quad z = z_0$$

The value  $\varrho_b$  is a parameter in the equations. The level  $z_0$  is related to the bottom-roughness. For homogeneous uniform flow one usually takes  $z_0 = k/33$ , where  $k$  is Nikuradse's equivalent sand-grain roughness.

### 4.3 Velocity and density profiles

Dimensionless variables are defined as follows

$$\begin{aligned} \eta &= z/h & U &= \kappa \bar{u}/u_* \\ \eta_2 &= a_2/h & \lambda &= l_\tau/\kappa h \\ \sigma &= \tau_i/\tau_b & s &= (\bar{\varrho} - \varrho_b)\kappa u_*/(f_i Sc) \end{aligned}$$

where  $u_* = (\tau_b/\rho)^{\frac{1}{2}}$  is the shear velocity at the bottom. The differential equations (4.2.1) then become

$$\frac{dU}{d\eta} = \begin{cases} \frac{\{1-(1-\sigma)\eta/\eta_2\}^{\frac{1}{2}}}{\eta(1-\eta)^{\frac{1}{2}}\{1-(1-\alpha/\eta_2)\eta/\eta_2\}} & 0 < \eta < \eta_2 \\ \frac{\sigma^{\frac{1}{2}}}{(1-\eta_2)^{\frac{1}{2}}(\alpha+\eta-\eta_2)} & \eta_2 < \eta < 1 \end{cases} \quad (4.3.1)$$

$$U(\eta_0) = 0$$

$$\frac{ds}{d\eta} = \begin{cases} (1-\eta)^{-\frac{1}{2}}\{1-(1-\alpha/\eta_2)\eta/\eta_2\}^{-1}\{1-(1-\sigma)\eta/\eta_2\}^{-\frac{1}{2}} & 0 < \eta < \eta_2 \\ (\alpha+\eta-\eta_2)^{-1}\{\sigma(1-\eta_2)\}^{-\frac{1}{2}} & \eta_2 < \eta < 1 \end{cases} \quad (4.3.2)$$

$$s(0) = 0$$

Mean dimensionless velocities and densities in each layer are denoted by  $U_{1,2}$  and  $s_{1,2}$ .

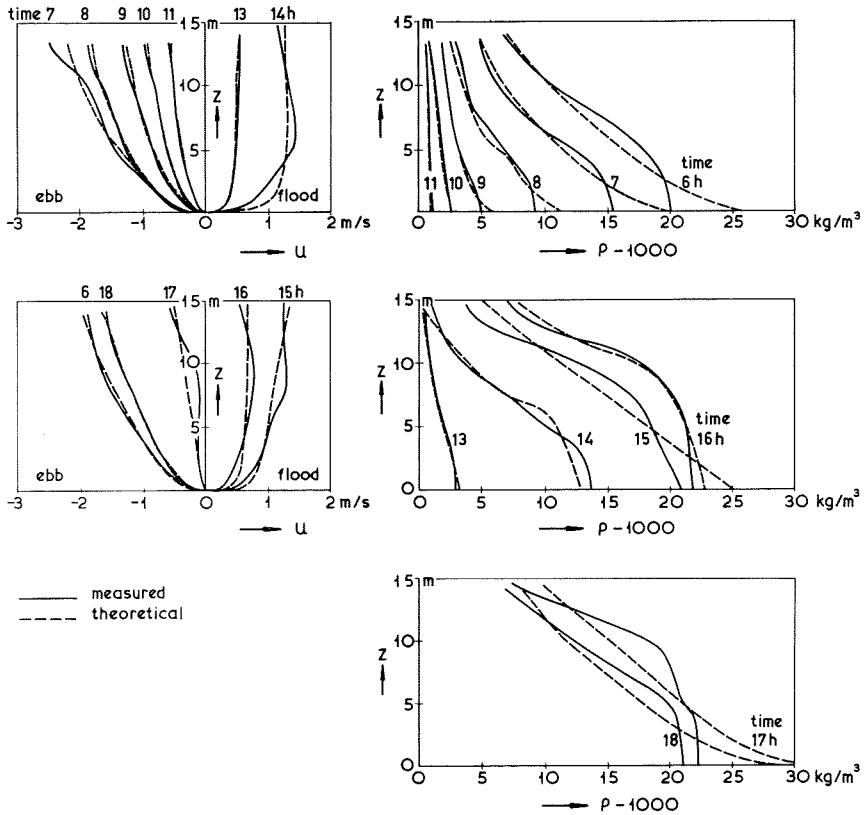


Fig. 8. Measured and theoretical velocity and density profiles for  $\alpha = \eta_2$ .  
Rotterdam Waterway 22-6-1956, km 1023.4.

Given the parameters  $\sigma, \eta_0, \eta_2, \alpha$  the dimensionless profiles of the velocity and density can be derived from eqs. (4.3.1) and (4.3.2). The integration is elementary and is not reproduced here. Also the mean dimensionless velocities and densities can be computed.

To find dimensional profiles, the true mean velocities and densities (either from measurements or from computations) are applied. The ratio

$$u_1/u_2 = U_1/U_2$$

will be a function of the above four parameters. Three of these ( $\eta_0, \eta_2$  and  $\alpha$ ) are "geometrical" parameters; the fourth ( $\sigma$ ) can be varied to give the desired ratio. The shear velocity then can be found from

$$u_* / \kappa = u_1 / U_1$$

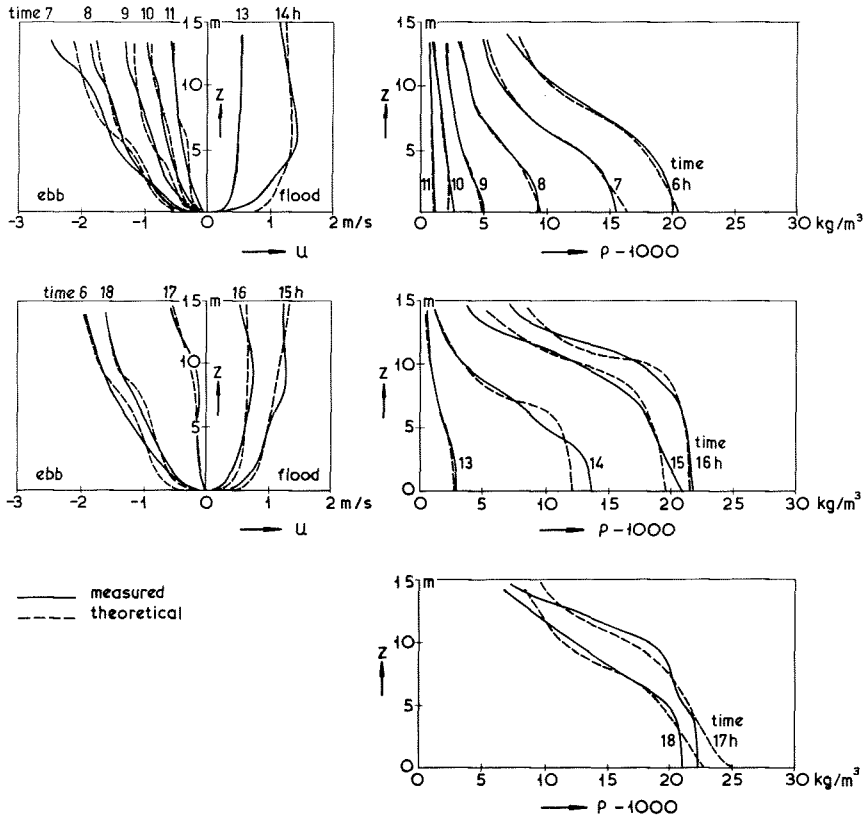


Fig. 9. Measured and theoretical velocity and density profiles for  $\alpha = 0.1$ . Rotterdam Waterway 22-6-1956, km 1023.4.

The same value of  $\sigma$  is applied in the density profile. There remain two parameters ( $\varrho_b$  and  $f_i Sc / \kappa u_*$ ) to be determined from the dimensional mean densities:

$$\varrho_1 = \varrho_b + s_1 f_i Sc / \kappa u_* \quad (4.3.3)$$

$$\varrho_2 = \varrho_b + s_2 f_i Sc / \kappa u_*$$

If the values  $u_{1,2}$  and  $\varrho_{1,2}$  are taken from the theoretical two-layer model, this procedure defines the corresponding profiles. The parameter  $\eta_2$  also follows from the model. The bottom roughness can be estimated in the usual way. The parameter  $\alpha$  in the mixing length then remains as an unknown. Its influence is investigated below by comparing theoretical with measured profiles.

To this end, measurements from the Rotterdam Waterway (22-6-'56) are used. Velocity and density profiles have been obtained by averaging the measured profiles

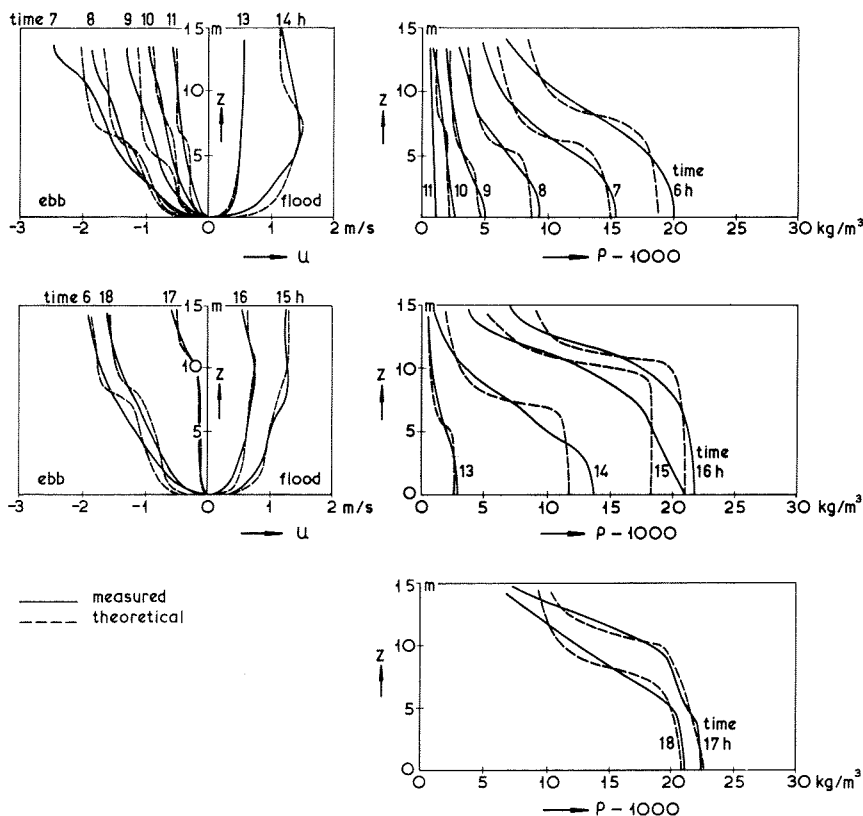
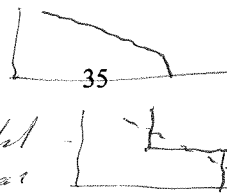


Fig. 10. Measured and theoretical velocity and density profiles for  $\alpha = 0.01$ . Rotterdam Waterway 22-6-1956, km 1023.4.

Kan niet altijd

aan een atoom dat  
de atoom samenhang geeft dat



at each cross-section. They are given in Fig. 8, 9 and 10; for the individual velocity-profiles see Fig. 25. The level of the interface has been determined by applying eq. (3.4.1). The mean velocities and densities have been applied in the above procedure. For  $\eta_0$  the value  $10^{-4}$  has been used, which corresponds to  $k \simeq 0.05$  m. The parameter  $\alpha$  has been varied.

From the results it is concluded that a useful approximation of the profiles is possible. Secondly, as could be expected, the best correspondence is not always at the same value of  $\alpha$ . The overall picture, however, including both density and velocity-profiles, is best for  $\alpha = 0.1$ . This can be used as a working approximation. It is essential in this comparison that the correct mean velocities and densities are applied. From this it may be concluded that a two-layer model can give reasonable profiles, provided the mean velocities and densities are reproduced well.

#### 4.4 Frictional and mixing coefficients

For the bottom and interfacial shear-stresses, frictional coefficients can be introduced as follows

$$\tau_b = \varrho_2 k_b u_2 |u_2| \quad (4.4.1)$$

$$\tau_i = \varrho_2 k_i (u_1 - u_2) |u_1 - u_2| \quad (4.4.2a)$$

$$\tau_i = \varrho_2 k_b (a_1/h) u_2 |u_2| + \varrho_2 k_i (u_1 - u_2) |u_1 - u_2| \quad (4.4.2b)$$

Similarly, an interfacial mixing coefficient is defined by

$$f_i = m_i (\varrho_2 - \varrho_1) |u_1 - u_2| \quad (4.4.3)$$

Eqs. (4.4.1) and (4.4.2a) are the same as those given by Schijf and Schönfeld. However, (4.4.2b) is proposed as an alternative to (4.4.2a). The reason is that in the limiting case of homogeneous flow the interfacial shear stress should not vanish. In that case  $\varrho_1 = \varrho_2$  and there is only one mean velocity, so  $u_1 = u_2$ . If a linear shear-stress profile is assumed, one has

$$\tau_i = \frac{a_1}{h} \tau_b \quad (4.4.4)$$

which is incorporated in (4.4.2b). The same condition follows from an analysis of eqs. (6.2.1) and (6.2.2) which coincide for the case of homogeneous flow if (4.4.4) is satisfied. Eq. (4.4.3) has also been used by O'Brien and Reid (1967).

The frictional and mixing coefficients can be expressed in terms of the parameters introduced in the preceding sections:

$$k_b/\kappa^2 = (U_2|U_2|)^{-1} \quad (4.4.5)$$

$$k_i/\kappa^2 = (\sigma - 1 + \eta_2) \{(U_1 - U_2)|U_1 - U_2|\}^{-1} \quad (4.4.6b)$$

$$m_i Sc/\kappa^2 = \{(s_2 - s_1)|U_1 - U_2|\}^{-1} \quad (4.4.7)$$

The right-hand members are functions of the geometrical parameters  $\eta_0$ ,  $\eta_2$ ,  $\alpha$  and the shear-stress ratio  $\sigma$ , which in its turn is determined by the ratio of the mean velocities. This means that the frictional and mixing parameters could be determined if in addition Von Kármán's constant  $\kappa$  and the turbulent Schmidt number  $Sc$  were known. The former can be understood as the product of Von Kármán's constant  $\kappa = 0.4$  and some function of the density stratification. The dependence of these parameters on the conditions in a stratified flow is not known very well. Therefore eqs. (4.4.5) to (4.4.7) cannot give more than a qualitative picture and the actual magnitude of the coefficients remains an empirical question. A further investigation of  $k_i$  is made in section 7.3.

#### 4.5 Convection through the interface

Little is known about the amount of water convected through the interface. If a sharp interface exists, an upward transport begins when interfacial waves start breaking. Schijf and Schönfeld (1953) show that interfacial waves grow unstable as soon as the internal Froude number

$$F = (u_1 - u_2) (\varepsilon g h)^{-\frac{1}{2}}$$

exceeds unity. Also some small-scale experiments have been done to determine the entrainment into a layer flowing over or under a stagnant one of different density (cf. e.g. Keulegan 1966). The entrainment is found to depend on the relative velocity and/or on a stability-parameter like  $F$ . Therefore there is some reason to assume that the vertical convective velocity relative to the interface  $w_i$  depends on  $F$ . The simplest dependence is a linear one. If variations in  $\varepsilon$  and  $h$  are not too important, one finds as a first guess

$$w_i = w_0 + w_1 |u_1 - u_2| \quad (4.5.1)$$

## BOUNDARY CONDITIONS

## 5.1 Initial conditions

Any instantaneous picture of the situation could be used as an initial condition. There is only one situation in which such a picture can be specified in all detail required, viz. a steady-flow situation. This situation is not realistic in a tidal estuary. Therefore the assumption must be made that the influence of the initial condition vanishes in the course of time, due to the frictional damping effects.

For the case with mixing (eqs. (3.3.3) to (3.3.8)) it is still rather difficult (though not impossible) to compute a steady situation. As the influence of the initial situation essentially is unwanted, one could just as well take a simple situation without mixing, and let the mixing increase gradually during the adjusting phase of the model. For the case without mixing (eqs. (3.3.9) to (3.3.12)) the steady situation can be derived analytically (Harleman 1961).

From eq. (3.3.10) one finds that  $u_2 = 0$  as there cannot be a net flow in the lower layer. From eq. (3.3.9) combined with the boundary condition for the river flow  $q_f$  one finds

$$u_1 = q_f/a_1$$

Introducing this into eq. (3.3.12) one obtains with eqs. (4.4.1) and (4.4.2)

$$g \frac{\partial h}{\partial x} - \varepsilon g \frac{\partial a_1}{\partial x} - gI - \frac{k_i u_1 |u_1|}{a_2} = 0$$

Now the surface slope can be eliminated between this equation and eq. (3.3.11):

$$-\frac{q_f^2}{a_1^3} \frac{\partial a_1}{\partial x} + \varepsilon g \frac{\partial a_1}{\partial x} - \frac{k_i q_f^2}{a_1^2 a_2} - \frac{k_i q_f^2}{a_1^3} (1 + \varepsilon) = 0$$

In this equation it is admissible to assume the water-depth  $h$  to be a constant (c.f. Chapter 6) and to neglect  $\varepsilon$  with respect to unity. Then it can be written in dimensionless form:

$$\left\{ F_f^{-2} \left( \frac{a_1}{h} \right)^3 - 1 \right\} \left( 1 - \frac{a_1}{h} \right) \frac{da_1}{dx} = k_i \quad (5.1.1)$$

where  $F_f = q_f (\varepsilon g h^3)^{-\frac{1}{2}}$  is the internal Froude number based on the freshwater discharge. The solution of eq. (5.1.1) is

$$k_i \left( \frac{L_w - x}{h} \right) = F_f^{-2} \left\{ \frac{1}{20} - \frac{1}{4} \left( \frac{a_1}{h} \right)^4 + \frac{1}{8} \left( \frac{a_1}{h} \right)^5 \right\} - \frac{1}{2} + \frac{a_1}{h} - \frac{1}{2} \left( \frac{a_1}{h} \right)^2 \quad (5.1.2)$$

where  $L_w$  is the length of the salt wedge. This length is determined by imposing the boundary condition at the river-mouth ( $x = 0$ ). As discussed in section 5.3, at that location the flow can be assumed to be critical, i.e.

$$(a_1/h)^3 = F_f^2 \quad (5.1.3)$$

One then finds for the length  $L_w$ :

$$k_i L_w / h = \frac{1}{20} F_f^{-2} - \frac{1}{2} + \frac{3}{4} F_f^{\frac{3}{2}} - \frac{3}{10} F_f^{\frac{5}{2}} \quad (5.1.4)$$

This relation is illustrated in Fig. 11. If the length of the salt wedge is known, it can be used to estimate the interfacial frictional coefficient  $k_i$ . It is noted that  $L_w$  becomes negative if  $F_f > 1$ . The formation of a salt wedge then is prevented by a high river-discharge.

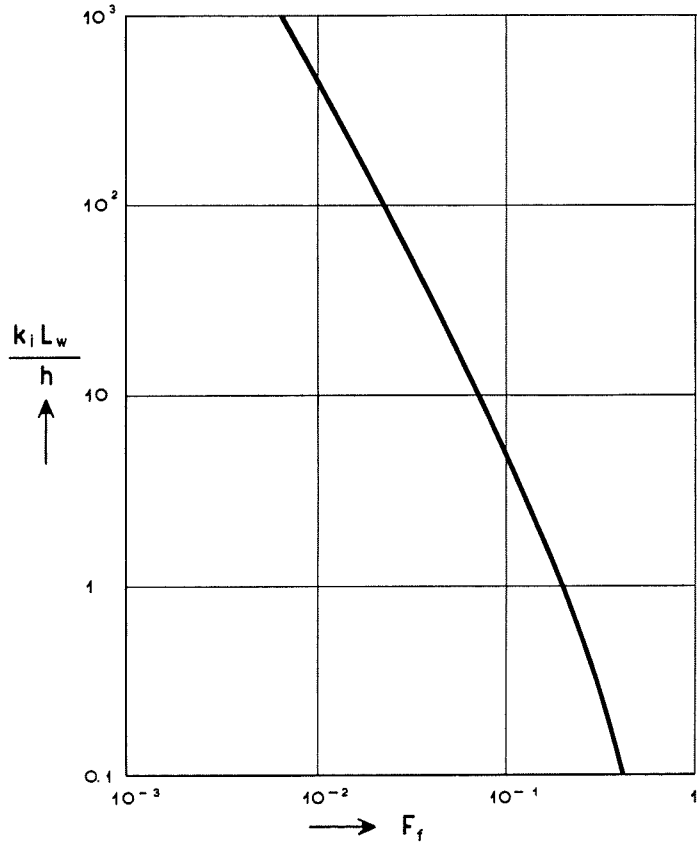


Fig. 11. Length of stationary salt-wedge.

## 5.2 Number and character of boundary conditions

For a hyperbolic system of differential equations, generally the number of boundary conditions to be specified at any boundary equals the number of characteristics entering the region at the instant under consideration (Courant and Hilbert 1962). In Appendix 3 it is derived that there exist six characteristic velocities. Two of these correspond to the surface wave mode:

$$c_s = \frac{a_1 u_1 + a_2 u_2}{h} \pm (gh)^{\frac{1}{2}} \quad (5.2.1)$$

The second pair corresponds to the internal wave mode:

$$c_i = \frac{a_1 u_2 + a_2 u_1}{h} \pm \left\{ \varepsilon g a_2 \frac{a_1}{h} (1 - F^2) \right\}^{\frac{1}{2}} \quad (5.2.2)$$

The third pair originates from the convection of dissolved salt by the mean flow:

$$c_u = u_{1,2} \quad (5.2.3)$$

The upstream boundary  $x = L$  is chosen outside the salt wedge area. There, as shown in section 3.3  $a_2 = 0$  and  $u_2 = u_1$ . So one or five characteristics point into the region, depending on the direction of flow. Supercritical flow with respect to the surface waves is assumed not to occur. The conditions to be specified are:

$$\text{river discharge} \quad a_1 u_1 = q_L(t) \quad (5.2.4a)$$

and in case of seaward flow:

$$\text{vanishing lower layer} \quad a_2 = 0 \quad (5.2.4b)$$

$$\text{density of fresh water} \quad \varrho_{1,2} = \varrho_f \quad (5.2.4c)$$

$$\text{equal velocities} \quad u_1 = u_2 \quad (5.2.4d)$$

At the seaward boundary things are much more complicated as the internal wave characteristics may change sign, resulting in supercritical flow. The condition corresponding to the characteristics (5.2.1) is still rather simple (vertical tide):

$$\text{water-level} \quad h(0, t) = \text{given} \quad (5.2.5)$$

The characteristics (5.2.2) may have any direction, as shown in Table 1 below for the Rotterdam Waterway on 22-6-1956. This means that two, one or no boundary conditions are required. The corresponding situations are denoted by supercritical inflow,

subcritical flow and super-critical outflow with respect to the internal waves. The required data could be obtained by measuring them in the prototype situation, but firstly this is not a simple measurement, and secondly it would seriously limit the predicting possibilities of the model.

The third pair of characteristics, too, gives difficulties, as they require the densities of inflowing water to be specified. The mixing in the adjacent sea region does not take place immediately, so the densities of the inflowing water are heavily dependent on the conditions in that region.

To meet the requirements for the boundary conditions, in section 5.4 a hypothesis is made for the situation at the river-mouth, taking the adjacent sea-region into account. For the case without mixing an alternative is possible by the assumption of critical flow at the river-mouth. This possibility is discussed in section 5.3. The densities being fixed, they do not require boundary conditions in this case.

Table 1. Characteristic velocities  
Rotterdam Waterway 22-6-1956, km 1030. Two-layer model with mixing.

time (h)	$a_2$ (m)	$a_1$ (m)	$\Delta\rho_2$ (kg/m <sup>3</sup> )	$\Delta\rho_1$ (kg/m <sup>3</sup> )	$u_2$ (m/s)	$u_1$ (m/s)	$F^2$	$c_i$ (m/s)
7	6.5	6.0	19	13	-1.0	-1.8	0.85	$-1.50 \pm 0.73$
8	6.0	6.0	15	9	-0.7	-1.3	0.92	$-0.96 \pm 0.40$
9	4.0	8.0	12	7	-0.4	-1.1	0.78	$-0.61 \pm 0.59$
10	3.5	8.5	13	6	0.2	-0.6	0.80	$-0.02 \pm 0.62$
11	3.5	8.5	14	5	0.4	-0.6	0.89	$0.14 \pm 0.54$
12	3.5	9.0	17	7	0.6	-0.2	0.51	$0.38 \pm 1.24$
13	3.5	9.0	20	7	0.9	0.4	0.16	$0.76 \pm 1.83$
14	9.0	4.0	21	8	1.1	0.9	0.03	$1.00 \pm 2.14$
15	11.0	2.0	23	12	1.0	0.9	0.01	$0.95 \pm 1.55$
16	11.5	1.0	24	20	0.5	0.5	0.00	$0.50 \pm 0.68$
17	11.0	1.5	24	20	0.3	-0.4	0.02	$-0.40 \pm 0.81$
18	10.0	2.5	24	17	-1.0	-1.3	0.10	$-1.25 \pm 1.25$

Attention should be paid to a possible "internal" boundary, which can be formed by a steep front of the salt wedge. At such a front, the differential equations may not be valid because of the occurrence of significant vertical accelerations, which causes deviations from the hydrostatic pressure-distribution. Techniques exist that admit discontinuous solutions ("weak solutions"), satisfying an integral form of the conservation laws expressed by the differential equations. The Lax-Wendroff-technique (Appendix 1) used in this study, is one of them. However, in these conservation laws too, the effect of vertical accelerations is not included. For the case of lock-exchange flow this may result in a rather different behaviour of the saline front (Abraham and Vreugdenhil 1970). On the other hand, in the tidal estuaries considered the flow does not show such strict layers and the phenomena of acceleration and deceleration at a front will be much less clear. Therefore the weak-solution approach is considered satisfactory and no further precautions are taken at a front.

### 5.3 Critical flow

The complicated flow pattern at the sharp transition between the estuary and the sea can be described only schematically for the present purpose. In a steady situation critical flow with respect to the internal waves can be assumed to exist at the transition (Stommel and Farmer 1952, Voogt 1966). There are several ways to make this plausible. Due to the sudden increase in the cross-section the upper layer will be very shallow in the sea-region. If the situation in the river-mouth would be subcritical, the salt water from the sea could penetrate the river, so the situation would not be steady. If, on the other hand, the flow would be supercritical, no influence of the sea could penetrate. Then, however, the shape of the salt wedge would be as sketched in Fig. 12, as follows from eq. (5.1.2).

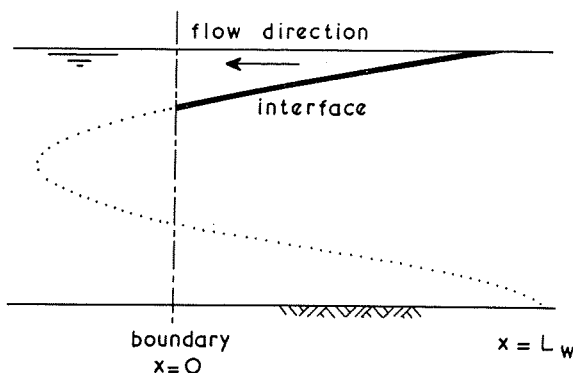


Fig. 12. Flow conditions in case of supercritical flow.

Clearly this is not consistent with the fresh water to be discharged. It is therefore concluded that the flow will be just critical, i.e., one of the  $c_i$  equals zero and the other is directed seaward. From Appendix 3 this is found to be the case if

$$\frac{u_1^2}{\varepsilon g a_1} + \frac{u_2^2}{\varepsilon g a_2} = 1 \quad (5.3.1)$$

For the case without mixing there is no net transport in the lower layer; then (5.1.3) results.

In unsteady conditions the above reasoning does not apply. Actually there is no reason why the flow would be critical, as the internal waves react rather slowly to changes in the conditions. From Table 1 in section 5.2, supercritical flow is seen to occur in prototype. Yet one could apply (5.3.1) as an approximation, speculating that the exact form of the boundary condition has a local influence only. The great advantage is that neither measurements nor a schematized sea are necessary to treat the boundary condition. It should be stressed, however, that this is only possible for the model without mixing. In the model with mixing the prediction of the densities still requires a consideration of the sea-region.

## 5.4 Schematized sea

In the model with mixing the phenomena in the adjacent sea region are important, as they determine the salinity of the inflowing water, and also influence the velocities and the level of the interface at the river-mouth. To obtain a self-contained model it appears unavoidable to include part of the sea region. Of course, the boundary conditions of this sea region are unknown again, but it is assumed that they do not influence the flow in the estuary in an essential way, if they are at a reasonable distance.

As the sea region is taken into account only to provide boundary conditions, a very detailed description is not necessary. The conditions will be different for different estuaries. Some model tests in this respect have been described by Kashiwamura and Yoshida (1969). The applicability of these results is not clear, as no tidal effects were included. Here a specialization is made to conditions prevailing near the mouth of the Rotterdam Waterway. Tidal flow there is directed roughly parallel to the coastline throughout the tidal cycle. Therefore a schematical one-dimensional channel is introduced to represent this sea region (Fig. 13). In this channel a two-layer flow is assumed in the same way as in the estuary itself.

The boundary conditions at the boundaries of the sea region are chosen as

$$\frac{\partial h_i}{\partial x} = 0 \quad \text{and} \quad \frac{\partial q_{1,2}}{\partial x} = 0$$

No condition for the water-level is required, as will become clear in the next Chapter. However, the net discharge  $q$  should be specified at one location as a function of time.

At the river-mouth conditions of continuity are imposed. For the net flow this gives

$$b_s(q_2 - q_3) = b_w q_1 \quad (5.4.1)$$

where the subscripts denote the branch numbers (Fig. 13).

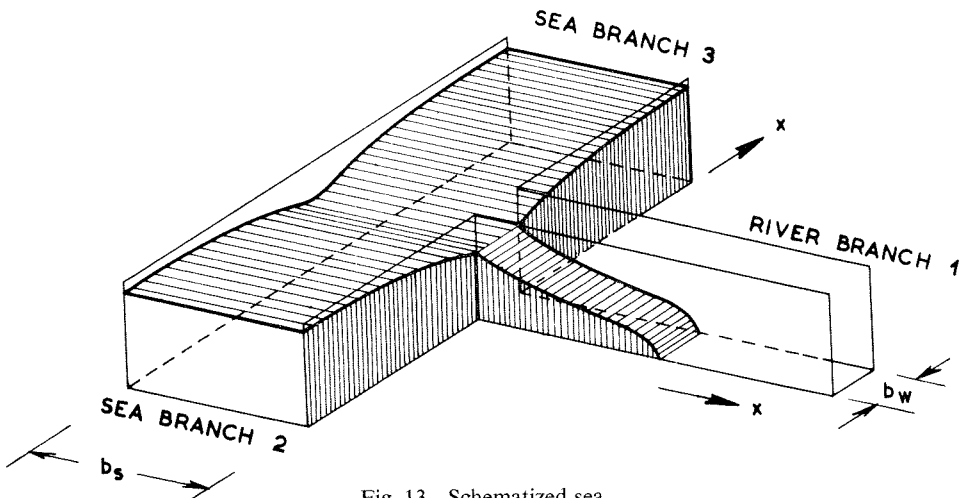


Fig. 13. Schematized sea.

For the lower layer

$$b_s\{(a_2u_2)_2 - (a_2u_2)_3\} = b_w(a_2u_2)_1 \quad (5.4.2)$$

Concerning the continuity of dissolved salt, complete mixing of the water flowing into the junction is assumed; for the upper and lower layers this gives

$$\sum_{\text{in}} b_k(q_1a_1u_1)_k = q_{1\text{out}} \sum_{\text{out}} b_k(a_1u_1)_k \quad (5.4.3)$$

$$\sum_{\text{in}} b_k(q_2a_2u_2)_k = q_{2\text{out}} \sum_{\text{out}} b_k(a_2u_2)_k \quad (5.4.4)$$

When applying the method to the model without mixing, the latter conditions do not of course apply. Finally, a dynamical condition should be introduced. The simplest possibility is to assume that the interface is continuous:

$$(a_2)_1 = (a_2)_2 = (a_2)_3 \quad (5.4.5)$$

This may not be realistic, however. An energy loss can be taken into account empirically by introducing the equations

$$\frac{1}{2}(q_2 - q_1)g\{(a_2)_2^2 - (a_2)_1^2\} = (1 - \beta_1)(q_1a_1u_1^2)_1 + (1 - \beta_2)(q_2a_2u_2^2)_1 \quad (5.4.6)$$

$$(a_2)_2 = (a_2)_3$$

with empirical coefficients  $\beta_1$  and  $\beta_2$ . If  $\beta_1 = \beta_2 = 1$  condition (5.4.5) is found again.

## 5.5 Supercritical flow

Two kinds of supercritical flow with respect to the internal waves can occur. If both  $c_i$  from eq. (5.2.2) are directed seaward, no boundary condition for the internal flow is required. This situation is called supercritical outflow. If both characteristics are directed upriver, two boundary conditions are required.

Some insight into this situation can be gained by comparison with the corresponding problem in homogeneous flow. A sloping channel, connected to a reservoir at the upstream end, works as a long weir. The maximum discharge occurs if the flow at the control section is critical (Chow 1959). A similar situation in two-layer flow is discussed by Rigger (1970). For quasi-steady conditions the discharge in the lower layer is shown to be maximal if critical flow occurs. In addition the return current is maximal if the flow is doubly critical, i.e. both characteristics  $c_i$  vanish. Although this condition only applies to steady flow, it could be used as a first approximation for the case

of supercritical flow. As shown in Appendix 3 the layer thickness and the velocity can be derived explicitly:

$$\left. \begin{aligned} a_2 &= \frac{1}{2}h\{1 + q(\varepsilon gh^3)^{-\frac{1}{2}}\} \\ u_2 &= (\varepsilon gh)^{\frac{1}{2}}a_2/h \end{aligned} \right\} (x = 0) \quad (5.5.1)$$

which constitute the two boundary conditions required.

The treatment of the internal flow boundary condition at the river-mouth, as discussed in the preceding sections, is summarized in Table 2.

Table 2. Boundary conditions at river-mouth

condition	critical flow method	schematized sea method
subcritical flow	critical flow (5.3.1)	continuity+dynamical condition, eqs. (5.4.1), (5.4.2) and (5.4.5) or (5.4.6)
supercritical outflow	none	river: none sea: (5.4.1), (5.4.2) and $(a_2)_2 = (a_2)_3$
supercritical inflow	doubly critical flow (5.5.1)	doubly critical flow (5.5.1) sea: (5.4.1), (5.4.2) and $(a_2)_2 = (a_2)_3$
for model with mixing in any condition	does not apply	for branches with inflow: (5.4.3) and/or (5.4.4)

## BAROTROPIC AND BAROCLINIC APPROXIMATIONS

**6.1 Singular perturbation problem**

In the mathematical model as formulated in the preceding sections, the relative density difference  $\varepsilon$  plays a central part, although it is small numerically ( $< 0.03$ ). For  $\varepsilon = 0$  the case of homogeneous tidal flow results, as discussed in section 6.2. Generally, however, for non-zero  $\varepsilon$  the flow pattern is influenced essentially, as the direction of flow even may be reversed. The large effects of small density differences indicate that the mathematical problem is a singular perturbation problem with respect to the small parameter  $\varepsilon$ . The same fact is seen more formally by considering the boundary conditions. For simplicity the analysis is shown only for the model without mixing, the general model showing the same features.

In the case of subcritical flow at the river-mouth, one boundary condition for the internal flow should be satisfied, as discussed in Chapter 5. Now in Appendix 3 it is shown that the behaviour of the "internal" characteristics  $c_i$  essentially changes if  $\varepsilon = 0$ . They then coincide with the water velocity, so they are directed upriver only if the water velocity does so. Consequently at ebb tide the required boundary condition cannot be satisfied. The mathematical problem resulting for  $\varepsilon = 0$  therefore cannot satisfy its full set of boundary conditions. This again indicates the singular character of the problem.

The small value  $\varepsilon$  is important in a different way in the numerical treatment of the problem. The characteristic velocities corresponding to the surface and internal wave modes have a rather different magnitude (Appendix 3). This is very unfavourable for a numerical solution of the equations (Appendix 1). The propagation of both kinds of waves can be reproduced simultaneously only if an uneconomically small grid-size is chosen. If, however, separate equations for each type of wave can be applied, different grids may be chosen and the computation may be much more economical. This separation corresponds to different approximations in the singular perturbation problem mentioned above (c.f. e.g. Van Dyke 1964, Cole 1968). The idea of a separation in surface and internal wave modes has been applied before by Csanady (1967, 1968) in an analytical model of layered flow in a circular lake, by O'Brien and Reid (1967), Tareyev (1968) and Weigand c.s. (1969) in oceanographical applications, and by Voogt (1966) for an estuary.

**6.2 Barotropic approximation**

First in eqs. (3.3.9) to (3.3.12) a slight reduction is introduced by combining eqs. (3.3.11) and (3.3.12) with the equations of continuity:

$$\frac{\partial u_1}{\partial t} + u_1 \frac{\partial u_1}{\partial x} + g \frac{\partial h}{\partial x} - gI + \frac{\tau_i}{\varrho_1 a_1} = 0 \quad (6.2.1)$$

$$\frac{\partial u_2}{\partial t} + u_2 \frac{\partial u_2}{\partial x} + (1-\varepsilon)g \frac{\partial h}{\partial x} + \varepsilon g \frac{\partial a_2}{\partial x} - gI + \frac{\tau_b - \tau_i}{\varrho_2 a_2} = 0 \quad (6.2.2)$$

An “outer” approximation now is formed by assuming a straightforward power series for small values of  $\varepsilon$ :

$$a_1 = a_1^{(0)} + O(\varepsilon) \quad \text{etc.}$$

Substituting this into the equations and taking the limit for  $\varepsilon = 0$  one obtains the system

$$\frac{\partial a_1^{(0)}}{\partial t} + \frac{\partial}{\partial x}(a_1^{(0)} u_1^{(0)}) = 0 \quad (6.2.3)$$

$$\frac{\partial a_2^{(0)}}{\partial t} + \frac{\partial}{\partial x}(a_2^{(0)} u_2^{(0)}) = 0 \quad (6.2.4)$$

$$\begin{aligned} \frac{\partial u_1^{(0)}}{\partial t} + u_1^{(0)} \frac{\partial u_1^{(0)}}{\partial x} + g \frac{\partial h^{(0)}}{\partial x} - gI + \frac{k_b}{h^{(0)}} u_2^{(0)} |u_2^{(0)}| + \\ + \frac{k_i}{a_1^{(0)}} (u_1^{(0)} - u_2^{(0)}) |u_1^{(0)} - u_2^{(0)}| = 0 \end{aligned} \quad (6.2.5)$$

$$\begin{aligned} \frac{\partial u_2^{(0)}}{\partial t} + u_2^{(0)} \frac{\partial u_2^{(0)}}{\partial x} + g \frac{\partial h^{(0)}}{\partial x} - gI + \frac{k_b}{h^{(0)}} u_2^{(0)} |u_2^{(0)}| + \\ - \frac{k_i}{a_2^{(0)}} (u_1^{(0)} - u_2^{(0)}) |u_1^{(0)} - u_2^{(0)}| = 0 \end{aligned} \quad (6.2.6)$$

It is shown in Appendix 3 that this system results in complex characteristic velocities, which implies an unstable character, unless  $u_1^{(0)} = u_2^{(0)}$ . This condition therefore is necessary to obtain a meaningful system. The two equations of continuity then can be added to give

$$\frac{\partial h^{(0)}}{\partial t} + \frac{\partial}{\partial x}(h^{(0)} u^{(0)}) = 0 \quad (6.2.7)$$

The two equations of motion become identical:

$$\frac{\partial u^{(0)}}{\partial t} + u^{(0)} \frac{\partial u^{(0)}}{\partial x} + g \frac{\partial h^{(0)}}{\partial x} - gI + \frac{k_b}{h^{(0)}} u^{(0)} |u^{(0)}| = 0 \quad (6.2.8)$$

where  $u^{(0)}$  stands for  $u_1^{(0)}$  or  $u_2^{(0)}$ . The latter two equations are the familiar ones describing the propagation of the tidal wave in homogeneous water. The approximation is called *barotropic* in contrast with the baroclinic approximation defined in section 6.3. Boundary conditions are the water-level at the river-mouth and the discharge at the upstream boundary. The layer thickness  $a_2^{(0)}$  can be determined using eq. (6.2.4), but, as pointed out before, the boundary condition at the river-mouth cannot always be satisfied. Higher order terms in the power series with respect to  $\varepsilon$  are not considered.

### 6.3 Baroclinic approximation

To obtain an approximation which can take the boundary condition at the river-mouth into account correctly, a transformation of the independent variables must be introduced. If the spatial coordinate is transformed, an analysis as shown hereafter gives the same result except for the fact that the frictional terms in the final equations (6.3.15) and (6.3.16) are missing. From a physical point of view this is not acceptable, so the time variable is transformed. The transformation-factor is derived from the characteristic velocities (Appendix 3). The time-variable for the “inner” approximation is defined as

$$t_i = \varepsilon^{\frac{1}{2}} t \quad (6.3.1)$$

The system of equations then becomes:

$$\varepsilon^{\frac{1}{2}} \frac{\partial a_1}{\partial t_i} + \frac{\partial}{\partial x} (a_1 u_1) = 0 \quad (6.3.2)$$

$$\varepsilon^{\frac{1}{2}} \frac{\partial a_2}{\partial t_i} + \frac{\partial}{\partial x} (a_2 u_2) = 0 \quad (6.3.3)$$

$$\varepsilon^{\frac{1}{2}} \frac{\partial u_1}{\partial t_i} + u_1 \frac{\partial u_1}{\partial x} + g \frac{\partial h}{\partial x} - gI + (1 + \varepsilon) \frac{k_b}{h} u_2 |u_2| + (1 + \varepsilon) \frac{k_i}{a_1} (u_1 - u_2) |u_1 - u_2| = 0 \quad (6.3.4)$$

$$\varepsilon^{\frac{1}{2}} \frac{\partial u_2}{\partial t_i} + u_2 \frac{\partial u_2}{\partial x} + (1 - \varepsilon) g \frac{\partial h}{\partial x} - gI + \varepsilon g \frac{\partial a_2}{\partial x} + \frac{k_b}{h} u_2 |u_2| - \frac{k_i}{a_2} (u_1 - u_2) |u_1 - u_2| = 0 \quad (6.3.5)$$

Now in this system clearly  $\varepsilon^{\frac{1}{2}}$  plays a part, so the following expansion is assumed:

$$a_1 = A_1^{(0)} + \varepsilon^{\frac{1}{2}} A_1^{(1)} + \dots \quad \text{etc.}$$

the capitals indicating the inner approximations. Introducing this into eqs. (6.3.2) to (6.3.5) and taking the limit for  $\varepsilon \rightarrow 0$  ( $t_i$  fixed) one obtains

$$\frac{\partial}{\partial x}(A_1^{(0)}U_1^{(0)}) = 0 \quad (6.3.6)$$

$$\frac{\partial}{\partial x}(A_2^{(0)}U_2^{(0)}) = 0 \quad (6.3.7)$$

$$U_1^{(0)}\frac{\partial U_1^{(0)}}{\partial x} + g\frac{\partial H^{(0)}}{\partial x} - gI + \frac{k_b}{H^{(0)}}U_2^{(0)}|U_2^{(0)}| + \frac{k_i}{A_1^{(0)}}(U_1^{(0)} - U_2^{(0)})|U_1^{(0)} - U_2^{(0)}| = 0 \quad (6.3.8)$$

$$U_2^{(0)}\frac{\partial U_2^{(0)}}{\partial x} + g\frac{\partial H^{(0)}}{\partial x} - gI + \frac{k_b}{H^{(0)}}U_2^{(0)}|U_2^{(0)}| - \frac{k_i}{A_2^{(0)}}(U_1^{(0)} - U_2^{(0)})|U_1^{(0)} - U_2^{(0)}| = 0 \quad (6.3.9)$$

Eqs. (6.3.6) and (6.3.7) can be integrated immediately. The constant of integration in (6.3.7) must be zero as there cannot be a net discharge in the lower layer. As the layer thickness will not vanish (boundary condition at  $x = 0$ ):

$$U_2^{(0)} = 0 \quad (6.3.10)$$

From the difference of eqs. (6.3.8) and (6.3.9) it follows that the velocities in both layers must be equal. Therefore the constant of integration for eq. (6.3.6), too, is zero and

$$U_1^{(0)} = 0 \quad (6.3.11)$$

So it is found that actually the velocities should be scaled with a factor  $\varepsilon^{\frac{1}{2}}$ . From (6.3.8) and (6.3.9) there remains

$$\frac{\partial H^{(0)}}{\partial x} = I$$

which can be integrated to

$$H^{(0)} = h(0, t_i) + Ix \quad (6.3.12)$$

the first term of which is prescribed by the boundary condition. From the equations of motion it is found very simply that the next term for the water-depth  $H^{(1)}$  must be zero. The first non-trivial set of equations, derived from eqs. (6.3.2) to (6.3.5) becomes

$$\frac{\partial A_1^{(0)}}{\partial t_i} + \frac{\partial}{\partial x}(A_1^{(0)}U_1^{(1)}) = 0 \quad (6.3.13)$$

$$\frac{\partial A_2^{(0)}}{\partial t_i} + \frac{\partial}{\partial x}(A_2^{(0)}U_2^{(1)}) = 0 \quad (6.3.14)$$

$$\frac{\partial U_1^{(1)}}{\partial t_i} + U_1^{(1)} \frac{\partial U_1^{(1)}}{\partial x} + g \frac{\partial H^{(2)}}{\partial x} + \frac{k_b}{H^{(0)}} U_2^{(1)} |U_2^{(1)}| + \frac{k_i}{A_1^{(0)}} (U_1^{(1)} - U_2^{(1)}) |U_1^{(1)} - U_2^{(1)}| = 0 \quad (6.3.15)$$

$$\begin{aligned} \frac{\partial U_2^{(1)}}{\partial t_i} + U_2^{(1)} \frac{\partial U_2^{(1)}}{\partial x} + g \frac{\partial H^{(2)}}{\partial x} - g \frac{\partial H^{(0)}}{\partial x} + g \frac{\partial A_2^{(0)}}{\partial x} + \\ + \frac{k_b}{H^{(0)}} U_2^{(1)} |U_2^{(1)}| - \frac{k_i}{A_2^{(0)}} (U_1^{(1)} - U_2^{(1)}) |U_1^{(1)} - U_2^{(1)}| = 0 \end{aligned} \quad (6.3.16)$$

Unknowns in this system are  $H^{(2)}$ ,  $U_1^{(1)}$ ,  $U_2^{(1)}$  and e.g.  $A_2^{(0)}$ ; afterwards  $A_1^{(0)}$  then follows from (6.3.12) with

$$H^{(0)} = A_1^{(0)} + A_2^{(0)} \quad (6.3.17)$$

The correction  $H^{(2)}$  is hardly interesting, so it is eliminated by subtracting eqs. (6.3.15) and (6.3.16):

$$\begin{aligned} \frac{\partial}{\partial t_i} (U_2^{(1)} - U_1^{(1)}) + \frac{\partial}{\partial x} (\frac{1}{2} U_2^{(1)2} - \frac{1}{2} U_1^{(1)2}) - gI + g \frac{\partial A_2^{(0)}}{\partial x} + \\ - \frac{k_i H^{(0)}}{A_1^{(0)} A_2^{(0)}} (U_1^{(1)} - U_2^{(1)}) |U_1^{(1)} - U_2^{(1)}| = 0 \end{aligned} \quad (6.3.18)$$

By the addition of eqs. (6.3.13) and (6.3.14), substitution of (6.3.12) and integration with respect to  $x$  there results

$$A_1^{(0)} U_1^{(1)} + A_2^{(0)} U_2^{(1)} = Q_L(t_i) + (L - x) \frac{dh(0, t_i)}{dt_i} \quad (6.3.19)$$

where  $x = L$  is the upstream boundary and  $Q_L$  is a constant of integration.

The inner approximation consists of the differential equations (6.3.14) and (6.3.18) for the unknowns  $A_2^{(0)}$  and  $U_2^{(1)}$ , while the other variables are expressed in terms of these two by means of eqs. (6.3.17) and (6.3.19). This system no longer contains the surface-wave mode. Correspondingly, it shows the internal wave characteristics  $c_i$  exactly. It is possible therefore to satisfy the seaward boundary condition. In this approximation, the flow is influenced essentially by pressure-differences arising from the non-homogeneity of the fluid. The approximation therefore is called *baroclinic* (for a definition of the terms barotropic and baroclinic cf. e.g. Neumann and Pierson 1966).

The system can also be derived heuristically. It is observed then that due to the large velocity of propagation of the surface waves, the latter are quite long compared to the length of the salt wedge. This implies that the differences in the water-level over the salt wedge are small, so that the water-surface may be assumed to be horizontal (eq. (6.3.12)). Eq. (6.3.19) then can be derived in the same way as above. The surface slope

(whether it is large or small) is eliminated by subtracting  $(1 - \varepsilon)$  times eq. (6.2.1) from (6.2.2). By applying a kind of Boussinesq approximation, i.e. by neglecting  $\varepsilon$  with respect to unity except in the gravity-terms one obtains

$$\frac{\partial}{\partial t}(u_2 - u_1) + \frac{\partial}{\partial x}(\frac{1}{2}u_2^2 - \frac{1}{2}u_1^2) - \varepsilon g I + \varepsilon g \frac{\partial a_2}{\partial x} - \frac{k_i h}{a_1 a_2}(u_1 - u_2)|u_1 - u_2| = 0 \quad (6.3.20)$$

which is identical to eq. (6.3.18), considering the transformations involved.

It is noted that within the basic assumptions of the model (hydro-static pressure distribution and negligible geostrophic effects) eq. (6.3.20) is equivalent to what is known in oceanography as Margules' equation (Neumann and Pierson 1966).

For convenience, the system of equations for the baroclinic approximation is summarized using the original variables. Eq. (6.3.20) is applied together with the equation of continuity

$$\frac{\partial a_2}{\partial t} + \frac{\partial}{\partial x}(a_2 u_2) = 0 \quad (6.3.21)$$

and  $u_1$  and  $a_1$  are expressed in terms of  $u_2$  and  $a_2$  by means of the relations

$$h = a_1 + a_2 = h(0, t) \quad (6.3.22)$$

$$q = a_1 u_1 + a_2 u_2 = q_L(t) + (L - x) \frac{d}{dt} h(0, t) \quad (6.3.23)$$

The boundary conditions for the internal flow are as discussed in section 5.3 or 5.4.

#### 6.4 Matching and uniform expansion

The baroclinic approximation as derived in the preceding section is determined except for the constant of integration  $Q_L(t_i)$ . This must be set by a procedure called matching. In the present context this procedure states that an "outer" representation of the baroclinic approximation (obtained by putting  $\varepsilon = 0$ ) should coincide with an "inner" representation of the barotropic approximation (Van Dyke 1964). It is shown simply that  $q_L(t) = \varepsilon^{\frac{1}{2}} Q_L(t_i)$  must be identified with the net discharge at  $x = L$ , which is derived from the barotropic approximation. It is seen that in this way the baroclinic approximation satisfies *all* boundary conditions. Therefore it cannot be far from uniformly valid.

A uniform expansion can be derived formally by adding the two expansions and subtracting the part they have in common. The common part is determined by forming an "inner" representation of the "outer" approximation or conversely. Because of the matching, both possibilities give the same result. Denoting the inner and outer

approximations by superscripts (*i*) and (*s*), the inner representation of the barotropic approximation (section 6.2) becomes

$$\varepsilon^{\frac{1}{2}} \frac{\partial}{\partial t_i} (h^{(i)}) + \frac{\partial}{\partial x} (h^{(i)} u^{(i)}) = 0 \quad (6.4.1)$$

$$\varepsilon^{\frac{1}{2}} \frac{\partial}{\partial t_i} (a_2^{(i)}) + \frac{\partial}{\partial x} (a_2^{(i)} u^{(i)}) = 0 \quad (6.4.2)$$

$$\varepsilon^{\frac{1}{2}} \frac{\partial}{\partial t_i} (u^{(i)}) + u^{(i)} \frac{\partial}{\partial x} (u^{(i)}) + g \frac{\partial}{\partial x} (h^{(i)}) - gI + k_b u^{(i)} |u^{(i)}| / h^{(i)} = 0 \quad (6.4.3)$$

with  $u^{(i)} = u_1^{(i)} = u_2^{(i)}$ . Assuming

$$h^{(i)} = h^{(i)(0)} + \varepsilon^{\frac{1}{2}} h^{(i)(1)} + \dots \quad \text{etc.}$$

one obtains by taking the limit for  $\varepsilon \rightarrow 0$ :

$$\frac{\partial}{\partial x} (h^{(i)(0)} u^{(i)(0)}) = 0 \quad (6.4.4)$$

$$\frac{\partial}{\partial x} (a_2^{(i)(0)} u^{(i)(0)}) = 0 \quad (6.4.5)$$

$$u^{(i)(0)} \frac{\partial}{\partial x} (u^{(i)(0)}) + g \frac{\partial}{\partial x} (h^{(i)(0)}) - gI + k_b u^{(i)(0)} |u^{(i)(0)}| / h^{(i)(0)} = 0 \quad (6.4.6)$$

Again in the lower layer no net discharge can occur so  $u^{(i)(0)} = 0$ . From (6.4.6) then

$$h^{(i)(0)} = h(0, t_i) + Ix \quad (6.4.7)$$

The next approximation becomes  $h^{(i)(1)} = 0$  and

$$\frac{\partial}{\partial t_i} (h^{(i)(0)}) + \frac{\partial}{\partial x} (h^{(i)(0)} u^{(i)(1)}) = 0 \quad (6.4.8)$$

$$\frac{\partial}{\partial t_i} (a_2^{(i)(0)}) + \frac{\partial}{\partial x} (a_2^{(i)(0)} u^{(i)(1)}) = 0 \quad (6.4.9)$$

$$\frac{\partial}{\partial t_i} (u^{(i)(1)}) + \frac{\partial}{\partial x} \left\{ \frac{1}{2} (u^{(i)(1)})^2 \right\} + g \frac{\partial}{\partial x} (h^{(i)(2)}) + k_b u^{(i)(1)} |u^{(i)(1)}| / h^{(i)(0)} = 0 \quad (6.4.10)$$

From (6.4.7) and (6.4.8) the velocity  $u^{(i)(1)}$  can be determined. Eq. (6.4.10) is unimportant as it only produces  $h^{(i)(2)}$ . Eq. (6.4.9) determines the common part for the layer thickness, which again does not satisfy the boundary condition. It is noted that

$$h^{(i)(0)} = H^{(0)} \quad \text{and} \quad u^{(i)(1)} = (A_1^{(0)}U_1^{(1)} + A_2^{(0)}U_2^{(1)})/H^{(0)}$$

A uniform approximation now is the following:

$$\begin{aligned} h &= h^{(0)} + H^{(0)} - h^{(i)(0)} = h^{(0)} \\ a_2 &= a_2^{(0)} + A_2^{(0)} - a_2^{(i)(0)} \\ a_1 &= h - a_2 \\ u_1 &= u^{(0)} + \varepsilon^{\frac{1}{2}} \{ U_1^{(1)} - u^{(i)(1)} \} \\ u_2 &= u^{(0)} + \varepsilon^{\frac{1}{2}} \{ U_2^{(1)} - u^{(i)(1)} \} \end{aligned} \tag{6.4.11}$$

In a similar way further approximations may be formed which describe e.g. the influence of the presence of the salt wedge on the tidal levels. For the present purpose, however, this is not necessary.

For the model with mixing a similar argument is given. The main result can be derived heuristically in the same way as shown in section 6.3. No essentially different features are present.

## APPLICATIONS OF THE MODEL WITHOUT MIXING

## 7.1 Rotterdam Waterway

In 1956 extensive measurements were executed in the Rotterdam Waterway by the Netherlands Public Works and Waterways Department (Rijkswaterstaat). At that time the Rotterdam Waterway (Fig. 14) was a relatively uniform channel. Some data on the width and depth in the seaward 18 km are given in Fig. 15. The data measured on 22-6-1956 are among the most complete; they are used to verify the computational method. For the case without mixing, the layer thickness has been determined from the measured salinity-profiles, after averaging in lateral direction, according to the definition eq. (3.4.3).

The river-mouth has been assumed to be at km 1032.5. The water-level measured at km 1030 is used as a boundary condition. River-discharge was about  $1000 \text{ m}^3/\text{s}$ . The density of the sea-water has been assumed to be  $1025 \text{ kg/m}^3$ , corresponding to  $\varepsilon = 0.025$ .

Before making a complete comparison between the computational results and the

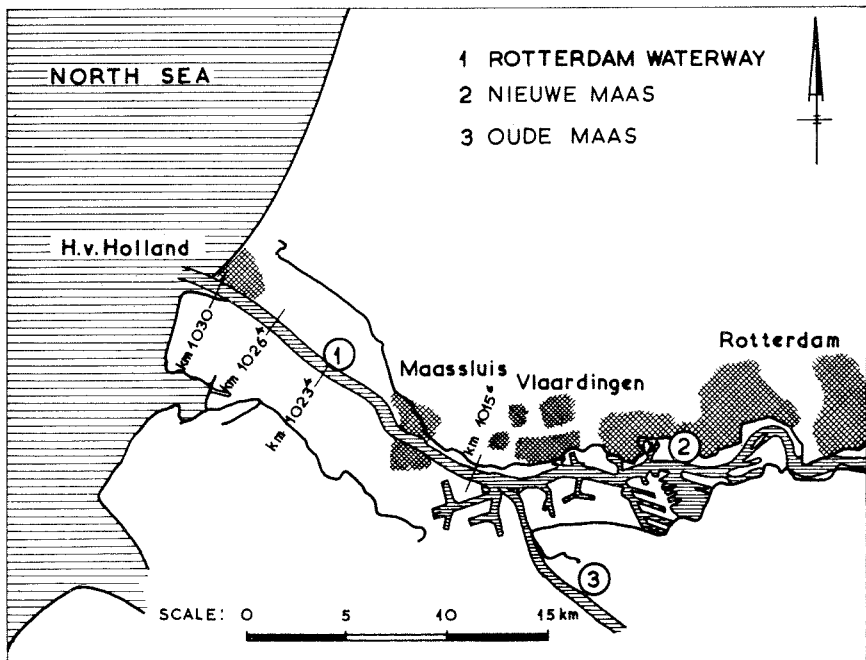
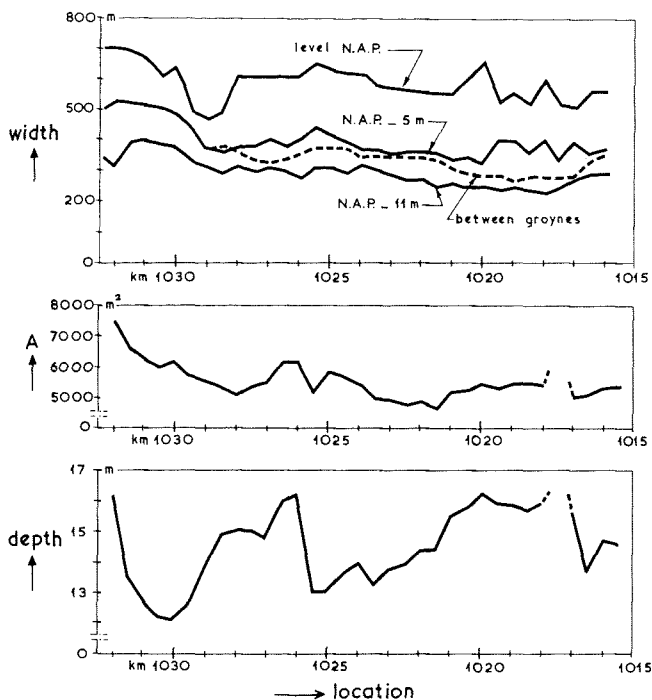


Fig. 14. Rotterdam Waterway 1956.

Fig. 15.  
Rotterdam Waterway 1956.  
Width, cross-sectional area  
below MSL (NAP) and mean  
depth between NAP -11 m  
depth-contours.



measured data, some questions should still be settled, viz. the treatment of the boundary conditions at the river-mouth and at the upstream section. First, a comparison is made between the critical flow method and the schematized sea method discussed in sections 5.3 and 5.4. For this purpose the tidal conditions have been schematized by taking  $q_L = q_f$  as a constant. The discharge curve at the river-mouth then depends fully on the water-level  $h(0, t)$ . This has been selected in such a way that the discharge curve approximates the measured one. The water-depth has been taken 12.5 m. Further data are given in Fig. 16, together with some results for the layer thickness as a function of time at four stations. Although no comparison with the measurements is made for these cases, the parameters have been adjusted such that the situation approximates the measured one. It is seen that the difference between the two methods is small and that it decreases with the distance from the sea. However, it has been found to be essential that in both methods the occurrence of supercritical flow is taken into account. The conjecture made in section 5.3 therefore is substantiated, namely that the exact form of the boundary condition is not very important, provided the essential features of supercritical flow are included. As a consequence of this test, the subsequent computations are treated by the simpler critical flow method.

The method of determining the tidal conditions used in the preceding cases is not consistent with the theory of Chapter 6. More correctly,  $q_L(t)$  is computed by means of a tidal computation for homogeneous water (barotropic mode), which then is intro-

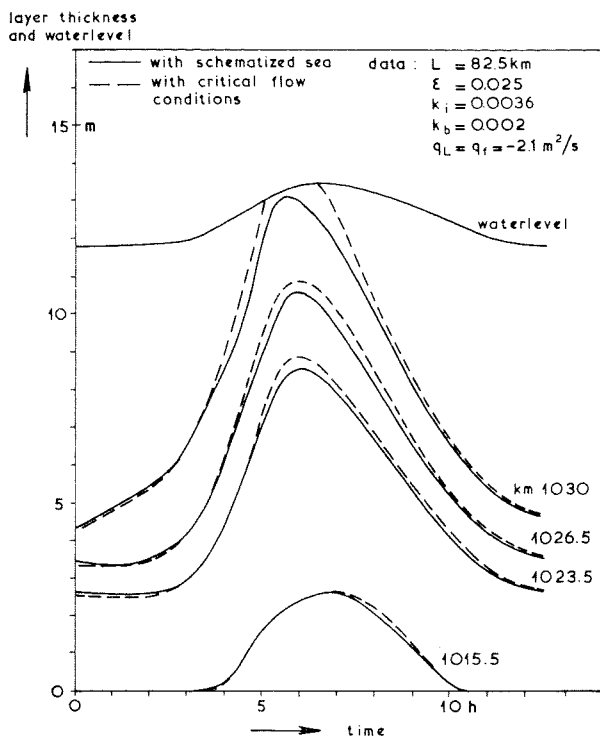


Fig. 16.  
Comparison of critical flow and schematized sea methods.

duced as a boundary condition for the baroclinic model. The value of  $L$  here is not very important, as it hardly influences the magnitude of the computed discharge  $q(x, t)$ . As the Rotterdam Waterway upstream of km 1015 was no longer a uniform channel, the tidal computation has been executed for a hypothetical channel, in the same way as discussed by Stigter and Siemons (1967). The resulting flow-pattern in the intrusion region is quite correct if the length of the hypothetical channel is chosen properly. The two methods of determining  $q_L$  have been compared in the cases 1 and 2 (computed  $q_L$  and fixed  $q_L$  respectively). Dimensions of the cross-section for this case were assumed to be  $12.5 \times 480$  m, corresponding to the seaward part of the estuary. Further data are given in Table 3.

Results are shown in Figs. 17, 18 and 19, together with the corresponding measurements. In Fig. 17 the amplitude of the discharge for case 1 is seen to be too small. Partly this is due to the fact that no distinction has been made between the storage and stream widths. The length  $L$  for case 2 has been chosen such that the flood and ebb volumes equal those of case 1. The resulting curve for  $q(x, t)$  at km 1030 is considerably less correct. One consequence of the method is that the phase-shift between the horizontal and the vertical tide is altered. Therefore all curves for case 2 have been shifted by two hours. The phase-shift is reproduced faithfully in case 1. The interfacial friction has been treated by eq. (4.4.2a). The coefficient  $k_i$  has been adjusted to

Table 3. Data for computations 1 and 2

depth $h$	12.5 m
storage width	480 m
stream width	480 m
density of sea water $\rho_2$	1025 kg/m <sup>3</sup>
density of fresh water $\rho_1$	1000 kg/m <sup>3</sup>
river discharge $Q_f$	1000 m <sup>3</sup> /s
Chézy-coefficient $C$	60 m <sup>1/2</sup> /s
coefficient of bottom friction $k_b$	0.0028
coefficient of interfacial friction $k_i$	0.0052
mesh width $\Delta x$ baroclinic	500 m
mesh width $\Delta x$ barotropic	2500 m
time step $\Delta t$	180 s
length $L$	case 1: 27 km case 2: 113 km
discharge per unit width $q_L$	case 1: variable case 2: $-2.1$ m <sup>2</sup> /s
length of tidal channel	105 km

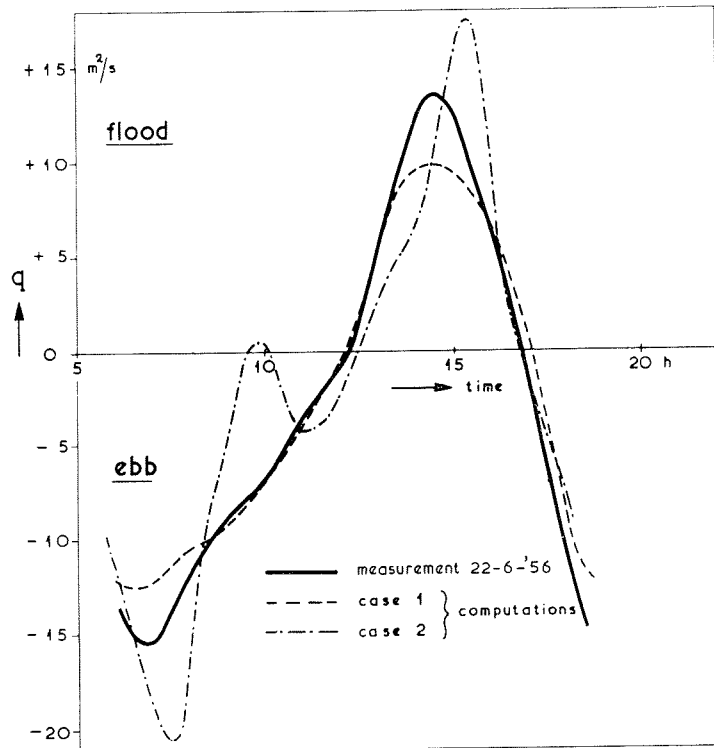


Fig. 17. Discharge at km 1030 for cases 1 and 2.

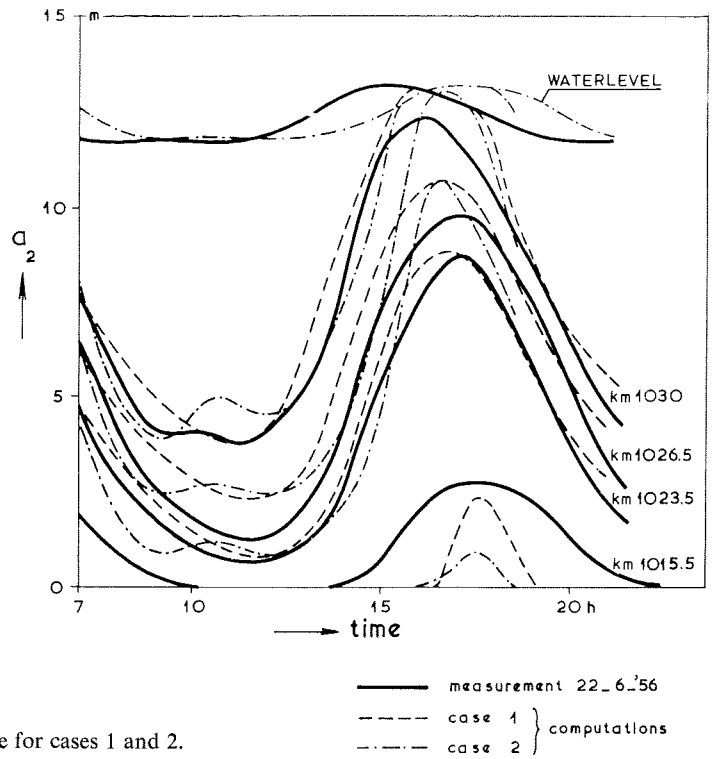


Fig. 18. Level of interface for cases 1 and 2.

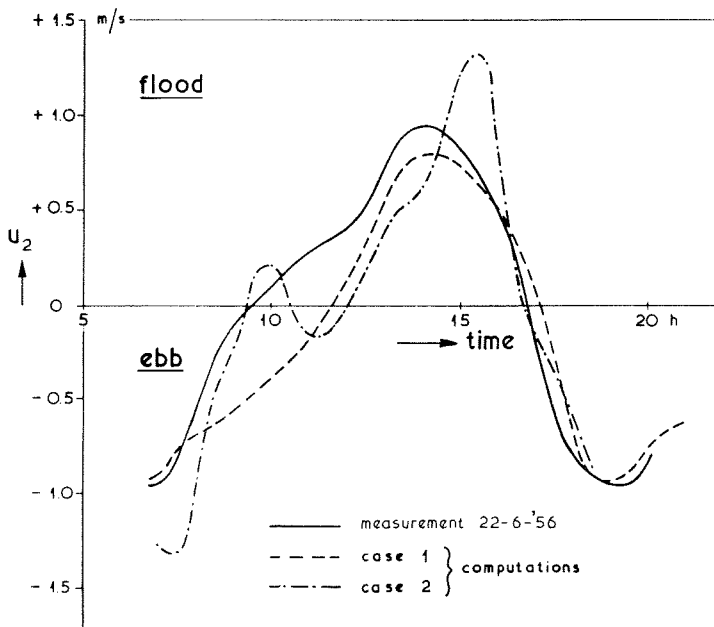


Fig. 19.  
Velocity in lower  
layer at km 1030 for  
cases 1 and 2.

obtain a good correspondence with the measurements. No reason has been found to use different values for cases 1 and 2. The main conclusion from Figs. 18 and 19 is that the more realistic curve for the discharge (case 1) gives the more correct results. Secondly, the phase of the discharge  $q$  is seen to determine the internal flow. The vertical tide being two hours late in case 2 is hardly noticed. Combining these two conclusions, it is found that a correct representation of the tidal flow is of major importance in reproducing the gravity-currents. If the situation is such that this can be done using the simple method of case 2, this will do, but otherwise a tidal computation cannot be dispensed with. As a third point, it is noted that the velocities even in case 1 are not reproduced very well. For the section at km 1030 this may be caused partly by local effects from the boundary (as shown in the preceding computations). Also the dimensions of the channel used are not quite representative for the entire region.

As a final check runs 3 and 4 are shown, in which expressions (4.4.2a) and (4.4.2b) respectively have been applied for the interfacial shear-stress. The cross-section was schematized to a rectangular one with dimensions  $14 \times 350$  m with a storage width of 600 m. These values can be considered representative for the seaward 18 kilometers shown in Fig. 15. The difference between the storage and stream width is taken into account in eqs. (6.2.7) and (6.3.23). In the other equations the stream-width is used. Further data are summarized in Table 4.

Table 4. Data for computations 3 and 4

depth $h$	14 m
storage width	600 m
stream width	350 m
density of sea-water $\rho_2$	1025 kg/m <sup>3</sup>
density of fresh water $\rho_1$	1000 kg/m <sup>3</sup>
river discharge $Q_f$	1000 m <sup>3</sup> /s
Chézy-coefficient $C$	60 m <sup>1/2</sup> /s
coefficient of bottom-friction $k_b$	0.0028
coefficient of interfacial friction $k_i$	0.007
mesh width $\Delta x$ baroclinic	500 m
mesh width $\Delta x$ barotropic	2500 m
time step $\Delta t$	180 s
length $L$	0
length of tidal channel	75 km

The value of  $k_i$  has been adjusted to obtain a good correspondence with the measurements. No reason has been found to use different values for cases 3 and 4. It is noted that the coefficient of bottom-friction  $k_b$  for case 4 does not appear explicitly in the equations for the baroclinic approximation (eq. (6.3.20)). The influence of the bottom friction of course is present by means of its effect on the interfacial coefficient  $k_i$ .

The numerical accuracy can be estimated using Fig. 33 from Appendix 1. For

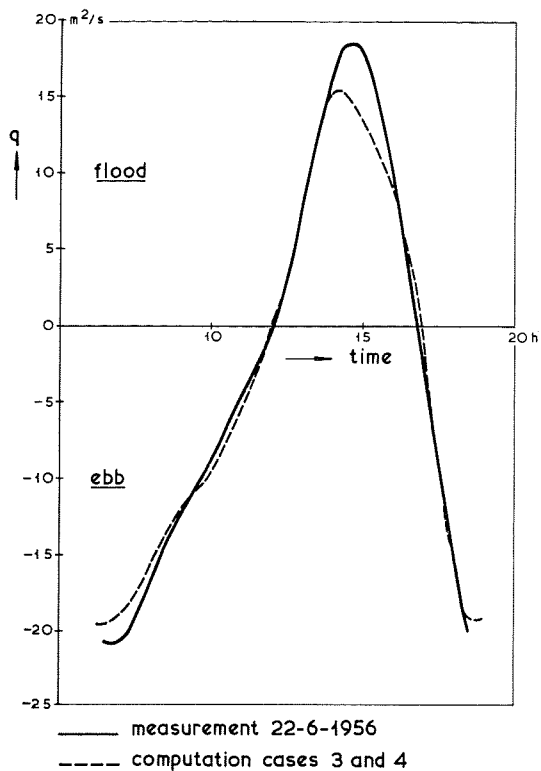


Fig. 20.  
Discharge at km 1030 for cases 3 and 4.

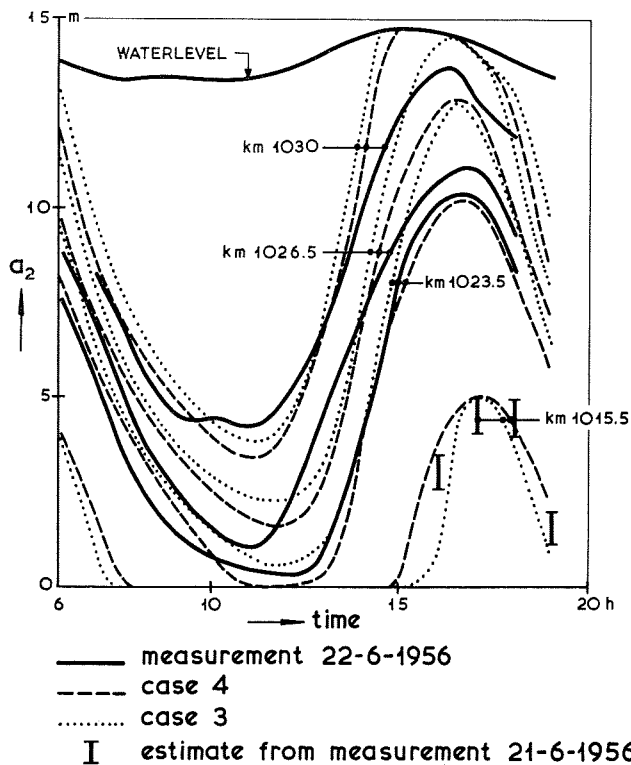


Fig. 21.  
Level of interface for cases  
3 and 4.

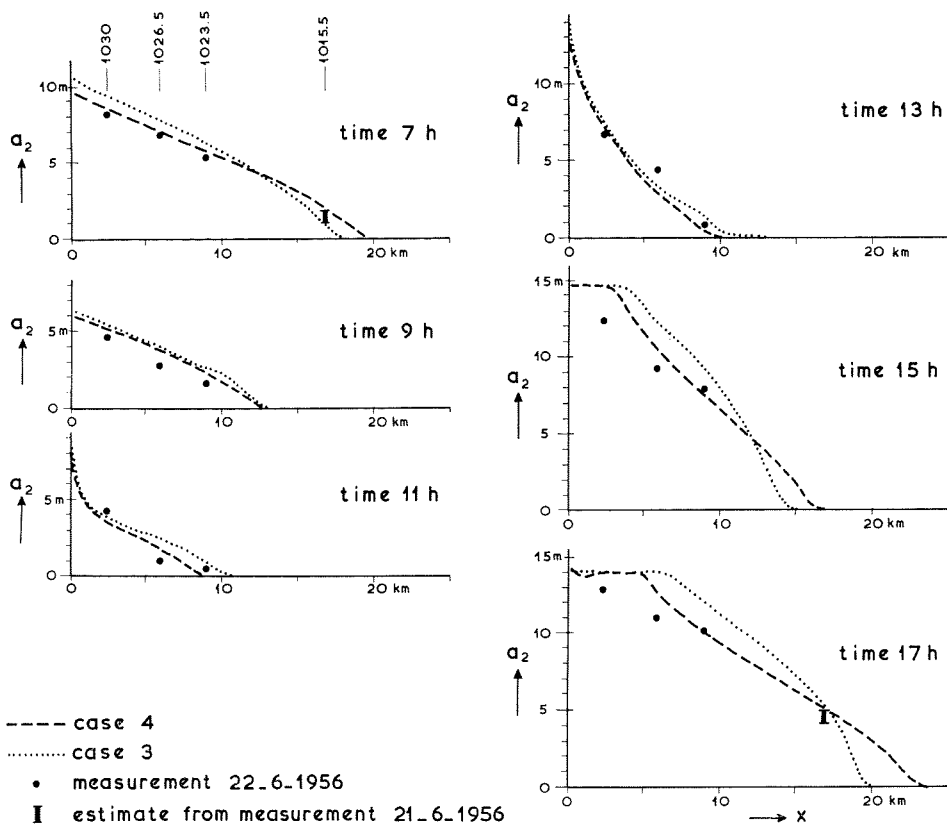


Fig. 22. Longitudinal sections of the interface for cases 3 and 4.

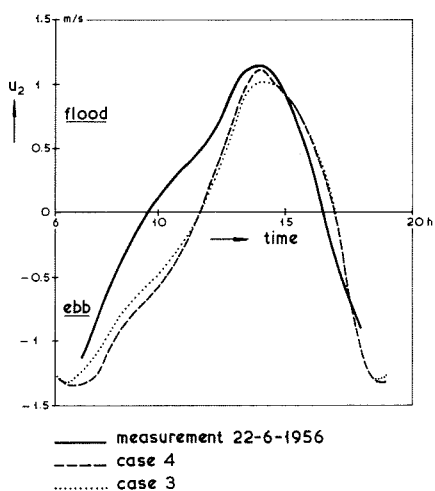


Fig. 23. Velocities in lower layer at km 1030 for cases 3 and 4.

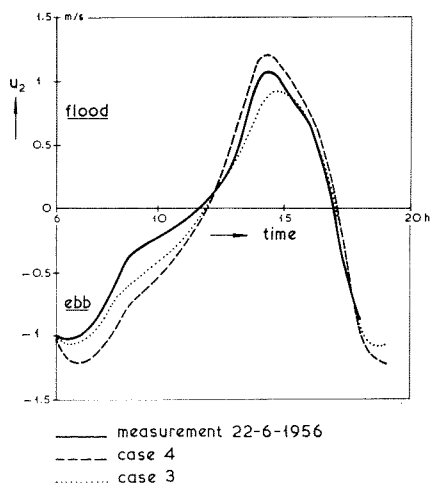


Fig. 24. Velocities in lower layer at km 1023.4 for cases 3 and 4.

waves with a period of about 6 hours, the following damping factors and relative velocities are found:

	barotropic	baroclinic
$\Delta x/l$	0.01	0.05
$\mu$	0.87	0.2
$D$	1.000	0.996
$c_r$	1.000	0.985

Results for cases 3 and 4 are shown in Figs. 20 to 24. They apply to the baroclinic mode, without the correction shown in section 6.4, which is assumed to be small. The discharge shown in Fig. 20 is more correct than in case 1 due to the difference between storage and stream width. A further improvement has not been attempted. The reproduction of the layer thickness is about as good as in case 1 above. There is some difference between cases 3 and 4, to be noticed both in Figs. 21 and 22. Measurements at km 1015.6 have been entered for orientation only, as they are from a different day (21-6-1956). Case 4 generally agrees better with the measurements than case 3. The velocities at kms 1030 and 1023.4, shown in Figs. 23 and 24, are of the correct order of magnitude. At km 1030 the same kind of differences with the measurements is found as in case 1. Indeed, the reproduction at km 1023.4 is more realistic. In these figures, case 3 gives slightly more accurate values than case 4. This is discussed more closely in the following section. In judging the preceding results it should be kept in mind that the measured data show a considerable scatter, at least in the order of 10% (see also the following section).

As a general conclusion, it can be stated that the two-layer model without mixing gives quite satisfactory results, considering the global nature of the model and the approximations involved in it. For many of the applications mentioned in the introduction the results will be very useful.

## 7.2 Velocity profiles

In the preceding section it has been found that the velocities are reproduced at the correct order of magnitude. For some applications a more detailed picture may be required; therefore a closer evaluation is made by means of the velocity profiles derived in section 4.3. To this end the procedure described in that section is applied to the results of cases 3 and 4 from section 7.1. Measured profiles are available at kms 1030 and 1023.4. At km 1030, however, deviations have been found, that possibly may be ascribed to the boundary condition (section 7.1). The profiles therefore have been determined only for km 1023.4 (Fig. 25). The parameter  $\eta_0$  has been taken  $10^{-4}$ , corresponding to a bottom roughness of  $k \simeq 0.05$  m. This is not quite consistent with the Chézy-coefficient used in the two-layer model, but this does not make much difference for the profiles. The parameter  $\alpha$  has been kept constant at 0.1, in accordance with the results in section 4.3. In Fig. 25, the individual profiles for the measurements are shown.

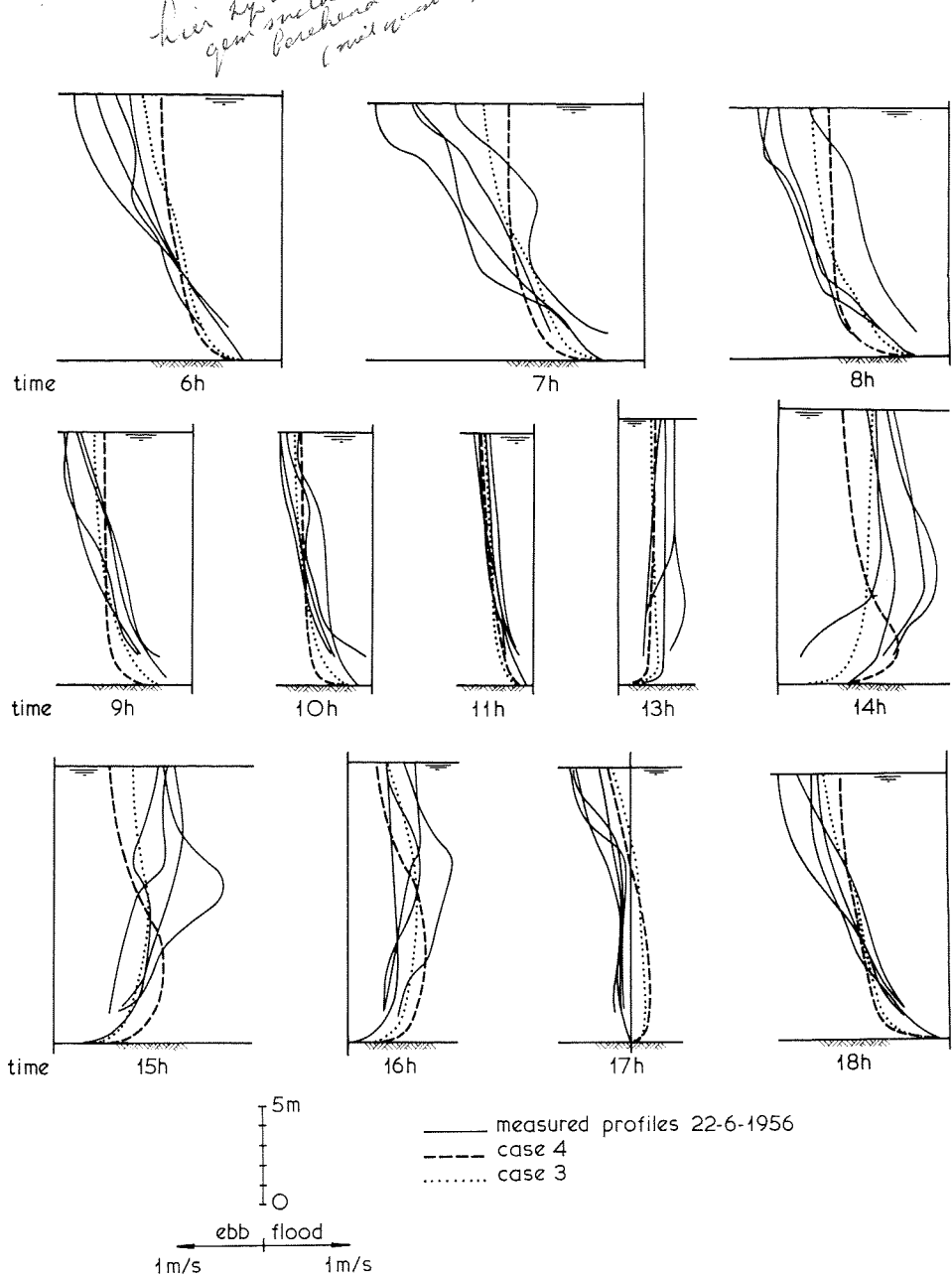


Fig. 25. Velocity profiles at km 1023.4 for cases 3 and 4.

Some remarks should be made. Firstly, it is seen that at 6 and 14 h the computed velocities are too small on the whole. This corresponds to the discharge curve shown in Fig. 20, so the effect should not be attributed to the two-layer model or the theoretical profiles. Secondly, in general a limited correspondence between measured and

theoretical profiles is seen. In a number of cases the theoretical profiles fall within the range of the measured ones. As the Rotterdam Waterway is not the uniform channel assumed in the computations, and therefore is not an ideal test case, this result is of some value. It should be realized, however, that it is caused to a large extent by the magnitudes of the mean velocities  $u_1$  and  $u_2$ . The theoretical profiles tend to have gradients that are smaller than the measured ones, i.e. the velocities in the lower part of the profiles are too large and those in the upper part are too small. This is more so for case 4 than for case 3, as can be concluded also from Fig. 24. As a much more perfect correspondence between theoretical and measured profiles is possible (c.f. section 4.3), it must be concluded that the reproduction of the velocities by the two-layer model still has a limited value. Also it is concluded that a definite choice between the expressions (4.4.2a) and (4.4.2b) cannot yet be made, as the effects are different if one considers the layer-thickness or the velocities. It may be necessary to find a more accurate expression instead of (4.4.2) to obtain a closer reproduction of the entire situation. This requires a more complete knowledge of the physical processes involved.

### 7.3 Interfacial friction

A theoretical prediction of the coefficient of interfacial friction  $k_i$  in section 4.4 has been shown to require a deeper insight into the physical process of turbulence in stratified surroundings. An empirical prediction suffers from a lack of data. In order to obtain some knowledge of the dependence of  $k_i$  on the conditions in the estuary, use has been made of systematic flume-tests, executed by the Delft Hydraulics Laboratory in commission of the Netherlands Public Works and Waterways Department. Dimensions of the flume are: width 0.67 m, depth 0.50 m, length 100 m. The reference situation can be considered an approximate scale model of the Rotterdam Waterway at scales 1:640 horizontally and 1:64 vertically (van Rees and Rigter 1969). Apart from experiments in the technique of hydraulic models, the systematic tests included variations of the water depth, river discharge, bottom roughness, tidal range and salinity of the sea-water. By hindcasting a number of these tests, using the two-layer model, a first approximation of the variations of  $k_i$  can be obtained. To this end, it must be assumed that the entire series of tests represents corresponding situations of a real estuary. There are indications that this is the case.

Table 5. Tidal flume, data situation T3

depth	13.8 m
tidal range at river-mouth	1.35 m
river discharge	950 m <sup>3</sup> /s
density sea-water	1024 kg/m <sup>3</sup>
width	430 m
Chézy-coefficient	60 m <sup>1/2</sup> /s

The reference situation T3 is characterized by the data in Table 5. The data are given in "prototype" dimensions by means of the above scales.

The computations have been made using constant values of  $q_L$  corresponding to the river discharge. The length  $L$  has been adjusted to obtain the observed amplitude of the tidal discharge at the river-mouth. For the interfacial shear-stress eq. (4.4.2b) has been applied. Values of  $k_i$  have been adjusted to obtain correspondence between test and computation in terms of either the maximal intrusion length (observed visually in the flume) or the variation of the mean density  $\langle \bar{\rho} \rangle$  at a few measuring sections. Both criteria give about the same result; therefore hereafter only the intrusion length is mentioned. The results of the computations are given in Table 6. For each situation the data are given only insofar as they differ from the reference situation. It is noted that the tidal range at the river-mouth generally was not quite constant, although it was kept constant at the tide generation in the model sea. The last column shows the values of  $k_i$ , corrected for this effect using the results of the test series with variable tidal range.

Table 6. Results of systematic tests

test no.	characteristic	tidal range (m)	maximal intrusion length (km)	$k_i$	$k_i$ reduced to tidal range of 1.35 m
T 3	cf. Table 5	1.35	26	0.0055	0.0055
T 106	$h = 10$ m	1.35	17	0.0040	0.0040
T 110	$h = 17$ m	1.46	39	0.0030	0.0025
T 116	$C = 80$ m <sup>3</sup> /s	1.38	32	0.0022	0.0021
T 114	$C = 40$ m <sup>3</sup> /s	1.38	19	0.0070	0.0067
T 121	$Q_f = 475$ m <sup>3</sup> /s	1.50	38	0.0025	0.0020
T 118	$Q_f = 1900$ m <sup>3</sup> /s	1.39	20	0.0015	0.0014
T 134		2.02	26	0.0150	
T 135		0.67	35	0.0012	

To give an impression of the reliability of these figures, it is noted that in general, other factors being equal, the intrusion length varies by a factor of 1.2 to 1.5 if the value of  $k_i$  is doubled or halved. The last digit in the specified values of  $k_i$  is not quite significant; the adjustment was not carried out to a high degree of accuracy. The results from Table 6 can be compared to the values obtained by assuming a stationary salt wedge, with the same length as the *mean* intrusion length for the non-steady case. Approximating this mean length by taking the average of the maximal and minimal intrusion lengths, the values of  $k_i$  have been computed from eq. (5.1.4). The results are given in Table 7 and Fig. 26. It should be realized that neither of the two sets of values is very accurate.

From Table 7 it can be concluded that the mean position of the salt wedge does *not* correspond to a stationary salt wedge with the same value of  $k_i$ . The difference is not systematic and may be either way. Therefore, on the one hand, if a value of  $k_i$  is known

Table 7. Comparison of non-steady and steady cases

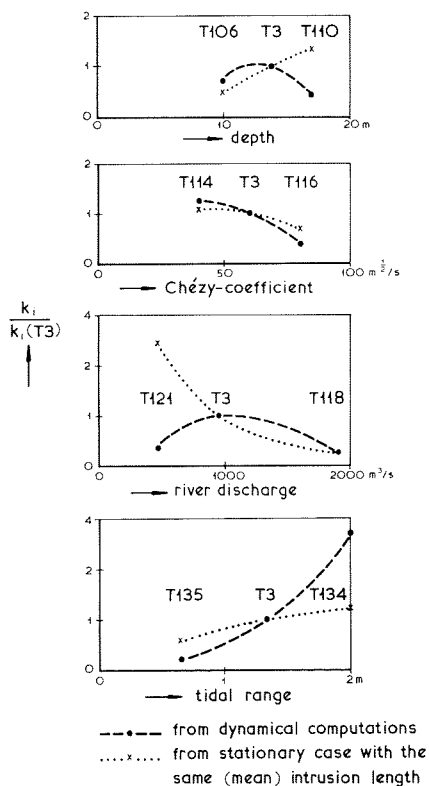
test no.	characteristic	mean intrusion length (km)	$k_i$ from Table 6 (last column)	$k_i$ from eq. (5.1.4)
T 3	cf. Table 5	17	0.0055	0.0049
T 106	$h = 10$ m	10	0.0040	0.0023
T 110	$h = 17$ m	29.5	0.0025	0.0066
T 116	$C = 80$ m $^{1/2}$ /s	25	0.0021	0.0033
T 114	$C = 40$ m $^{1/2}$ /s	16	0.0067	0.0052
T 121	$Q_f = 475$ m $^3$ /s	31	0.0020	0.0120
T 118	$Q_f = 1900$ m $^3$ /s	14.5	0.0014	0.0013
T 134	tide 2.02 m	14	0.0150	0.0059
T 135	tide 0.67 m	30.5	0.0012	0.0027

a stationary salt wedge generally will not give a correct picture. On the other hand, the value of  $k_i$  cannot be estimated from the mean position by assuming it to be stationary.

From the results of the non-steady computations in Table 6 and Fig. 26, the value of  $k_i$  can be estimated for a limited range of conditions around those of the Rotterdam Waterway (represented by T 3). The trends, especially for the water depth and the

river discharge, are such that an extrapolation seems dangerous.

As the above conclusions are derived from model tests, a verification with data from nature will be important to improve the utility of the figures.

Fig. 26. Dependence of interfacial frictional coefficient  $k_i$  on conditions.

## APPLICATION OF THE MODEL WITH MIXING

Considering the success of the computations by means of the model without mixing, and on the other hand the difficulty of specifying the parameters for the model with mixing, only one experiment with the latter is shown. It is applied again to the Rotterdam Waterway (22-6-1956). Data for the computation are given in Table 8.

Table 8. Data for case with mixing

depth $h$	14 m
storage width	600 m
stream width	350 m
density of undiluted sea-water	1025 kg/m <sup>3</sup>
density of undiluted fresh water	1000 kg/m <sup>3</sup>
river discharge $Q_f$	1000 m <sup>3</sup> /s
Chézy-coefficient $C$	60 m <sup>1/2</sup> /s
coefficient of bottom friction $k_b$	0.0028
coefficient of interfacial friction $k_i$	0.0006
mesh width $\Delta x$	500 m
time step $\Delta t$	180 s
length $L$	0
mixing coefficient $m_i$	0.0006
coefficients for convection $w_0$	0.0001
$w_1$	-0.00016

The tidal discharge has been obtained by means of a tidal computation as in cases 3 and 4 of section 7.1. The boundary condition at the river-mouth has been treated by the schematized sea method. Eq. (5.4.5) was applied at the junction. The width of the schematized sea has been taken at 5000 m; it extends 20 km on either side of the junction. The interfacial shear stress has been represented by eq. (4.4.2b). The density  $\rho_i$  at the interface has been taken from eq. (3.4.1) which is correct if the convective velocity  $W_i$  in the definition (cf. eq. (3.2.7)) is constant with respect to  $x_2$ .

Results are shown in Figs. 27 to 32. The measurements have been treated by eq. (3.4.1) to obtain the layer thickness. The velocities and densities shown are mean values in the layers thus defined. The layer thicknesses shown in Fig. 28 afterwards have been reduced to a uniform water depth of 14 m. The discharge shown in Fig. 27 is identical with Fig. 20; it is repeated for convenience. The level of the interface (Fig. 28) at flood tide is approximately correct for the three measuring sections. The irregular behaviour is probably caused by the conditions at the junction. At ebb tide the mean level is still about correct, but the slope is too large. The velocities (Figs. 29, 30) have the right order of magnitude. They are reproduced at about the same quality as in the case without mixing. The deviations at km 1030 are present in both models.

conductivity

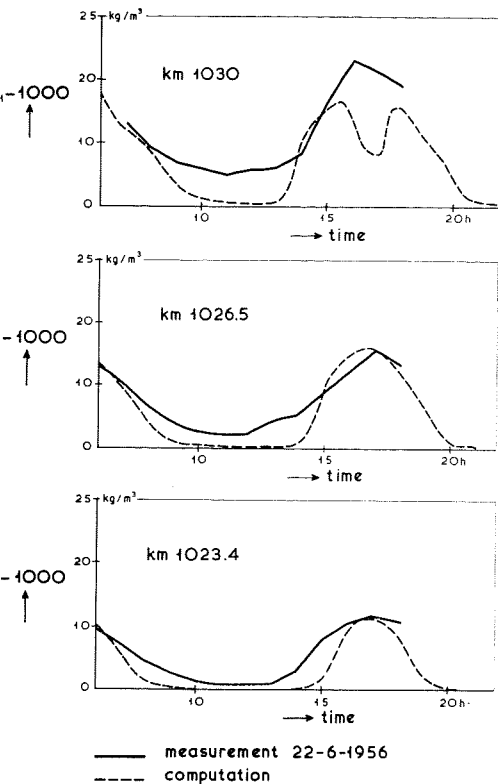


Fig. 31. Densities in upper layer for model with mixing.

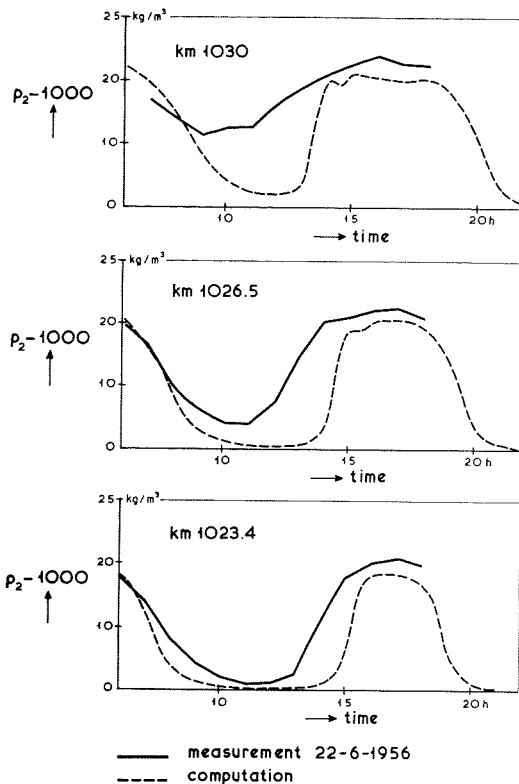


Fig. 32. Densities in lower layer for model with mixing.

This shows that they are not caused by dynamical effects, present in the model with mixing, but not in the model without. It has already been suggested that they originate from the boundary. Velocity profiles have not been computed, but it is clear that they will not have a better quality than those in Fig. 25. The velocities in the upper layer are too small at 14–15 h, which again corresponds to the deviation in the discharge curve (Fig. 27).

The new aspect of the model with mixing is found in the variable densities (Figs. 31, 32). In both figures the densities at flood tide are roughly correct. At ebb tide the density falls too low in both layers, which means that the salinity intrusion recedes too far in the computation. At flood tide, the densities at the tip of the salt wedge are not shown. They may also be too low. This would indicate that the distribution of the quantities of salt and water exchanged between the layers is not correct.

It is noted that the computation is not yet quite in equilibrium, as can be seen from the figures. Neither is the prototype, however. Therefore to make a closer comparison, one would need a larger interval of measurements (e.g. two tidal cycles). Generally it can be stated that the reproduction of the situation by the model with mixing is not

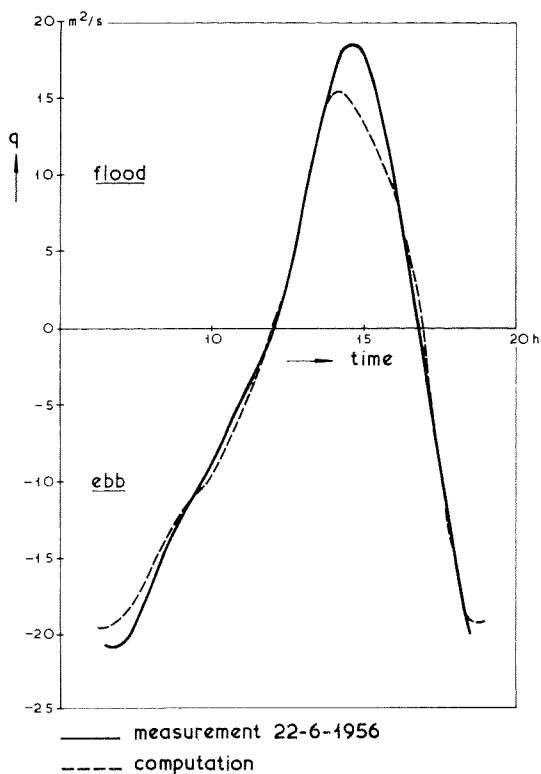


Fig. 27. Discharge at km 1030 for model with mixing.

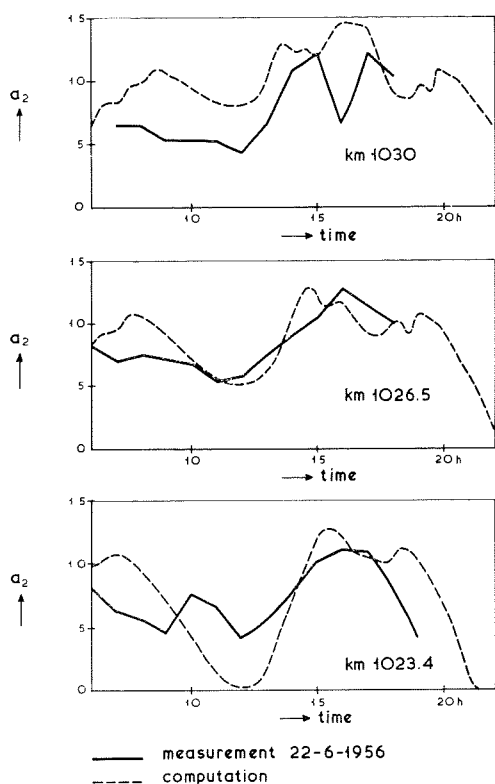


Fig. 28. Level of the interface for model with mixing.

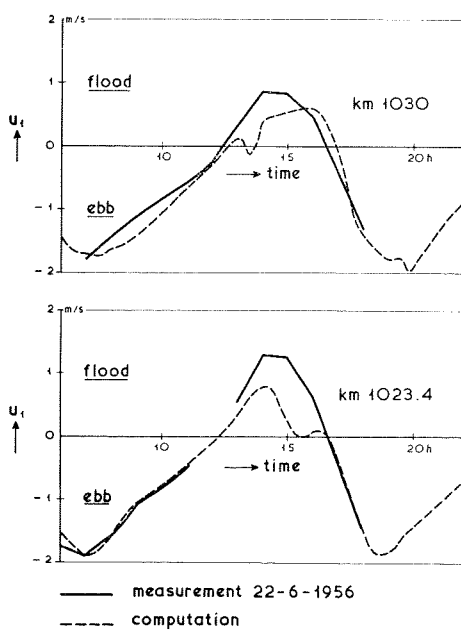


Fig. 29. Velocities in upper layer for model with mixing.

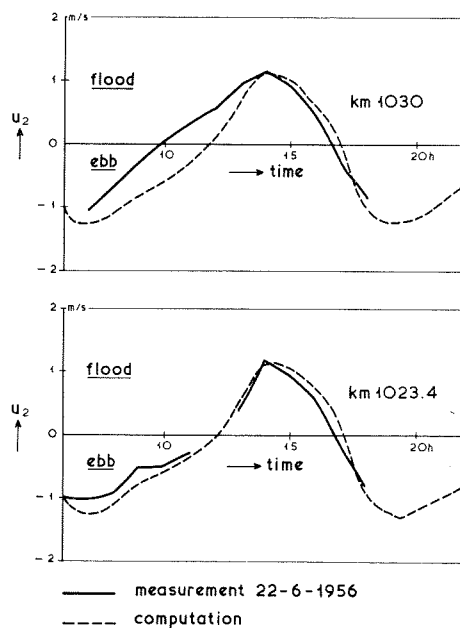


Fig. 30. Velocities in lower layer for model with mixing.

better than by the model without mixing. Of course, the information obtained is somewhat more detailed in the former case.

This behaviour of the model with mixing cannot be explained by the neglects involved in the derivation. The neglect of the dispersive salt transport and the approximation of the pressure terms in Appendix 4 are shown to be justified for this model. No neglects are made at the interface. The effect therefore must be attributed to the specification of the empirical quantities: turbulent shear stress, turbulent mass flux and convective transport through the interface. A better reproduction than obtained with the model without mixing can be obtained only if these empirical quantities are specified more correctly than in the above example. Variation of the parameters has a relatively small effect, so the expressions used are possibly not quite adequate. More justified expressions, however, require a more complete knowledge of the turbulent flow, which at present does not appear to be available. Therefore it must be concluded that the applicability of the model with mixing is still limited to those cases in which a sufficient knowledge of the turbulent processes exists. In such cases a rather complete picture can be produced with it.

## CONCLUSIONS

In this Chapter the conclusions from the preceding sections are summarized and combined. First, the performance of the two-layer models is discussed. Of course, judgment depends on the application intended, and the degree of detail required for it. For a number of the applications mentioned in the introduction it can be stated that the computations give quite reasonable results, not only for a fully stratified estuary, but also for a partly mixed one like the Rotterdam Waterway.

The baroclinic approximation, in which the long surface waves have been eliminated, produces a sufficient degree of accuracy. This has important computational advantages. Firstly, the mesh width and time-step can be chosen more or less optimally for the internal waves, without limitations because of the surface waves. In a possible tidal computation (barotropic mode) different values for the mesh width and the time-step may be used. Secondly, the computation can be limited to the region of actual salt intrusion. The economy, provided by these two reasons, will be even more effective in possible two-dimensional applications, which can be considered an extension of the present study. There is one condition for this satisfactory performance of the baroclinic approximation: the net discharge should be represented as a function of time to a good degree of accuracy. Whether or not a tidal computation is needed depends on the situation. In simple cases the discharge can be approximated by considering storage only. This conclusion leads to the remark that the method used by Voogt (1966) can give good results, even though the fixed water-level assumed in the method is not justified theoretically. The condition is that the discharge at the boundary is specified correctly.

The boundary conditions at the river-mouth have been found to be of considerable importance. Essentially, supercritical flow in either direction may occur with respect to the internal waves. These effects should be included in the mathematical model. Within this restriction the details of the treatment are not very important, as evidenced by the correspondence between the results of the critical-flow method and the schematized-sea method. It is stressed that both methods are practically independent of measured data, which is a great advantage if the model is used for prediction purposes. The discharge in the sea region required for the schematized-sea method can probably be derived with sufficient accuracy from basic tidal data. It is recalled that the critical-flow method is not sufficient for the model with mixing.

Concerning the models with and without interfacial mixing, two remarks should be made. Due to the more correct representation of the densities, the model with mixing will be superior in the reproduction of the hydrodynamic phenomena. However, this advantage is offset to a large extent by the difficulty of specifying the empirical quan-

tities involved. Physical knowledge at present is insufficient for this purpose. Even if a correct representation of some situation is obtained, the prediction of the parameters remains a great problem. Therefore the model without mixing will be generally preferred, unless of course information on the density or salinity essentially is required.

The empirical parameters present the most important problem in the applications. Concerning the formulation for the interfacial shear stress, it can be concluded that neither of the two proposed expressions in eq. (4.4.2) is ideal. One produces more correct values for the level of the interface (i.e. for the mean density); the other results in more accurate velocities. It would seem important, however, that at any rate eq. (4.4.4) is satisfied in the marginal case of homogeneous flow. A real improvement probably requires more experimental data. Apart from this difficulty, the value of the interfacial shear stress coefficient  $k_i$  can be determined by hindcasting a known situation. The difficulty mentioned by Boulot and Daubert (1969) that the salt wedge probably never is in dynamical equilibrium, does not make this determination impossible. It should be realised that the resulting value applies only to the investigated situation. It is not permissible to assume the salt wedge to be stationary at its mean position. Some idea of the influence of different conditions has been obtained by considering a number of flume tests. Further verification of the trends will be important. Similar approximations for the parameters in the case with mixing have so far been impossible, because the model is not very suitable for hindcasting, considering the relatively large number of empirical parameters.

It is concluded that the two-layer model without mixing is satisfactory for applications requiring only mean velocities in each layer, and cross-sectional mean densities. The latter can be derived from the layer thickness, by means of eq. (3.4.3). Reproduction of the shear stress at the bottom has not been verified, as experimental data are lacking. For applications in which velocity profiles are important an approximation can be given. The accuracy probably can hardly be increased by considering a more elaborate description of turbulent processes, as it depends mainly on the accuracy of the mean velocities. The profiles provide not more than a kind of interpolation between the mean velocities computed by means of the two-layer model. If, in addition, density profiles are required, in principle the model with mixing can produce them, but this will be successful only if the empirical quantities can be specified satisfactorily.

For any application a number of data are required apart from those defining the problem. The main ones are the vertical tide  $h$  and the horizontal tide  $q$  in at least one cross-section. As stated above, the boundary conditions at the river-mouth can be reasonably predicted. Empirical parameters can be predicted less well. Therefore, as in the case of a hydraulic model, calibration of the model will be necessary. This requires measurements of at least some density or salinity profiles, and preferably also some velocity measurements.

Finally, some extensions and possible fields of application are mentioned.

- a. Although the present study is mainly concerned with estuaries, this is not the only possibility. The method can be applied to any system of channels (e.g. the Euro-poort harbour complex in the Netherlands). The main problem of this extension will be found in the formulation and treatment of the boundary conditions at the junctions.
- b. A non-tidal application is the propagation of a salt-water front during the exchange process of a shipping-lock. This situation is discussed by Abraham and Vreugdenhil (1970). The behaviour of a steep salt water front is more important in this case than in the case of an estuary, discussed in the present study. Empirical data on the behaviour are necessary for a good reproduction.
- c. An important application is the case of thermal stratification, e.g. cooling water circulation, or circulation of pollutants in thermally stratified reservoirs. Except for a reformulation of the equations in terms of temperature, the same techniques can be applied as in the present case. Mixing, entrainment, radiation and similar phenomena should be formulated in a representative way.
- d. The influence of wind on the circulation can be incorporated relatively simply in the model, assumed that the wind stress and its effect on the shear stress in the water-layers can be specified. This is the same kind of information as required for e.g. storm-surge calculations, wind set-up in lakes and the like.
- e. By means of the velocity profiles (and possibly the density profiles) an impression can be obtained of the dispersion of pollutants in any of the above cases.
- f. All these and similar applications can be extended to two-dimensional areas. The computational problems involved have been investigated in other branches of applied mathematics. Again the turbulent shear stress should be reconsidered, as not only its magnitude but also its direction should be known.

## REFERENCES

- ABBOTT, M. B. and I. TORBE, 1963, On flows and fronts in a stratified fluid, *Proc. Roy. Soc. A* **273**, 12-40.
- ABRAHAM, G. and C. B. VREUGDENHIL, 1970, Discontinuities in stratified flows, *J. Hydr. Res.* (to appear).
- BONNEFILLE, R. and J. GODDET, 1959, Etude des courants de densité en canal, 8th Congress IAHR, Montreal, paper C 14.
- BOULOT, F., P. BRACONNOT and PH. MARVAUD, 1967, Détermination numérique des mouvements d'un coin salé, *La Houille Blanche* **22**, 8, 871-877.
- BOULOT, F. and A. DAUBERT, 1969, Modèle mathématique de la salinité sous une forme stratifiée en régime non-permanent, 13th Congress IAHR, Kyoto, paper C 38.
- BOUSSINESQ, J., 1903, *Théorie analytique de la chaleur*, Gauthier-Villars, Paris.
- BOWDEN, K. F., 1962, The mixing processes in a tidal estuary, *Int. Conf. Water Poll. Res.*, London 1962, paper 3-33.
- BRADSHAW, P., 1967, The turbulence structure of equilibrium boundary layers, *J. Fluid Mech.* **29**, 4, 625-645.
- BRADSHAW, P., D. H. FERRISS and N. P. ATWELL, 1967, Calculation of boundary-layer development using the turbulent energy equation, *J. Fluid Mech.* **28**, 3, 593-616.
- BURGH, P. VAN DER, 1968, Prediction of the extent of salt water intrusion into estuaries and seas, *J. Hydr. Res.* **6**, 4, 267-288.
- CHOW, VEN TE, 1959, *Open channel hydraulics*, McGrawhill, New York.
- COLE, J. D., 1968, *Perturbation methods in applied mathematics*, Blaisdell Publ. Cy., Waltham, Mass.
- COURANT, R. and D. HILBERT, 1962, *Methods of mathematical physics II*, Interscience Publ., New York.
- CSANADY, G. T., 1967, Large scale motion in the Great Lakes, *J. Geoph. Res.* **72**, 16, 4151-4162.
- CSANADY, G. T., 1968a, Wind-driven summer circulation in the Great Lakes, *J. Geoph. Res.* **73**, 8, 2579-2589.
- CSANADY, G. T., 1968b, Motions in a model Great Lake due to a suddenly imposed wind, *J. Geoph. Res.* **73**, 20, 6435-6447.
- DORODNITSYN, A. A., 1964, "Exact" numerical methods in the boundary-layer theory, *Fluid Dynamics Trans.* **1**, 59-71.
- VAN DYKE, M., 1964, *Perturbation methods in fluid mechanics*, Academic Press, New York.
- ECKART, C., 1962, The equations of motion of sea-water, in: M. N. Hill (ed.), *The Sea*, vol. I p. 31-41, Interscience Publ. New York.
- ELLISON, T. H., 1957, Turbulent transport of heat and momentum from an infinite rough plane, *J. Fluid Mech.* **2**, 5, 456-466.
- ELLISON, T. H. and J. S. TURNER, 1960, Mixing of a dense fluid in a turbulent pipe flow, *J. Fluid Mech.* **8**, 4, 514-544.
- FRANCIS, J. R. D., H. STOMMEL, H. G. FARMER and D. PARSON, 1953, Observation of turbulent mixing processes in a tidal estuary, *Woods Hole Oceanogr. Inst.*, Tech. Rep. 53-22.
- HANSEN, D. V., 1967, Salt balance and circulation in partially mixed estuaries, in: G. H. Lauff (ed.), *Estuaries*, Washington, 1967, p. 45-51.
- HANSEN, D. V. and M. RATTRAY, 1966, New dimensions in estuary classification, *Limnology and Oceanography* **11**, 3, 319-326.
- HARLEMAN, D. R. F., 1961, Stratified flow, Chapter 26 in *Handbook of Fluid Dynamics* (V. L. Streeter, ed.), McGrawhill, New York.
- HARLEMAN, D. R. F. and G. ABRAHAM, 1966, One-dimensional analysis of salinity intrusion in the Rotterdam Waterway, Delft Hydr. Lab., Publ. no. 44.

- HARLEMAN, D. R. F. and A. T. IPPEN, 1967, Two-dimensional aspects of salinity intrusion in estuaries, Tech. Bull. 13, Committee on Tidal Hydraulics, Corps of Engineers, U.S. Army.
- HINZE, J. O., 1959, Turbulence, McGrawhill, New York.
- IPPEN, A. T. and D. R. F. HARLEMAN, 1961, One-dimensional analysis of salinity intrusion in estuaries, Tech. Bull. 5, Committee on Tidal Hydraulics, Corps of Engineers, U.S. Army.
- KASAHARA, A., E. ISAACSON and J. J. STOKER, 1965, Numerical studies of frontal motion in the atmosphere I, *Tellus* **17**, 3, 261–277.
- KASHIWAMURA, M. and S. YOSHIDA, 1969, Flow pattern of density current at a river-mouth, 13th Congress IAHR, Kyoto, paper C 20.
- KENT, R. E. and D. W. PRITCHARD, 1959, A test of mixing length theories in a coastal plain estuary, *J. Mar. Res.* **18**, 1, 62–72.
- KEULEGAN, G. H., 1966, The mechanism of an arrested saline wedge, Ch. 11 in: A. T. Ippen (ed.), *Estuary and coastline hydrodynamics*, McGrawhill, New York.
- LEENDERTSE, J. J. 1967, Aspects of a computational model for long-period water-wave propagation, RAND Memorandum RM 5294-PR, also Thesis Delft 1967.
- LUMLEY, J. L. and H. A. PANOFKY, 1964, The structure of atmospheric turbulence, Interscience Publ., New York.
- NEUMANN, G. and W. J. PIERSON, Jr., 1966, Principles of physical oceanography, Prentice-Hall Inc., New York.
- O'BRIEN, G. G., M. A. HYMAN and S. KAPLAN, 1951, A study of the numerical solution of partial differential equations, *J. Math. Phys.* **29**, 223–251.
- O'BRIEN, J. J. and R. O. REID, 1967, The nonlinear response of a two-layer baroclinic ocean to a stationary axially symmetric hurricane I, II, *J. Atm. Sci.* **24**, 2, 197–215.
- OKUBO, A., 1964, Equations describing the diffusion of an introduced pollutant in a one-dimensional estuary, *Studies on Oceanography* 1964, 216–226.
- OSWATITSCH, K., 1959, *Physikalische Grundlagen der Strömungslehre*, Handbuch der Physik VIII/1 (Strömungsmechanik I), Springer, Berlin 1959.
- PRANDTL, L., 1929, Einfluss stabilisierender Kräfte auf die Turbulenz, *Vorträge a.d. Gebiete der Aerodynamik und verwandter Gebiete* (Aachen 1929) p. 1–7.
- REES, A. J. VAN and B. P. RIGTER, 1969, Flume study on salinity intrusion in estuaries, 13th Congress IAHR, Kyoto, paper C 33.
- RICHTMYER, R. D. and K. W. MORTON, 1967, *Difference-methods for initial-value problems*, Interscience Publ., New York.
- RIGTER, B. P., 1970, Density-induced return-currents in outlet channels, *J. ASCE* **96**, HY 2, 529–546.
- RYABENKI, V. S. and A. F. FILIPPOV, 1960, Über die Stabilität von Differenzen-gleichungen, VEB Deutscher Verlag der Wissenschaften, Berlin.
- SCHMITZ, H. P., 1964, Modellrechnungen zu winderzeugten Bewegungen in einem Meer mit Sprungschicht, *Deutsche Hydrogr. Z.* **17**, 5, 201–230.
- SCHMITZ, H. P., 1967, A numerical approximation of the monsoon-generated circulation in the Arabian Sea, *Deutsche Hydrogr. Z.* **20**, 5, 205–217.
- SCHIFF, J. B. and J. C. SCHÖNFELD, 1953, Theoretical considerations on the motion of salt and fresh water, IAHR Congr. Minnesota.
- STEWART, R. W., 1959, The problem of diffusion in a stratified fluid, *Adv. Geophysics* **6**, 303–311.
- STIGTER, C. and J. SIEMONS, 1967, Calculation of longitudinal salt-distribution in estuaries as a function of time, Publ. no. 52, Delft Hydraulics Laboratory.
- STOMMEL, H. and H. G. FARMER, 1952, Abrupt change in width in two-layer open-channel flow, *J. Mar. Res.* **11**, 2, 205–214.
- TAREYEV, B. A., 1968, Non-geostrophic disturbances and baroclinic instability in two-layered oceanic flow, *Izv., Atmosph. and Oceanic Physics* **4**, 12, 730–734.
- TOWNSEND, A. A., 1956, *The structure of turbulent shear flow*, Cambridge Univ. Press.
- TOWNSEND, A. A., 1958, Turbulent flow in a stably stratified atmosphere, *J. Fluid Mech.* **3**, 4, 361–372.
- TOWNSEND, A. A., 1961, Equilibrium layers and wall turbulence, *J. Fluid Mech.* **11**, 1, 97–120.
- VLIEGENTHART, A. C., 1969, Dissipative difference schemes for shallow water equations, *J. Eng. Math.* **3**, 2, 81–94.
- VOOGT, J., 1966, Investigation of the salt wedge by means of the method of characteristics, Rijks-waterstaat Nota MFA 6612 (in Dutch).

- VREUGDENHIL, C. B., 1968, Discussion of the paper „Difference solutions to the shallow-water equations” by Liggett and Woolhiser, J. ASCE **94**, EM1, 334–339.
- VREUGDENHIL, C. B., 1969, On the effect of artificial-viscosity methods in calculating shocks, J. Eng. Math. **3**, 4, 285–288.
- VREUGDENHIL, C. B., 1970, Two-layer model of stratified flow in an estuary, La Houille Blanche, **25**, 1, 35–40.
- WADA, A., 1969, Numerical analysis of flow and thermal diffusion caused by outfall of cooling water, 13th Congress IAHR, Kyoto, paper C 36.
- WEIGAND, J. G., H. G. FARMER, S. J. PRINSENBURG and M. RATTRAY, Jr., 1969, Effects of friction and surface tide angle of incidence on the coastal generation of internal tides, J. Mar. Res. **27**, 2, 241–259.
- WOOSTER, W. S., A. J. LEE and G. DIETRICH, 1969, Redefinition of salinity, J. Mar. Res. **27**, 3, 358–360.

## NOTATION

		dimension
$a_{1,2}$	thickness of upper and lower layer	m
$A_{1,2}$	cross-sectional area of upper and lower layer	$m^2$
$A$	matrix in system of differential equations	
$b_s$	width of the "sea"	m
$b_w$	width of the estuary	m
$B$	matrix in system of differential equations	
$c$	velocity of propagation	m/s
$c_r$	relative velocity of propagation	—
$C_{1,2}$	wetted perimeter of upper and lower layer	m
$D$	damping factor	—
$D_s$	molecular diffusion of salt	$kg/m^3/s$
$f$	turbulent mass-flux	$kg/m^2/s$
$f$	terms in differential equations	
$F_{1,2}$	dispersive mass-flux	kg/s
$F$	internal Froude number $(u_1 - u_2)(\epsilon gh)^{-\frac{1}{2}}$	—
$F_i$	internal Froude number $U(gh\Delta\rho/\rho)^{-\frac{1}{2}}$	—
$F_f$	internal Froude number $q_f(\epsilon gh^3)^{-\frac{1}{2}}$	—
$g$	acceleration due to gravity	$m/s^2$
$h$	water-depth	m
$h_b$	bottom-level	m
$h_i$	level of the interface	m
$h_s$	water-level	m
$I$	bottom-slope, also identity-matrix	
$k$	wave-number	$m^{-1}$
$k_{b,i}$	coefficients for friction at bottom and interface	—
$l$	wave-length	m
$l_{1,2}$	length parameters in energy equations	m
$l_{t,f}$	mixing-lengths for momentum and mass transfer	m
$L$	length-scale, also: length of estuary considered	m
$L_w$	length of stationary salt wedge	m
$m_i$	mixing coefficient at interface	—
$M$	amplification matrix	—
$n_j$	normal vector	—
$N$	dimension of $A$	—
$p$	pressure	$N/m^2$

$q$	discharge per unit width	$\text{m}^2/\text{s}$
$q_L$	value of $q$ at $x = L$	$\text{m}^2/\text{s}$
$q_f$	river-discharge per unit width	$\text{m}^2/\text{s}$
$Q$	discharge	$\text{m}^3/\text{s}$
$r$	relative intensity of turbulence, also: eigenvalue	—
$R$	matrix in system of differential equations	
$Re$	Reynolds number $Uh/\nu$	—
$Rf$	flux Richardson number	—
$Ri$	local Richardson number	—
$s$	dimensionless density difference	—
$S$	salinity	—
$Sc$	turbulent Schmidt number	—
$t$	time	$\text{s}$
$T$	time-scale, also: propagation factor	$\text{s}$
$u_i$	longitudinal velocity at the interface	$\text{m}/\text{s}$
$\bar{u}$	mean velocity	$\text{m}/\text{s}$
$u_*$	shear velocity $(\tau_b/\varrho_0)^{\frac{1}{2}}$	$\text{m}/\text{s}$
$\mathbf{u}$	vector of unknowns in differential equations	
$U$	scale of longitudinal velocity	$\text{m}/\text{s}$
	also: dimensionless velocity	—
$v_j$	component of velocity in $x_j$ direction	$\text{m}/\text{s}$
$w_i$	vertical velocity relative to the interface	$\text{m}/\text{s}$
$W_i$	local vertical velocity relative to the interface	$\text{m}/\text{s}$
$W$	parameter denoting amount of work	—
$x_j$	coordinate ( $x_1$ longitudinal, $x_2$ lateral, $x_3$ vertical upward)	$\text{m}$
$z$	vertical coordinate	$\text{m}$
$z_0$	level of zero velocity	$\text{m}$
$\alpha$	parameter in mixing-length	—
$\beta$	relative error in pressure term	—
$\beta_{1,2}$	coefficients of energy loss at the river-mouth	—
$\delta_{ij}$	Kronecker-delta ( $= 1$ if $i = j$ , else 0)	—
$\Delta t$	time-step	$\text{s}$
$\Delta x$	mesh width	$\text{m}$
$\Delta \varrho$	density difference	$\text{kg}/\text{m}^3$
$\varepsilon$	relative density difference	—
$\eta$	dimensionless vertical coordinate	—
$\theta$	coefficient of molecular diffusion	$\text{m}^2/\text{s}$
$\kappa$	Von Kármán's constant	—
$\lambda$	dimensionless mixing length	—
$\lambda_M$	amplification factor, eigenvalue of $M$	—
$\mu$	parameter in difference equations $c \Delta t/\Delta x$	—

$\nu$	coefficient of kinematic viscosity	$\text{m}^2/\text{s}$
$\xi$	parameter in difference equations ( $k\Delta x$ )	—
$\varrho$	density	$\text{kg}/\text{m}^3$
$\varrho_{\text{sea}}$	density of sea-water	$\text{kg}/\text{m}^3$
$\varrho_f$	density of fresh water	$\text{kg}/\text{m}^3$
$\varrho_M$	spectral radius of $M$	—
$\sigma$	ratio of shear stresses $\tau_i$ and $\tau_b$	—
$\tau$	turbulent shear stress	$\text{N}/\text{m}^2$
—	time average	
'	deviation from time average	
$s$	surface	
$i$	interface	
$b$	bottom	
$1$	mean value in upper layer	
$2$	mean value in lower layer	
$\langle \rangle$	cross-sectional mean value	
$( )_t$	tidal mean value	

## SUMMARY

A great deal of literature has been devoted to gravity currents in estuaries. However, more or less detailed theoretical models of these phenomena are scarce. This is partly due to the fact that the equations have been difficult to solve if they describe the situation with some generality. This difficulty is surmounted by the use of digital computers. A more fundamental drawback is the lack of knowledge concerning the physical processes of turbulent flow in a stratified fluid. This precludes a detailed two- or three-dimensional description of the flow-pattern.

Some schematical models exist which give an overall picture of the flow, still taking variations in space (along the estuary) and time (with the tide) into account. One of these is the two-layer model that is the subject of the present study. It is found that a great part of the information required for engineering applications can be obtained from it.

A salt water and a fresh water layer are assumed to be present, either with or without mixing between them. Although flow in most estuaries is not strictly stratified, the two-layer schematization can be useful. This follows from an investigation of the approximations involved in the derivation of the equations. Empirically, the same fact is demonstrated by applying the two-layer model to the partly mixed Rotterdam Waterway.

Knowledge of the turbulent flow processes, though in a less detailed form, is still required for a two-layer model, mainly to describe turbulent friction and mixing at the interface, as well as convection through it. If the interface is assumed to be impermeable, only the turbulent friction remains as an empirical parameter. Although the dynamical processes are reproduced less well in this case, the applicability is found to be superior, due to the small number of empirical parameters. Too little is yet known concerning the exchange of salt and water between the layers to permit a more detailed reproduction by means of the model with mixing. The latter therefore will be applied only if information on the salinity is required.

The two-layer models result in mean velocities in each layer, and for the case with mixing also in mean densities. These parameters can be applied to define a family of velocity and density profiles. Combined with a crude model of the turbulent structure, this turns out to give reasonably realistic profiles. Therefore as an extension of the two-layer model an estimate of the velocity (and density) profiles can be given.

The theory is verified by means of the 1956 measurements in the Rotterdam Waterway. A satisfactory correspondence is found, especially for the case without mixing. An estimate of the interfacial frictional coefficient as a function of the global conditions is obtained by hindcasting a number of flume tests.

Although the present study is concerned mainly with estuaries, the two-layer model can be applied to several other cases of stratified flow, notably those concerned with thermal stratification. Such applications, however, require specific descriptions of empirical quantities, like mixing, friction, radiation.

## SAMENVATTING

Een grote hoeveelheid literatuur is gewijd aan gelaagde stroming in getij-rivieren. Enigszins gedetailleerde modellen van deze verschijnselen zijn echter schaars. Dit wordt gedeeltelijk veroorzaakt doordat de vergelijkingen, die nodig zijn om de situatie in zijn algemeenheid te beschrijven, moeilijk opgelost kunnen worden. Deze moeilijkheid kan worden overwonnen door de toepassing van een rekentug. Een meer fundamentele moeilijkheid wordt gevormd door het gebrek aan inzicht in de processen die zich afspelen bij de turbulente stroming in een gelaagde vloeistof. Hierdoor wordt een gedetailleerd twee- of drie-dimensionaal beeld van het stroombeeld uitgesloten.

Er bestaan een aantal schematische voorstellingen, die een globaal beeld van de stroming geven, maar toch rekening houden met de variaties in plaats (langs de getij-rivier) en tijd (met het getij). Het twee-lagen-model, dat in dit onderzoek aan de orde wordt gesteld, is er één van. Het blijkt dat een groot deel van de voor technische toepassingen benodigde gegevens uit dit model kunnen worden afgeleid.

Er wordt verondersteld dat er een zoute en een zoete laag bestaan, al of niet met uitwisseling. Hoewel de meeste getijrivieren geen stroming in twee duidelijke lagen vertonen, kan het model toch van toepassing zijn. Dit volgt uit een beschouwing van de bij de afleiding van de vergelijkingen gemaakte benaderingen. Hetzelfde feit wordt getoond door toepassing van het twee-lagen model op de gedeeltelijk gemengde Nieuwe Waterweg.

Ook voor een twee-lagen model moet er een zekere kennis van de turbulente processen zijn, hoewel minder gedetailleerd. Deze heeft vooral betrekking op de turbulente wrijving en menging aan het grensvlak en op de convectie door het grensvlak. Wanneer het grensvlak als ondoorlatend wordt beschouwd, blijft van deze grootheden alleen de turbulente wrijving over. Hoewel in dit geval de dynamische processen wat minder goed worden weergegeven, zijn de toepassingsmogelijkheden groter in verband met het kleine aantal empirische parameters. Er is nog te weinig bekend van de uitwisseling van water en zout door het grensvlak om door middel van het model met menging een nauwkeuriger beeld van de situatie te verkrijgen. Dit model zal dus alleen toegepast worden als er gegevens over de zoutconcentratie vereist zijn.

Uit de twee-lagen modellen worden gemiddelde snelheden in iedere laag afgeleid, alsmede gemiddelde dichtheden voor het geval met menging. Met behulp van deze parameters en een ruw model van de turbulentie kan een familie van snelheids- en dichtheids-profielen worden gedefinieerd. Langs deze weg blijkt een redelijk realistische beschrijving van de profielen mogelijk te zijn. De snelheids- (en dichtheids-) profielen kunnen dus als uitbreiding van het twee-lagen model worden verkregen.

De theorie wordt getoetst aan de hand van in 1956 uitgevoerde metingen in de Nieuwe Waterweg. Er wordt een bevredigende overeenstemming gevonden, vooral voor het geval zonder menging. Door het narekenen van een aantal goot-proeven wordt een schatting gemaakt van de wrijvings-coëfficiënt aan het grensvlak als functie van de omstandigheden.

Hoewel dit onderzoek hoofdzakelijk op getij-rivieren is gericht, kan het twee-lagen model ook voor andere gevallen van gelaagde stroming gebruikt worden, met name voor gevallen van thermische gelaagdheid. Zulke toepassingen vereisen echter wel een eigen beschrijving van empirische grootheden zoals menging, wrijving, straling.

## APPENDIX

### 1 Numerical method

The system of differential equations derived in Chapter 3 is a quasi-linear hyperbolic system in one spatial dimension. As a method of solution a finite-difference method is chosen. The alternative formed by the method of characteristics has not been applied mainly for two reasons. Firstly, the mesh-spacing may become very irregular, which introduces unpredictable inaccuracies. Secondly, the possibility of an extension to two spatial dimensions is kept in mind, for which the method of characteristics is of a considerably greater complication.

The choice of a specific finite-difference method is determined by several considerations. The most important one is the numerical accuracy. A specified accuracy should be reached, spending as little effort as possible. Secondly, when applied to a non-linear system as present here, the method should not be subject to non-linear instabilities. Thirdly, it should not give difficulties when steep fronts occur, schematized mathematically by discontinuities.

No attempt has been made to find a difference-method which is optimal with respect to the above requirements. From the known methods, a choice has been made for the Lax-Wendroff method (c.f. Richtmyer and Morton 1967; this reference is denoted by RM in this section). It is an explicit method. Although an implicit method is less restrictive with respect to stability considerations, it need *not* be much more economical, as the numerical accuracy does not allow much larger step-widths than can be used for an explicit method. This is shown in some more detail in a paper by Vreugdenhil (1968), where the Lax-Wendroff method is found to compare favourably to other methods in this respect. As to non-linear instabilities, no rigorous criterion is known to prevent them, but it is generally considered important that a method is dissipative. Below, this is shown to be the case. Finally, the truncation error works as an artificial viscosity, which makes possible the automatic calculation of shocks. This too is discussed below.

The Lax-Wendroff method is applied in its one-step version (RM p. 302). The reason is that the intermediate step in the two-step version has a lower order of accuracy. This may cause difficulties in the treatment of the boundary conditions. As far as possible the system of equations is written in the form of conservation laws, i.e.,

$$\frac{\partial \mathbf{u}}{\partial t} + \frac{\partial \mathbf{f}}{\partial x} + \mathbf{h} = 0 \quad (\text{A } 1.1)$$

where  $\mathbf{u}$  is the vector of dependent variables and  $\mathbf{f}$  and  $\mathbf{h}$  are vector functions of it.

The dynamical equation (6.3.20) is not a physical conservation law. Moreover, it cannot even be written in this form for the case with mixing. The system always can be written as

$$\frac{\partial \mathbf{u}}{\partial t} + A \frac{\partial \mathbf{u}}{\partial x} + \mathbf{h} = 0 \quad (\text{A } 1.2)$$

If eq. (A 1.1) applies,  $A$  is the Jacobian of  $\mathbf{f}$  with respect to  $\mathbf{u}$ . For simplicity the following derivations are applied to eq. (A 1.1). For the form (A 1.2) results are shown, obtained along the same lines. It is noted that for the present problem the presence of the functions  $q$  and  $h$ , known from eqs. (6.3.22) and (6.3.23), causes the occurrence of additional terms in the non-derivative part  $\mathbf{h}$  in (A 1.2) and in the Lax-Wendroff scheme.

The Lax-Wendroff method consists in forming an approximation of the Taylor-series

$$\mathbf{u}_j^{n+1} = \mathbf{u}_j^n + \Delta t \left( \frac{\partial \mathbf{u}}{\partial t} \right)_j^n + \frac{1}{2} \Delta t^2 \left( \frac{\partial^2 \mathbf{u}}{\partial t^2} \right)_j^n + \dots$$

which by means of the differential equation is written as

$$\mathbf{u}_j^{n+1} = \mathbf{u}_j^n - \Delta t \left( \frac{\partial \mathbf{f}}{\partial x} + \mathbf{h} \right)_j^n + \frac{1}{2} \Delta t^2 \left\{ \frac{\partial}{\partial x} \left( A \frac{\partial \mathbf{f}}{\partial x} \right) \right\}_j^n + \dots \quad (\text{A } 1.3)$$

The notation  $\mathbf{u}_j^n$  is to be understood as  $\mathbf{u}(j\Delta x, n\Delta t)$ . In the last term of eq. (A 1.3) the term  $\mathbf{h}$  has been omitted, which means that it is represented to a lower order of accuracy. This is mainly because it consists of empirical quantities that do not justify a painstaking treatment. When the conservation law form cannot be carried through, eq. (A 1.3) is written in subscripted form as

$$(u_i)_j^{n+1} = (u_i)_j^n - \Delta t \left( A_{ik} \frac{\partial u_k}{\partial x} + h_i \right)_j^n + \frac{1}{2} \Delta t^2 \left\{ B_{ikl} A_{lm} \frac{\partial u_m}{\partial x} \frac{\partial u_k}{\partial x} + A_{ik} \frac{\partial}{\partial x} \left( A_{kl} \frac{\partial u_l}{\partial x} \right) \right\}_j^n$$

where the summation convention again is used. Here

$$B_{ikl} = \frac{\partial A_{ik}}{\partial u_l}$$

The derivatives with respect to  $x$  are now approximated by finite differences, producing the Lax-Wendroff scheme

$$\begin{aligned} \mathbf{u}_j^{n+1} = & \mathbf{u}_j^n - \frac{1}{2} \frac{\Delta t}{\Delta x} (\mathbf{f}_{j+1}^n - \mathbf{f}_{j-1}^n) - \Delta t \mathbf{h}_j^n + \\ & + \frac{1}{2} \left( \frac{\Delta t}{\Delta x} \right)^2 \{ A_{j+\frac{1}{2}}^n (\mathbf{f}_{j+1}^n - \mathbf{f}_j^n) - A_{j-\frac{1}{2}}^n (\mathbf{f}_j^n - \mathbf{f}_{j-1}^n) \} \end{aligned} \quad (\text{A } 1.4)$$

The matrices  $A_{j+\frac{1}{2}}^n$  and  $A_{j-\frac{1}{2}}^n$  are approximated by the mean of the values at the adjacent mesh-points.

The truncation error is determined by expanding all terms of eq. (A 1.4) into a Taylor series with respect to the central mesh-point  $(j, n)$ . The empirical term being represented at a lower accuracy, it is left out for this purpose. Then

$$u_j^{n+1} - u_j^n = \Delta t \frac{\partial u}{\partial t} + \frac{1}{2} \Delta t^2 \frac{\partial^2 u}{\partial t^2} + \frac{1}{6} \Delta t^3 \frac{\partial^3 u}{\partial t^3} + \dots$$

The  $k$ -th element of this vector equation reads in subscripted form:

$$\Delta t \frac{\partial u_k}{\partial t} + \frac{1}{2} \Delta t^2 \frac{\partial}{\partial x} \left( A_{ki} \frac{\partial f_i}{\partial x} \right) - \frac{1}{6} \Delta t^3 \frac{\partial}{\partial x} \left\{ B_{kim} \frac{\partial f_i}{\partial x} \frac{\partial f_m}{\partial x} + A_{ki} \frac{\partial}{\partial x} \left( A_{im} \frac{\partial f_m}{\partial x} \right) \right\} + \dots$$

Here

$$A_{ki} = \frac{\partial f_k}{\partial u_i} \quad \text{and} \quad B_{kim} = \frac{\partial^2 f_k}{\partial u_i \partial u_m}$$

All quantities apply to the central mesh-point. Further

$$(f_k)_{j+1}^n - (f_k)_{j-1}^n = 2\Delta x \frac{\partial f_k}{\partial x} + \frac{1}{3} \Delta x^3 \frac{\partial^3 f_k}{\partial x^3} + \dots$$

and the term

$$\frac{1}{2} (A_{j+1}^n + A_j^n) (f_{j+1}^n - f_j^n) - \frac{1}{2} (A_j^n + A_{j-1}^n) (f_j^n - f_{j-1}^n)$$

gives in subscripted form

$$\Delta x^2 \frac{\partial}{\partial x} \left( A_{ki} \frac{\partial f_i}{\partial x} \right) + O(\Delta x^4)$$

Combining these expressions one finds from (A 1.4):

$$\frac{\partial u_k}{\partial t} + \frac{\partial f_k}{\partial x} = \frac{1}{6} \Delta t^2 \frac{\partial}{\partial x} \left\{ B_{kim} \frac{\partial f_i}{\partial x} \frac{\partial f_m}{\partial x} + A_{ki} \frac{\partial}{\partial x} \left( A_{im} \frac{\partial f_m}{\partial x} \right) \right\} - \frac{1}{6} \Delta x^2 \frac{\partial^3 f_k}{\partial x^3} + \dots \quad (\text{A 1.5})$$

A similar result can be obtained starting from eq. (A 1.2). This indicates that the method has a second order accuracy according to the definition (RM p. 68)

$$\|u(x, t + \Delta t) - Mu(x, t)\| = O(\Delta t^3)$$

where  $M$  is the operation defined by eq. (A 1.4), applied to a solution of the differential equation. Then, as stated e.g. by Ryabenki and Filippov (1960), the discretization-error is also of the second order in  $\Delta t$ , i.e.

$$\|u_j^n - u(x, t)\| = O(\Delta t^2)$$

if the method is stable in the sense of Lax and Richtmyer. Here  $u(x, t)$  represents the solution of the differential equation.

The stability and the overall accuracy of the method are investigated for a linearized problem, i.e. the matrix  $A$  is assumed to be constant. In this case, whether or not the conservation law form is valid, the difference equation (A 1.4) simplifies to

$$\begin{aligned} u_j^{n+1} = & \left\{ -\frac{1}{2} \frac{\Delta t}{\Delta x} A + \frac{1}{2} \left( \frac{\Delta t}{\Delta x} A \right)^2 \right\} u_{j+1}^n + \left\{ I - R\Delta t - \left( \frac{\Delta t}{\Delta x} A \right)^2 \right\} u_j^n + \\ & + \left\{ \frac{1}{2} \frac{\Delta t}{\Delta x} A + \frac{1}{2} \left( \frac{\Delta t}{\Delta x} A \right)^2 \right\} u_{j-1}^n \end{aligned} \quad (\text{A } 1.6)$$

where  $R$  is the Jacobian of  $h$  with respect to  $u$  and  $I$  is the identity-matrix. The entire set of operations in a time-step can therefore be expressed by a block-tridiagonal matrix  $M$  with the elements shown in eq. (A 1.6). Now the matrix  $R$  generally will not have the same eigenvectors as  $A$ . First the effect of  $R$  is ignored. The eigenvectors of  $A$  are denoted by  $U_m$ . The number of them is  $N$ , the dimension of  $A$ . The eigenvalues of  $A$  are the characteristic velocities  $c$ . Now it is easily seen that the eigenvectors of the matrix  $M$  are of the form

$$\begin{pmatrix} \vdots \\ U_m e^{ijk\Delta x} \\ U_m e^{i(j+1)k\Delta x} \\ U_m e^{i(j+2)k\Delta x} \\ \vdots \end{pmatrix}$$

where  $k$  can be interpreted as a wave-number. The eigenvectors  $U_m$  indicate specific wave modes. The corresponding eigenvalues of  $M$  are found to be

$$\lambda_M = 1 - \mu_m^2(1 - \cos \xi_k) - i\mu_m \sin \xi_k \quad (\text{A } 1.7)$$

where  $\mu_m = c_m \Delta t / \Delta x$  and  $\xi_k = k\Delta x$ . The number of eigenvectors is  $N$  times half the number of mesh-points  $L/2\Delta x$ . The wave number  $k$  assumes the  $L/2\Delta x$  values

$$2\pi/L, 4\pi/L, \dots, \pi/\Delta x$$

(assuming  $L/\Delta x$  to be even for simplicity).

The eigenvectors form a complete system, so the initial condition for the difference-equation can be written

$$\mathbf{u}_j^0 = \sum_{s=1}^{L/2\Delta x} \sum_{m=1}^N c_{ms} U_m \exp(ijs2\pi\Delta x/L) \quad (\text{A } 1.8)$$

Then

$$\mathbf{u}_j^n = \sum_{s=1}^{L/2\Delta x} \sum_{m=1}^N \lambda_M^n c_{ms} U_m \exp(ijs2\pi\Delta x/L) \quad (\text{A } 1.9)$$

It is seen that each component in eq. (A 1.8) is multiplied in each time-step by a factor  $\lambda_M$  depending on the wave-number and on the type of wave. The representation (A 1.8) is also used in the Lax-Richtmyer theory of stability (RM p. 61). The spectral radius  $\varrho_M$  of  $M$  satisfies

$$\varrho_M^2 = 1 - 4\mu^2(1 - \mu^2) \sin^4 \frac{1}{2}\xi \quad (\text{A } 1.10)$$

where subscripts have been omitted. Now a difference-approximation is called dissipative of order  $2n$  if (RM p. 109) there exists a constant  $\delta > 0$  such that for  $|\xi| \leq \pi$

$$\varrho_M \leq 1 - \delta |\xi|^{2n}$$

where  $n$  is a positive integer. It follows that the method is dissipative of order 2 if  $|\mu| < 1$ . This character, however, disappears if  $\mu = 0$ , i.e. at locations where critical flow occurs. It has proved not to be necessary to take precautions for this case.

For stability, the condition

$$\varrho_M \leq 1 \quad (\text{A } 1.11)$$

is required for fixed values of the time step  $\Delta t$  and for any length of the time interval. This is stability in the sense of O'Brien, Hyman and Kaplan (1951). The condition actually prevents exponential growth of any component in eq. (A 1.8) with time if the time step is fixed. It follows from eq. (A 1.10) that the method is stable if  $|\mu| < 1$ .

It is noted that eq. (A 1.11) is somewhat stronger than the Von Neumann condition, necessary for stability in the sense of Lax and Richtmyer (fixed time interval and vanishing time step  $\Delta t$ , RM p. 70). Generally it is impossible to show that this condition is also sufficient without considering the specific form of the system of differential equations. For the linearized system discussed hereafter it can be shown to be sufficient using one of the conditions mentioned by Richtmyer and Morton (RM p. 85).

So far, the effect of the non-derivative terms  $\mathbf{h}$  in the equations has been ignored. For the general case the eigenvectors of the matrix  $M$  are unknown. However, for the specific systems of differential equations discussed in this study a similar analysis can be done including the non-derivative terms. Generally, this is still a complicated

matter. Below the analysis is shown for a linearized system of equations describing the flow of a salt water layer below a deep fresh water layer which is almost motionless. The equations are identical to those for a single layer of water, except for the reduced gravity.

$$\frac{\partial a_2}{\partial t} + a_2 \frac{\partial u_2}{\partial x} = 0$$

$$\frac{\partial u_2}{\partial t} + \varepsilon g \frac{\partial a_2}{\partial x} + r u_2 = 0$$

where  $r u_2$  denotes the linearized frictional term. The matrices  $A$  and  $R$  (assumed constant) read for this case:

$$A = \begin{pmatrix} 0 & a_2 \\ \varepsilon g & 0 \end{pmatrix} \quad R = \begin{pmatrix} 0 & 0 \\ 0 & r \end{pmatrix}$$

The characteristic velocities are  $c = \pm(\varepsilon g a_2)^{\frac{1}{2}}$ . Applying the difference method (A 1.6), the matrix  $M$  will have similar eigenvectors as shown before, but the vectors  $U_m$  no longer are eigenvectors of  $A$ . The vector  $u_j^n$  at a specific point during a time step is multiplied by the matrix

$$G = I - R\Delta t - \left( A \frac{\Delta t}{\Delta x} \right)^2 (1 - \cos \xi) - i \frac{\Delta t}{\Delta x} A \sin \xi$$

The eigenvalues  $\lambda$  follow from

$$\begin{vmatrix} 1 - \mu^2(1 - \cos \xi) - \lambda & -i \frac{\Delta t}{\Delta x} a_2 \sin \xi \\ -i \varepsilon g \frac{\Delta t}{\Delta x} \sin \xi & 1 - \mu^2(1 - \cos \xi) - r\Delta t - \lambda \end{vmatrix} = 0$$

This gives

$$\lambda = 1 - \frac{1}{2}r\Delta t - \mu^2(1 - \cos \xi) \pm i \{ \mu^2 \sin^2 \xi - (\frac{1}{2}r\Delta t)^2 \}^{\frac{1}{2}}$$

which corresponds to eq. (A 1.7). Introducing  $\varphi = \sin^2 \frac{1}{2} \xi$  it is found for the case that the eigenvalues are complex:

$$|\lambda|^2 = 1 - 4\mu^2(1 - \mu^2)\varphi^2 - r\Delta t(1 - 2\mu^2\varphi)$$

This expression has a maximum for

$$\varphi = \frac{1}{4}r\Delta t(1 - \mu^2)^{-1}$$

Then

$$\varrho_M^2 = 1 - r\Delta t + \frac{1}{4}\mu^2(r\Delta t)^2(1 - \mu^2)^{-1}$$

which is smaller than unity if

$$\mu^2 < (1 + \frac{1}{4}r\Delta t)^{-1} \quad (\text{A } 1.12)$$

It is straightforward to show that the eigenvalues  $\lambda$  never exceed unity in absolute value if this condition is satisfied. Even though this analysis is not generally valid because of the simplification of the equations, it is indicated that the admissible range for  $\mu$  is limited somewhat by the presence of the non-derivative terms. It is noted that  $r\Delta t$  generally is small. In addition, it is stressed that the above stability analysis is a local one. It does not guarantee global stability, especially because of the boundary conditions.

Although the truncation error is of the second order, as shown in eq. (A 1.5), this does not say very much concerning the actual accuracy with which waves are reproduced. This can be investigated by means of the propagation factor (e.g. Leendertse 1967, Vliegthart 1969). For simplicity the term  $\mathbf{h}$  is again neglected. From eqs. (A 1.8) and (A 1.9) it was seen that each wave-component is multiplied in each time-step by a complex number  $\lambda_M$ , which introduces a damping and a phase shift. If one component is singled out for the investigation, the solution of the differential equation after one physical period  $2\pi(kc)^{-1}$  reads at the grid-points

$$\mathbf{u} = \mathbf{U}_m e^{-2\pi i} e^{ikj\Delta x}$$

For the difference-equation the same time-interval is covered by  $2\pi(kc\Delta t)^{-1} = 2\pi/(\mu\xi)$  time-steps. Its solution therefore is

$$\mathbf{u} = \mathbf{U}_m \lambda_M^{2\pi/(\mu\xi)} e^{ikj\Delta x}$$

The propagation factor  $T$  now is defined as the ratio of the solutions of the difference and differential equations

$$T = \lambda_M^{2\pi/(\mu\xi)} e^{2\pi i} \quad (\text{A } 1.13)$$

Its modulus denotes the relative damping factor  $D$  per physical wave-period. The ratio of the argument to the phase-shift  $-2\pi$  of the physical wave gives the relative velocity of propagation of the computed wave  $c_r$ .

$$D = |\lambda_M|^{2\pi/(\mu\xi)} \quad (\text{A } 1.14)$$

$$c_r = -\arg(\lambda_M)/(\mu\xi)$$

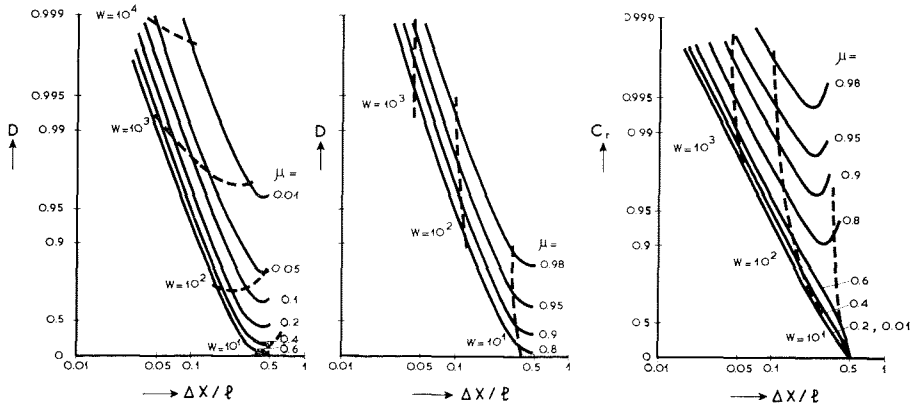


Fig. 33. Damping factor  $D$  and relative velocity of propagation  $c_r$  for the Lax-Wendroff method. Dashed lines: equal amounts of work  $W$  (arbitrary units).

The quantities  $D$  and  $c_r$  should both be as close to unity as possible. They can be derived from eq. (A 1.7) for various values of  $\mu$  and  $\xi$ . The result is given in Fig. 33. Here  $\xi = 2\pi\Delta x/l$ , where  $l$  is the wave-length considered. The accuracy therefore depends on the number of meshes in one wave-length and on the parameter  $\mu$ , which denotes the orientation of the grid relative to the characteristics.

In the figure also lines of equal amounts of work have been drawn. The number of operations to cover the region is proportional to  $(\Delta x \Delta t)^{-1}$ . If the wave-length  $l$  and the velocity of propagation  $c$  are constant, the amount of work is defined as

$$W = \frac{l^2}{c \Delta x \Delta t} = \mu^{-1} (\Delta x/l)^{-2} \quad (\text{A 1.15})$$

When designing a computation one chooses a combination of  $\mu$  and  $\xi$  which satisfies conditions for  $D$  and  $c_r$  set in advance, with the smallest amount of work.

An important difficulty arises if the velocities of propagation show considerable differences. This situation occurs in the present study if the full system of equations is considered (section A 3). Because of stability considerations one should have  $|\mu| < 1$  (or alternatively eq. (A 1.12)) for any wave present. This is most restrictive for the surface waves. The corresponding value of  $\mu$  for the internal wave-mode then may be less than 0.05. From Fig. 33 it is seen that the method is then quite inaccurate, unless very small values of  $\Delta x/l$  and corresponding small time-steps are applied, which makes the computation expensive. This will be even more the case for applications in two spatial dimensions.

Concerning shock-like conditions (salt fronts), it is known that the Lax-Wendroff method can take care of weak solutions (RM p. 337). These satisfy global conservation laws expressing the same physical principles as the differential equations do for local conditions. The velocity of propagation of a front is given by

$$c[u] = [f] \quad (\text{A 1.16})$$

where [ ] denotes the difference of the values on either side of the shock. It has been pointed out already that the dynamical equation (6.3.20) is not a conservation law, so that the resulting behaviour of the shock is not correct. As shown by Abraham and Vreugdenhil (1970), this may be important if considerable energy losses occur due to deceleration of the upper layer behind the front. However, in a tidal estuary the fronts are not expected to be very marked and to influence the flow in an essential way. Therefore the straightforward application of the Lax-Wendroff method is considered to be acceptable.

The shape of a front deviates from a discontinuity by the action of the artificial viscosity. This is to be identified with the truncation error shown in eq. (A 1.5). For a single equation with constant coefficients, this reads (up to fourth order terms)

$$\frac{\partial u}{\partial t} + c \frac{\partial u}{\partial x} = -\mu(1-\mu^2) \frac{\Delta x^3}{6\Delta t} \frac{\partial^3 u}{\partial x^3} + \mu^2(1-\mu^2) \frac{\Delta x^4}{24\Delta t} \frac{\partial^4 u}{\partial x^4} \quad (\text{A 1.17})$$

which can be solved analytically for a given initial condition (Vreugdenhil (1969)). It is found that the two terms shown are completely responsible for the shape of the front, found numerically, including secondary waves. In the original Lax-Wendroff method additional artificial viscosity terms were added, but in the present case this turned out to be unnecessary.

Finally, the treatment of the boundary conditions is mentioned. Generally (i.e. at subcritical flow-conditions) a first order accurate implicit finite difference representation of the equations of continuity is used to complete the system of equations at a boundary. During supercritical outflow the same procedure is applied to the dynamical equation too. The equations (3.3.3) and (3.3.4) are treated in this way only as long as boundary conditions for the density are required (cf. section 5.2). At the river-mouth a system of non-linear algebraic equations results, which can be solved by iteration. During supercritical inflow the conditions for the level of the interface and the velocity are prescribed explicitly (eq. (5.5.1)).

## 2 Energy equations

The equation describing the energy balance can be obtained as follows. By subtracting  $\frac{1}{2}v_kv_k$  times eq. (2.1.1) from  $v_k$  times eq. (2.1.6) one obtains

$$\begin{aligned} v_k \frac{\partial}{\partial t} (\rho v_k) - \frac{1}{2} v_k v_k \frac{\partial \rho}{\partial t} + v_k \frac{\partial}{\partial x_j} (\rho v_k v_j) - \frac{1}{2} v_k v_k \frac{\partial}{\partial x_j} (\rho v_j) + \\ + v_k \frac{\partial p}{\partial x_k} + \rho g v_3 - \rho v v_k \frac{\partial^2 v_k}{\partial x_j \partial x_j} = 0 \end{aligned}$$

In this equation the first two terms give

$$\frac{1}{2} v_k v_k \frac{\partial \rho}{\partial t} + \rho \frac{\partial}{\partial t} (\frac{1}{2} v_k v_k) = \frac{\partial}{\partial t} (\frac{1}{2} \rho v_k v_k)$$

Similarly, the third and fourth terms result in

$$\frac{1}{2}v_k v_k \frac{\partial}{\partial x_j}(\rho v_j) + \rho v_j \frac{\partial}{\partial x_j}(\frac{1}{2}v_k v_k) = \frac{\partial}{\partial x_j}(\frac{1}{2}\rho v_k v_k v_j)$$

Finally

$$v_k \frac{\partial p}{\partial x_k} = \frac{\partial}{\partial x_k}(p v_k)$$

due to eq. (2.1.5) so the energy equation becomes

$$\frac{\partial}{\partial t}(\frac{1}{2}\rho v_k v_k) + \frac{\partial}{\partial x_j}(\frac{1}{2}\rho v_k v_k v_j) + \frac{\partial}{\partial x_k}(p v_k) + \rho g v_3 - \rho v v_k \frac{\partial^2 v_k}{\partial x_j \partial x_j} = 0 \quad (\text{A } 2.1)$$

The quantity  $\frac{1}{2}\rho v_k v_k$  can be identified as the kinetic energy per unit volume. Taking the time-average of eq. (A 2.1) and applying the Boussinesq approximation, the equation for the total energy is obtained:

$$\begin{aligned} & \frac{\partial}{\partial t}(\frac{1}{2}\bar{\rho} \bar{v}_k \bar{v}_k + \frac{1}{2}\bar{\rho} \overline{v'_k v'_k}) + \frac{\partial}{\partial x_j}(\frac{1}{2}\bar{\rho} \bar{v}_k \bar{v}_k \bar{v}_j + \frac{1}{2}\bar{\rho} \overline{v'_k v'_k \bar{v}_j} + \\ & + \frac{1}{2}\bar{\rho} \overline{v'_k v'_k v'_j}) + \frac{\partial}{\partial x_j}(\bar{\rho} \bar{v}_k \overline{v'_k v'_j}) + \frac{\partial}{\partial x_k}(\bar{p} \bar{v}_k + \overline{p' v'_k}) + \\ & + \bar{\rho} \bar{v}_3 g + \overline{\rho' v'_3 g} - \bar{\rho} v \bar{v}_k \frac{\partial^2 \bar{v}_k}{\partial x_j \partial x_j} - \overline{\rho v v'_k \frac{\partial^2 v'_k}{\partial x_j \partial x_j}} = 0 \end{aligned} \quad (\text{A } 2.2)$$

In a similar way, an equation for the energy associated with the mean flow can be derived from eqs. (2.2.1) and (2.2.3):

$$\begin{aligned} & \frac{\partial}{\partial t}(\frac{1}{2}\bar{\rho} \bar{v}_k \bar{v}_k) + \frac{\partial}{\partial x_j}(\frac{1}{2}\bar{\rho} \bar{v}_k \bar{v}_k \bar{v}_j) + \bar{v}_k \frac{\partial}{\partial x_j}(\bar{\rho} \overline{v'_k v'_j}) + \frac{\partial}{\partial x_k}(\bar{p} \bar{v}_k) + \bar{\rho} \bar{v}_3 g - \bar{\rho} v \bar{v}_k \frac{\partial^2 \bar{v}_k}{\partial x_j \partial x_j} = 0 \\ & \quad \quad \quad 1 \quad \quad \quad 2 \quad \quad \quad 3 \quad \quad \quad 4 \quad \quad \quad 5 \quad \quad \quad 6 \end{aligned} \quad (\text{A } 2.3)$$

Here a term

$$\frac{1}{2}\bar{v}_k \bar{v}_k \frac{\partial}{\partial x_j}(\overline{\rho' v'_j})$$

has been neglected. It would have cancelled exactly, had the Boussinesq approximation not been made. The difference between eqs. (A 2.2) and (A 2.3) gives the equation for the turbulence-energy:

$$\begin{aligned} & \frac{\partial}{\partial t}(\frac{1}{2}\bar{\rho} \overline{v'_k v'_k}) + \frac{\partial}{\partial x_j}(\frac{1}{2}\bar{\rho} \overline{v'_k v'_k \bar{v}_j} + \frac{1}{2}\bar{\rho} \overline{v'_k v'_k v'_j}) + \bar{\rho} \overline{v'_k v'_j} \frac{\partial \bar{v}_k}{\partial x_j} + \\ & \quad \quad \quad 1 \quad \quad \quad 2 \quad \quad \quad 3 \\ & + \frac{\partial}{\partial x_k}(\overline{p' v'_k}) + \overline{\rho' v'_3 g} - \bar{\rho} v v'_k \frac{\partial^2 v'_k}{\partial x_j \partial x_j} = 0 \\ & \quad \quad \quad 4 \quad \quad \quad 5 \quad \quad \quad 6 \end{aligned} \quad (\text{A } 2.4)$$

These three energy-equations have the same structure. For eqs. (A 2.3) and (A 2.4) the terms can be characterized as follows:

term no.	mean flow, eq. (A 2.3)	turbulence, eq. (A 2.4)
1	local rate of change of kinetic energy per unit volume	
2	convection by mean flow	convection by mean flow and by fluctuating components of velocity
3	loss of energy due to work done by turbulent shear stresses against translation of fluid elements	source of energy due to work done by turbulent shear stresses in rotation of fluid elements
4	work done by pressure and gravity;	"diffusion" by fluctuations of pressure
5	loss or gain depending on situation	loss of potential energy by transfer of mass against gravity
6	direct viscous dissipation of energy	major part: dissipation by viscosity (Townsend 1956)

These equations are discussed e.g. by Ellison (1957), Townsend (1958), Stewart (1959). They can be simplified by considering the order of magnitude in the same way as in section 2.3. The main terms then turn out to be:

mean flow:

$$\frac{d}{dt}(\frac{1}{2}\bar{\rho}\bar{v}_k\bar{v}_k) - \bar{u}\frac{\partial\tau}{\partial z} + \bar{u}\frac{\partial\bar{p}}{\partial x} + \bar{v}\frac{\partial\bar{p}}{\partial y} = 0 \quad (\text{A } 2.5)$$

turbulence:

$$\frac{d}{dt}(\frac{1}{2}\bar{\rho}\overline{v'_kv'_k}) + \frac{\partial}{\partial x_j}(\frac{1}{2}\bar{\rho}\overline{v'_kv'_kv'_j} + \overline{p'v'_j}) - \tau\frac{\partial\bar{u}}{\partial z} + g\bar{f} - \bar{\rho}v'_k\frac{\partial^2\bar{v'_k}}{\partial z^2} = 0 \quad (\text{A } 2.6)$$

where

$$x_{1,2,3} = x, y, z$$

$$v_{1,2,3} = u, v, w$$

$$\tau = -\bar{\rho}\overline{v'_1v'_3}$$

$$f = \overline{\rho'v'_3}$$

$$\frac{d}{dt} = \frac{\partial}{\partial t} + \bar{v}_j\frac{\partial}{\partial x_j}$$

A discussion of the mechanism of the turbulent process in terms of the energy flow is given by Stewart (1959). A somewhat simplified picture is the following. In eq. (A 2.5) some term represents a source of energy; this may be either the convective term or the pressure-term.

This energy is used to overcome the loss of energy, represented by the part of the work by the shear stress ( $\bar{u}\partial\tau/\partial z$ ). This energy is transferred to the turbulent motion, but not at the same location. This follows from the fact that the terms  $\bar{u}\partial\tau/\partial z$  and  $\tau\partial\bar{u}/\partial z$  cancel when they are integrated over the water-depth, but not locally. The energy, thus available for the turbulence, together with energy possibly contributed by convection, is lost into potential energy due to the upward turbulent mass-flux ( $gf$ ) and in dissipation due to viscosity. The portion of the gain of energy going into potential energy is represented by the flux Richardson number  $Rf$ :

$$Rf = \frac{g \bar{q}'w'}{\bar{q} \bar{u}'w' \frac{\partial\bar{u}}{\partial z}} \quad (\text{A } 2.7)$$

The second term in eq. (A 2.6) serves to redistribute the energy over different heights (turbulent diffusion). In unsteady flow, the process of energy-transfer is not in equilibrium because of the local “storage” of kinetic energy. Schematically the situation is given in Fig. 34.

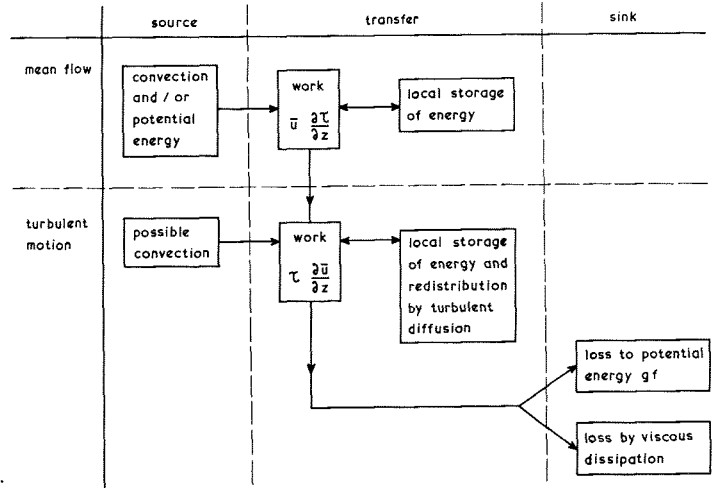


Fig. 34. Energy transfer.

In the same way an equation describing the intensity of the turbulent density-fluctuations can be derived. To this end, eq. (2.2.1) is subtracted from eq. (2.1.1):

$$\frac{\partial q'}{\partial t} + \frac{\partial}{\partial x_j} (\bar{q} v'_j + q' \bar{v}_j + q' v'_j - \overline{q' v'_j}) - \theta \frac{\partial^2 q'}{\partial x_j \partial x_j} = 0$$

Multiplying by  $q'$  and taking the time-average:

$$\frac{\partial}{\partial t} (\frac{1}{2} \overline{q'^2}) + \frac{\partial}{\partial x_j} (\frac{1}{2} \overline{q'^2} \bar{v}_j + \frac{1}{2} \overline{q'^2 v'_j}) + \overline{q' v'_j} \frac{\partial \bar{q}}{\partial x_j} - \theta \overline{q'} \frac{\partial^2 q'}{\partial x_j \partial x_j} = 0 \quad (\text{A } 2.8)$$

The terms can be interpreted in a similar way as those in eqs. (A 2.3) and (A 2.4). By considering the order of magnitude of the terms, the equation can be simplified to

$$\frac{d}{dt}(\frac{1}{2}\overline{q'^2}) + \frac{\partial}{\partial z}(\frac{1}{2}\overline{q'^2 w'}) + f\frac{\partial \bar{q}}{\partial z} - \overline{\theta q' \frac{\partial^2 q'}{\partial z^2}} = 0 \quad (\text{A } 2.9)$$

The mixing-length hypothesis, applied in Chapter 4, can be derived from eqs. (A 2.6) and (A 2.9) by further neglecting the convective and turbulent diffusion terms and by considering steady flow. In addition to this, expressions for the dissipative terms have to be found.

The dissipation by viscosity is effectuated in the smallest eddies. The generation mainly takes place in the large-scale eddies. The transfer from large to small scales is a process of non-linear interaction. Of course, the actual dissipation is governed by viscosity. However, the *amount* of energy to be dissipated is determined by the large-scale eddies, as follows from the process described above. This means that the dissipation process adjusts itself to the amount of energy being transferred, and that it will not show an explicit dependence on the Reynolds number. In this respect it has been noted (e.g. Bradshaw 1961) that the turbulence spectra in equilibrium boundary layers, when scaled to the shear velocity  $(\tau/\rho)^{\frac{1}{2}}$ , almost coincide, especially for the small eddies, i.e. for the part which determines the dissipation. Therefore a first approximation for the dissipative term, taking dimensional considerations into account, is

$$\overline{\bar{q} v v'_k \frac{\partial^2 v'_k}{\partial x_j \partial x_j}} = -\bar{q} \frac{|\tau/\bar{q}|^{\frac{3}{2}}}{l_1} \quad (\text{A } 2.10)$$

A similar expression is given by Bradshaw, Ferriss and Atwell (1967) and Townsend (1961). Making similar assumptions for the diffusion term in eq. (A 2.9),

$$\overline{\theta q' \frac{\partial^2 q'}{\partial x_j \partial x_j}} = \frac{-f^2}{l_2 |\tau/\bar{q}|^{\frac{3}{2}}} \quad (\text{A } 2.11)$$

In these equations  $l_1$  and  $l_2$  are length parameters.

With these expressions and with the neglects mentioned above, eqs. (A 2.6) and (A 2.9) become:

$$\tau \frac{\partial \bar{u}}{\partial z} - gf - \bar{q} \frac{|\tau/\bar{q}|^{\frac{3}{2}}}{l_1} = 0 \quad (\text{A } 2.12)$$

$$\frac{\partial \bar{q}}{\partial z} + \frac{f}{l_2 |\tau/\bar{q}|^{\frac{3}{2}}} = 0 \quad (\text{A } 2.13)$$

From these equations the turbulent shear stress  $\tau$  and the turbulent mass-flux  $f$  can be expressed as

$$|\tau/\bar{q}|^{\frac{1}{2}} = l_1 \frac{\partial \bar{u}}{\partial z} \left\{ \frac{1}{2} \pm \frac{1}{2} \left( 1 - 4 \frac{l_2}{l_1} Ri \right)^{\frac{1}{2}} \right\} \text{sign}(\tau) \quad (\text{A } 2.14)$$

$$f = -l_1 l_2 \frac{\partial \bar{q}}{\partial z} \frac{\partial \bar{u}}{\partial z} \left\{ \frac{1}{2} \pm \frac{1}{2} \left( 1 - 4 \frac{l_2}{l_1} Ri \right)^{\frac{1}{2}} \right\} \text{sign}(\tau) \quad (\text{A } 2.15)$$

where

$$Ri = -g \frac{\partial \bar{q}}{\partial z} \bar{q}^{-1} \left( \frac{\partial \bar{u}}{\partial z} \right)^{-2}$$

is the local Richardson number. For homogeneous flow,  $Ri = 0$  and eq. (A 2.14) reduces to the familiar mixing-length hypothesis. Generally, one could define mixing-lengths  $l_\tau$  for momentum-transfer and  $l_f$  for mass-transfer by

$$|\tau/\bar{q}|^{\frac{1}{2}} = l_\tau \frac{\partial \bar{u}}{\partial z} \text{sign}(\tau)$$

$$f = -l_f^2 \frac{\partial \bar{q}}{\partial z} \frac{\partial \bar{u}}{\partial z} \text{sign}(\tau)$$

which corresponds to eqs. (A 2.14) and (A 2.15) if

$$l_\tau = l_1 \left\{ \frac{1}{2} + \frac{1}{2} \left( 1 - 4 \frac{l_2}{l_1} Ri \right)^{\frac{1}{2}} \right\} \quad (\text{A } 2.16)$$

$$l_f^2 = l_1 l_2 \left\{ \frac{1}{2} + \frac{1}{2} \left( 1 - 4 \frac{l_2}{l_1} Ri \right)^{\frac{1}{2}} \right\}$$

Qualitatively, these expressions are in accordance with literature where a dependence on the Richardson number has been found (e.g. Ellison and Turner 1960, Francis c.s. 1953, Kent and Pritchard 1959, Bowden 1962). The positive sign has been chosen because of the observed tendency. A quantitative application of eq. (A 2.16) is not possible without further assumptions, the behaviour of the length-parameters  $l_1$  and  $l_2$  being unknown.

### 3 Characteristics

The equation for the characteristic velocities

$$c = \frac{dx}{dt}$$

resulting from the system of differential equations (3.3.3). . . (3.3.8) reads

$$(c - u_1)(c - u_2) [\{(c - u_1)^2 - ga_1\} \{(c - u_2)^2 - ga_2\} - (1 - \varepsilon)g^2 a_1 a_2] = 0 \quad (\text{A } 3.1)$$

Two characteristic velocities can be derived immediately:

$$c_u = u_{1,2} \quad (\text{A } 3.2)$$

The remaining ones are the roots of the equation

$$\phi(c) \equiv \{(c - u_1)^2 - ga_1\} \{(c - u_2)^2 - ga_2\} - (1 - \varepsilon)g^2 a_1 a_2 = 0 \quad (\text{A } 3.3)$$

The latter equation also results from the system without mixing (3.3.9) to (3.3.12), the only difference being that the value of  $\varepsilon$  is then fixed.

A graphical method to investigate eq. (A 3.3) is described by Abbott and Torbe (1963). Its character can also be investigated analytically. The larger of the values  $a_1$  and  $a_2$  is denoted by  $a_+$ , the smaller by  $a_-$ . The corresponding velocities are denoted by  $u_+$  and  $u_-$ . Now it is easily seen that  $\phi(c)$  is negative at

$$c = u_1 \pm (ga_1)^{\frac{1}{2}} \quad \text{and} \quad u_2 \pm (ga_2)^{\frac{1}{2}}$$

The derivative  $\phi'(c)$  has one zero in each of the intervals

$$(u_+ - (ga_+)^{\frac{1}{2}}, u_- - (ga_-)^{\frac{1}{2}})$$

$$(u_- - (ga_-)^{\frac{1}{2}}, u_- + (ga_-)^{\frac{1}{2}})$$

$$(u_- + (ga_-)^{\frac{1}{2}}, u_+ + (ga_+)^{\frac{1}{2}})$$

This means that  $\phi(c)$  must have two zeros (and not more than two) outside these intervals. As  $u_1$  and  $u_2$  are small relative to  $(ga_+)^{\frac{1}{2}}$ , these roots will be of the order  $(ga_+)^{\frac{1}{2}}$  or larger. From the constant term in eq. (A 3.3) it is concluded then that the other pair of zeros must be of the order  $(ga_+)^{\frac{1}{2}}$  or smaller. These roots certainly are included in the interval

$$|c| < \frac{1}{2}(ga_+)^{\frac{1}{2}}$$

If one assumes in addition

$$|u_{1,2}| < \frac{1}{2}(ga_+)^{\frac{1}{2}}$$

one has from eq. (A 3.3):

$$\begin{aligned} \phi(c) &= (c - u_-)^2(c - u_+)^2 - ga_+(c - u_-)^2 - ga_-(c - u_+)^2 + \varepsilon g^2 a_1 a_2 = \\ &= (c - u_-)^2 \{(c - u_+)^2 - ga_+\} - ga_-(c - u_+)^2 + \varepsilon g^2 a_1 a_2 \leq \\ &\leq -ga_-(c - u_+)^2 + \varepsilon g^2 a_1 a_2 \end{aligned}$$

If  $\varepsilon = 0$ , it is seen that  $\phi(c)$  is negative in this region, so the pair of small roots is complex then. There is one exception, viz. the case in which  $u_1 = u_2$ . Then the small roots are

$$c_i = u_1 = u_2$$

Except for this case, the system is not fully hyperbolic if  $\varepsilon = 0$ , which indicates an unstable behaviour.

For the general case eq. (A 3.3) is illustrated in Fig. 35. The larger pair of roots can be found analytically by introducing

$$c = c_0 + c_1$$

into eq. (A 3.3), where  $c_0 \sim (gh)^{\frac{1}{2}}$  and  $c_1 \sim u_{1,2}$ , which is an order of magnitude smaller. By retaining the largest terms in the equation, one finds

$$c_0 = \pm (gh)^{\frac{1}{2}}$$

The second largest terms give

$$c_1 = (a_1 u_1 + a_2 u_2)/h$$

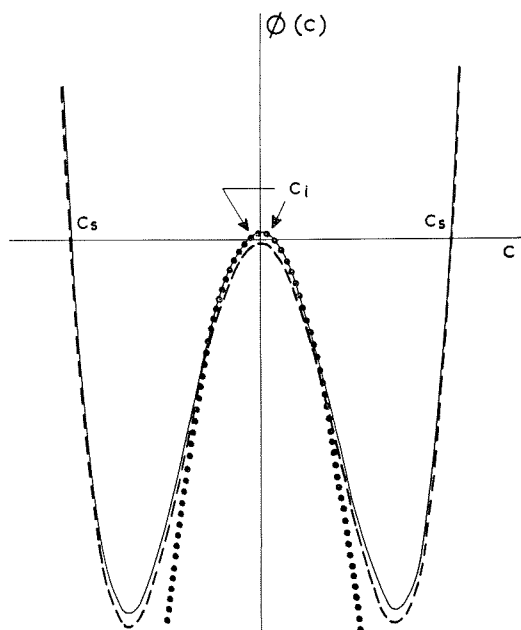


Fig. 35.  
Characteristic  
equation.

- FULL EQUATION (A.3.3)
- THE SAME WITH  $\varepsilon = 0$
- ..... APPROXIMATION FOR SMALL  $c$  (A.3.5)

so the velocity of propagation for the surface wave mode is given approximately by

$$c_s = (a_1 u_1 + a_2 u_2)/h \pm (gh)^{\frac{1}{2}} \quad (\text{A } 3.4)$$

The smaller pair of roots now must be of the order  $\varepsilon^{\frac{1}{2}}$  as stated above. Then the product  $(c - u_1)^2(c - u_2)^2$  in the equation can be neglected. There remains

$$-ga_1(c - u_2)^2 - ga_2(c - u_1)^2 + \varepsilon g^2 a_1 a_2 = 0 \quad (\text{A } 3.5)$$

which is shown in Fig. 35 as a dotted line. The roots are the velocities of propagation for the internal wave mode

$$c_i = (a_1 u_2 + a_2 u_1)/h \pm \{\varepsilon g a_1 a_2 h^{-1}(1 - F^2)\}^{\frac{1}{2}} \quad (\text{A } 3.6)$$

where  $F = (u_1 - u_2)(\varepsilon gh)^{-\frac{1}{2}}$  is the internal Froude number. From this expression, too, it can be concluded that  $c_i$  is real for  $\varepsilon = 0$  only if  $u_1 = u_2$ .

The order of magnitude of  $c_i$  and  $c_s$  is determined by the square roots in eqs. (A 3.4) and (A 3.6). The ratio is

$$c_i/c_s \sim \{\varepsilon a_1 a_2 h^{-2}(1 - F^2)\}^{\frac{1}{2}}$$

Here  $\varepsilon < 0.03$  for sea-water and  $a_1 a_2 h^{-2} < 0.25$ . Also  $F$  may not be negligible with respect to unity. The ratio therefore is certainly smaller than 0.087 and may be as small as 0.01.

Usually the velocities  $u_{1,2}$  will not be important compared to  $(gh)^{\frac{1}{2}}$ , so neither of the surface wave velocities  $c_s$  will become zero. The internal wave velocities, however, can change sign very well. *Critical flow* occurs if one of the  $c_i$  vanishes. From eq. (A 3.5) this is seen to occur if

$$\frac{u_1^2}{\varepsilon g a_1} + \frac{u_2^2}{\varepsilon g a_2} = 1 \quad (\text{A } 3.7)$$

If both  $c_i$  vanish, the flow is said to be *doubly critical*. Then one has in addition to (A 3.7)

$$\frac{u_1}{a_1} = -\frac{u_2}{a_2} \quad (\text{A } 3.8)$$

as can be derived from (A 3.6). From eqs. (A 3.7) and (A 3.8), combined with

$$h = a_1 + a_2$$

$$q = a_1 u_1 + a_2 u_2$$

it is possible to derive  $a_2$  and  $u_2$  explicitly:

$$\left. \begin{aligned} a_2 &= \frac{1}{2}h + \frac{1}{2}q(\varepsilon gh)^{-\frac{1}{2}} \\ u_2 &= \frac{1}{2}q/h + \frac{1}{2}(\varepsilon gh)^{\frac{1}{2}} \end{aligned} \right\} \quad (\text{A } 3.9)$$

#### 4 Estimates of approximations

In the derivation of the two-layer model (Chapter 3) two assumptions have been made, which can be checked to some extent using measurements. To this end, measurements in the Rotterdam Waterway (Fig. 14) are applied, made on 22-6-1956. In the relevant region the following data have been obtained at hourly intervals during about one tidal cycle.

km	1030	1026.5	1023.4
water level	1	1	1
vertical velocity profiles	4	none	4
vertical salinity profiles	3	4	4

The level of the interface and the mean velocities in each layer, used in Chapters 7 and 8, have been determined from these measurements. Of course these data are not representative for any estuary. However, the Rotterdam Waterway is a good example of a partly mixed estuary. This gives some confidence that the following results have some more general validity.

The first approximation to be evaluated is the neglect of the dispersive terms  $F_1$  and  $F_2$  in section 3.2. If they are retained for a moment, the equation of mass-conservation for the lower layer (3.2.7) gives, after averaging over one tidal cycle and over the entire length of the salt wedge:

$$(\varrho_2 A_2 u_2)_t + (F_2)_t = \int_0^L (b_i f_i)_t dx + \int_0^L (w_i \varrho_i b_i)_t dx \quad (\text{A } 4.1)$$

assuming the situation to be in equilibrium. The notation  $( )_t$  is used to indicate a tidal mean value. The terms in the left-hand member are taken at km 1030, to be identified with  $x = 0$  for the moment. Eq. (3.2.6) after a similar operation results in

$$(A_2 u_2)_t = \int_0^L (b_i w_i)_t dx \quad (\text{A } 4.2)$$

which means that the net flow into the lower layer at km 1030 must have left the lower layer through the interface. Subtracting  $\varrho_0$  times eq. (A 4.2) from eq. (A 4.1) gives a picture of the salt balance:

$$(\Delta \varrho_2 A_2 u_2)_t + (F_2)_t = \int_0^L (b_i f_i)_t dx + \int_0^L (w_i \Delta \varrho_i b_i)_t dx \quad (\text{A } 4.3)$$

The left-hand members of the latter two equations can be derived from the measurements. To make an estimate of the right-hand member of (A 4.3), an assumption is made concerning  $\Delta \varrho_i$ . For simplicity it is assumed to be constant at  $10 \text{ kg/m}^3$ . The last term in (A 4.3) then is approximated by

$$\Delta \varrho_i \int_0^L (b_i w_i)_t dx$$

which can be computed from (A 4.2). The third term in eq. (A 4.3) then can be found from the balance of the equation. Results are shown in Fig. 36. It should be noted that the four terms need not balance at each instant, but only in the mean values. These can be summarized as follows:

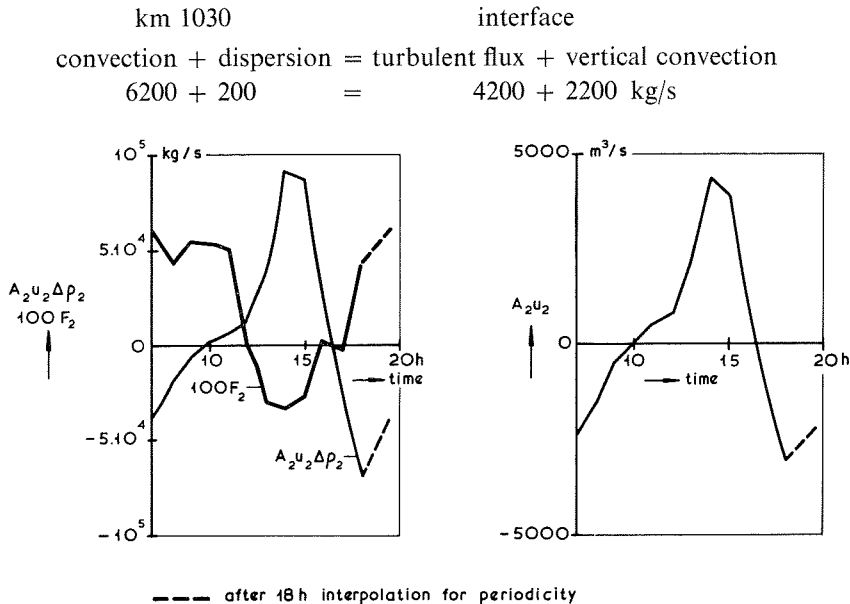


Fig. 36. Salt and water balance (Rotterdam Waterway 22-6-1956).

The figure for the dispersion term is not very accurate because of the small number of velocity and salinity profiles in the cross-section. Yet it is clear that it is quite small with respect to the other terms.

A more serious approximation is made in section 3.3 in the pressure terms. It has already been noted in that section that this approximation is quite justified for the upper layer. In the lower layer, however, the ratio between the neglected integral and the essential term

$$\beta = \frac{\frac{\partial}{\partial x} \int_{h_b}^{h_i} (x_3 - h_b) (\bar{\varrho} - \varrho_2) dx_3}{\frac{\partial}{\partial x} \{ \frac{1}{2} (\varrho_2 - \varrho_1) a_2^2 \}} \quad (\text{A } 4.4)$$

Table 9. Error in pressure-term for case without mixing. Measurements from Rotterdam Waterway 22-6-1956.

time	h	$\frac{1}{2}\Delta qa_2^2 (\Delta \rho = 25 \text{ kg/m}^3)$			$\int_{h_b}^{h_i} (x_3 - h_b)(\bar{\rho} - 1025)dx_3$	difference in				$\beta$					
		km	1030	1026.5	1023.4	km	$\frac{1}{2}\Delta qa_2^2$	between kms			integral				
(h)	(m)	(kg/m)	1030	1026.5	1023.4	(kg/m)	1030	1026.5	1023.4	1030	1026.5	1023.4	1030	1026.5	1023.4
6	—	—	—	901	607	—	—	294	41	—	—	—	—	0.14	—
7	13.40	925	515	280	—	143	410	235	44	34	44	0.08	0.19	—	—
8	13.35	440	206	95	—	103	234	111	30	43	30	0.18	0.27	—	—
9	13.40	244	77	26	—	69	161	51	10	42	17	0.26	0.33	—	—
10	13.30	220	29	8	—	63	191	21	3	52	8	0.27	0.38	—	—
11	13.40	195	12	2	—	51	183	10	1	46	4	0.25	0.40	—	—
12	13.60	238	46	3	—	54	192	43	1	39	14	0.20	0.33	—	—
13	14.00	393	221	8	—	67	172	213	3	22	42	0.13	0.20	—	—
14	14.60	1248	580	157	—	140	668	423	38	66	36	0.10	0.09	—	—
15	14.75	1711	984	663	—	108	727	321	94	3	11	0.00	0.03	—	—
16	14.60	2315	1334	1004	—	88	981	330	114	31	5	0.03	0.02	—	—
17	14.30	2090	1431	1109	—	105	659	322	122	-14	-3	0.02	0.01	—	—
18	13.75	1622	1019	847	—	140	603	172	129	18	-7	0.03	0.04	—	—

Table 10. Error in pressure-term for case with mixing. Measurements from Rotterdam Waterway 22-6-1956.

time	$h$ (m)	$\Delta \varrho = \varrho_2 - \varrho_1$ km			$\frac{1}{2} \Delta \varrho a_s^2$ km			$\int_{h_0}^{h_i} (x_3 - h_b)(\bar{\varrho} - \varrho_2) dx_3$ km			difference in $\frac{1}{2} \Delta \varrho a_s^2$ between kms			integral			$\beta$		
		1030	1026.5	1023.4	1030	1026.5	1023.4	1030	1026.5	1023.4	1030	1026.5	1023.4	1030	1026.5	1023.4	1030	1026.5	1023.4
(h)		(kg/m <sup>3</sup> )			(kg/m)			(kg/m)			(kg/m)			(kg/m)					
6	-	-	7.6	8.9	-	133	184	-	2	5	-	-51	-3	-	-0.5	-	-	-	0.06
7	13.40	6.4	7.3	7.8	156	88	85	2	1.5	2	68	3	0.5	0.5	-0.2	0.07	0.04	0.01	0.17
8	13.35	5.5	3.7	4.6	71	63	36	1	0.7	0.5	8	27	0.3	0.3	0.2	0.04	0.01	0.01	0.01
9	13.40	4.9	2.8	2.4	44	21	8	0.7	0.2	0.1	23	13	0.5	0.5	0.1	0.02	0.01	0.01	0.01
10	13.30	6.8	2.4	1.1	28	23	13	0.7	0.2	0.1	5	10	0.5	0.5	0.1	0.10	0.01	0.01	0.01
11	13.40	8.1	2.0	0.7	68	16	4	2	0.1	0.0	52	12	1.9	1.9	0.1	0.04	0.01	0.01	0.01
12	13.60	12.2	5.3	0.9	67	43	9	2	0.7	0.0	24	34	1.3	1.3	0.7	0.05	0.02	0.02	0.02
13	14.00	13.8	10.7	3.1	192	168	8	6	4	0.1	24	160	2	2	4	0.08	0.03	0.03	0.03
14	14.60	12.0	14.7	9.0	665	381	119	19	11	3	284	262	7	7	8	0.02	0.01	0.01	0.01
15	14.75	8.6	13.1	12.0	615	514	403	9	11	12	101	111	-2	-2	-1	0.02	0.01	0.01	0.01
16	14.60	1.2	11.0	10.6	43	570	431	0.2	9.7	9.9	-527	139	-10	-10	-0.2	0.02	0.00	0.00	0.00
17	14.30	1.7	10.4	9.2	84	580	348	0.3	11	7	-496	232	-11	-11	4	0.02	0.02	0.02	0.02
18	13.75	5.1	8.8	9.5	190	300	248	2	5	6	-110	52	-3	-3	-1	0.03	0.03	0.03	0.02

may assume appreciable values. The denominator is the term which is mainly responsible for the characteristic velocities of the internal wave mode. The values of  $\beta$  will be different for the models with and without mixing, as the level of the interface and the densities in each layer are different.

The gradients in eq. (A 4.4) can be determined between km. 1030 and 1026.5 and between km. 1026.5 and 1023.4. The results are given in Tables 9 and 10. The large distance between the measuring sections probably causes the gradients to be inaccurate. However, a reasonable estimate of the order of magnitude is considered possible.

It is concluded that for the case with mixing the values of  $\beta$  generally do not exceed a few percents. There are some exceptions, but these are due to small values of the denominator of eq. (A 4.4). The neglect of the integral turns out to be fully justified. The error is so small that a possible improved representation, using density profiles e.g. from section 4.3, does not make sense, considering the uncertainties in other, empirical, parameters in the mathematical model.

For the case without mixing the figures for  $\beta$  are considerably larger. Again, the largest values are due to the smaller values of the denominator. The largest error (66) is only 7 percent of the largest gradient (981). Yet errors up to 20% are not uncommon. This means that the neglect of the integral in this case is rather doubtful. A closer approximation using density profiles is impossible in this case, as no density profiles can be derived.